The Institute of Paper Chemistry

Appleton, Wisconsin

Doctor's Dissertation

Counterdiffusion of Carbon Dioxide and Nitrogen Through Dry and Partially Saturated Fiber Beds

James Francis Matters

June, 1965

COUNTERDIFFUSION OF CARBON DIOXIDE AND NITROGEN THROUGH DRY AND PARTIALLY SATURATED FIBER BEDS

A thesis submitted by

James Francis Matters

B.S. in Ch.E. 1960, Drexel Institute of Technology
M.S. 1962, Lawrence College

in partial fulfillment of the requirements
of The Institute of Paper Chemistry
for the degree of Doctor of Philosophy
from Lawrence University,
Appleton, Wisconsin

June, 1965

TABLE OF CONTENTS

SUMMARY

During the hot surface drying of fiber beds, the ordinary diffusion of water vapor (mass transport due to only a concentration gradient) is an important phenomenon throughout the drying cycle. In relation to this problem, the objectives of this thesis were (1) to determine the mechanisms governing the process of gaseous ordinary diffusion through fiber beds at varying degrees of liquid saturation, and (2) to evaluate the effect of varying the saturation of the fiber bed on the diffusion resistance.

The experimental program consisted primarily of studying the steady-state, uniform pressure, isothermal counterdiffusion of carbon dioxide and nitrogen through partially saturated beds of nylon fibers in an open system. The beds were partially saturated with a nonvolatile liquid, dioctyl phthalate, to degrees within the range of 10 to 70% of the void volume. For each bed, the diffusion mechanism was evaluated by making runs at several pressures within the range of 0.2 to 1.0 atmosphere. A guarded-ring type of diffusion chamber was used for this study.

At the lower pressures used, the observed diffusion fluxes were independent of pressure. As the pressure increased, the bulk phase transport of carbon dioxide was augmented by surface transport. With decreasing degree of saturation, the bulk phase transport rates increased, and the surface transport rate of carbon dioxide decreased.

In the bulk phase, normal diffusion prevailed at all pressures and degrees of saturation. This diffusion process was not equimolal. When the degree of saturation was less than 0.5 and the surface transport of carbon dioxide was negligible, the value of the flux ratio (nitrogen to carbon dioxide) was approximately equal to -1.25, as predicted by momentum transport theory. However, for degrees of saturation greater than 0.5, the value of the flux ratio was about

-1.34. This result was consistent with the results of analyses of the frequency of molecule-wall collisions and the related transport of axial momentum.

As the degree of saturation decreased, the effective normal diffusion coefficient increased. Analysis of this behavior was made in terms of the diffusibility and a geometric model expression for this parameter. Among other things, the results of this analysis indicated a marked difference between partially saturated beds in which the gas occupied more than half of the void space and those in which the liquid was the predominant fluid. In the former case, the diffusibility was proportional to the nonwetting-phase degree of saturation raised to a power n, where n was greater than unity. In the latter case, this proportionality no longer held, and the observed diffusion resistance was much less than that expected from the results obtained for the beds in which the gas was the predominant fluid. These differences were attributed to the effects of pore branching and pore tortuosity on the diffusion resistance.

When normal diffusion was accompanied by appreciable surface transport, the calculated values of the effective normal diffusion coefficient were less than the values determined for the normal diffusion process itself. Furthermore, the absolute value of the flux ratio for normal diffusion in the presence of significant surface transport was less than the minimum value predicted by momentum transport theory for normal diffusion.

Small axial pressure differences, also, had a significant effect on the normal diffusion process. While the observed gas transport rates were affected quite significantly by such pressure differences, the effective normal diffusion coefficient was independent of them. These results were in accord with momentum transport considerations and with recently reported experimental and theoretical developments.

INTRODUCTION

Quite generally, this study was concerned with the ordinary counterdiffusion of a binary gas mixture in porous media. Diffusion may be defined as the transport, under the influence of a physical stimulus, of an individual component through a mixture. When the driving force is a concentration gradient of the diffusing component, the process is referred to as ordinary diffusion. This type of transport of gases or vapors results from the random thermal motion of the molecules. Molecules can move from regions of higher to lower concentration and also in the opposite direction. Since there are more molecules in the regions of higher concentration, there will be a net transport toward the regions of lower concentration. In the absence of a container, the ordinary counterdiffusion of gases is governed solely by intermolecular collisions. Molecule-wall collisions have an important effect on this transport process when it takes place in some sort of apparatus.

Gaseous diffusion in a porous medium is affected further by the effects of its complex spatial geometry. In many cases of practical interest, the ordinary diffusion process is complicated by the effects of pressure and temperature gradients and surface transport. Fundamental to the solutions of these problems has been the characterization of the ordinary diffusion process itself.

For the drying of fiber beds, ordinary diffusion appears to be an important mechanism for the transport of water vapor (1). In such a system, the vapor transport is complicated further by phenomena associated with the volatile liquid phase present. Elucidation of this transport process has been hindered not only by all of the above complexities but also by a lack of knowledge concerning the process of ordinary diffusion in a drying system.

Early investigations concerned with the drying of porous materials, including paper and fiber beds, were based on the premise that the drying rate curves were indicative of relatively simple drying phenomena. However, more recent studies in this area have revealed relatively complex interrelationships of heat and mass transfer phenomena to be associated with the characteristic drying rate curves. Efforts in regard to fiber beds have been expended in the areas of liquid and vapor movement, heat transfer, and temperature and moisture distributions (1-4).

Using a simplified system of glass fibers, Cowan (1) carried out studies which elucidated the internal heat and mass transfer processes occurring during hot surface drying. As part of his analysis of the internal mass transfer mechanisms, Cowan considered the diffusion of water vapor which had originated at the hot surface. Although Cowan's analysis of the diffusion process was somewhat oversimplified, it indicated that ordinary diffusion was probably an important mode of water vapor transport during the hot surface drying of fiber beds. In this analysis it was necessary to assume that the air through which the water vapor diffused was stagnant. However, it is considered more accurate to view this diffusion process as one of counterdiffusion of water vapor and air. The present study was directed toward elucidating this transport phenomenon.

Depending on the size of the pores, i.e., a characteristic linear dimension, relative to the mean free path of the gas, ordinary diffusion through a porous medium may proceed via normal diffusion, Knudsen diffusion, or a process intermediate between these two extremes. As the pore size-mean free path ratio decreases, the diffusion process may undergo a transition from normal to Knudsen diffusion. The limiting values of the pore size-mean free path ratio corresponding to the transition region have not been well defined (5). For a counterdiffusion process, the value of the ratio of the diffusion fluxes must be known in

order to characterize the process completely. This quantity has been the subject of much controversy and is now considered to depend on the magnitude of the pore size relative to the mean free path (6, 7).

During the drying of a fiber bed, the amount of liquid in the bed is progressively reduced. It is well known that as a fiber bed is desaturated, liquid is removed from void spaces that are progressively smaller in size. Therefore, the ordinary diffusion mechanism may vary with degree of saturation*.

Aside from the effect of pore size on the diffusion mechanism, the over-all effect of the complex geometry of a porous medium is to make the medium seem much thicker with respect to diffusion than an equally thick free space. This effect is generally analyzed in terms of an effective diffusion coefficient. The approaches used have been primarily empirical in nature. In general, most studies have been made with two-phase (solid-gas) porous media composed of granular particles. Studies concerned with fibrous networks and/or three-phase systems (solid-liquid-gas) are virtually nonexistent. Introduction of a liquid phase into a porous medium will appreciably alter the geometry of the gas-filled pores, and the results of investigations on two-phase systems will not, in general, be applicable to three-phase systems (8).

The specific objectives of this thesis were (1) to determine the mechanisms governing the process of gaseous ordinary diffusion through fiber beds at varying degrees of saturation, and (2) to evaluate the effect of varying the saturation of the fiber bed on the diffusion resistance.

*Degree of saturation is the fraction of the void volume occupied by liquid.

For the hot surface drying of fiber beds, the ordinary diffusion process will be complicated by the effects of temperature, pressure, and moisture gradients, adsorption phenomena, liquid movement, and condensation and evaporation processes. Therefore, the use of a drying system would not permit a precise evaluation of the ordinary diffusion process. The use of water as the saturant presents additional experimental problems because of its high volatility.

By means of an open system and under conditions of uniform temperature and pressure, steady-state measurements of gaseous ordinary counterdiffusion were made with fiber beds partially saturated with a nonvolatile liquid (dioctyl phthalate). Additional considerations led to the use of beds of nylon fibers, rather than wood pulp fibers, and carbon dioxide and nitrogen as the gas system, rather than water vapor and air.

To a certain extent this investigation was phenomenological in nature. The characterization of the observed diffusion process was based on certain aspects of the kinetic theory of gases, momentum transport theory, and relevant mass transport phenomena. Because of the extreme complexity of partially saturated fibrous structures, the evaluation of the effects of the liquid phase on the diffusion resistance was best made empirically at the present time. The fundamental analysis of the diffusion process and the empirical evaluation of the ordinary diffusion resistance elucidate the effects of partially saturated fiber beds on the process of gaseous diffusion. The results of this study provide also for a more knowledgeable analysis of the transport of water vapor in a drying system and a framework for future studies concerned with this phenomenon.

ORDINARY DIFFUSION THEORY

In the following discussion, the theories pertinent to the ordinary diffusion of gases in porous media are presented. Specifically, the steady-state counterdiffusion of two ideal gases, A and B, under conditions of uniform temperature and pressure in an open system is considered. This discussion will be limited to diffusion in the gas phase only. Transport due to the motion of adsorbed gas molecules is neglected.

The case important to this study is that of a one-dimensional diffusion along the z-direction. For this situation, the mechanisms governing the ordinary counterdiffusion of Gases A and B in a porous medium are the exchange of z-momentum resulting from collisions of unlike molecules and that due to molecule-wall collisions (9). Viscous shearing stresses are negligible. The relative significance of these two mechanisms depends on the magnitude of the pore size relative to the mean free path of the gas molecules.

If the pore size is much greater than the mean free path, intermolecular collisions will be the limiting mechanism. This process is referred to as normal or bulk diffusion. When the pore size is much smaller than the mean free path, the limiting mechanism will be the molecule-wall collisions. Diffusion of this type is referred to as Knudsen diffusion or free-molecule flow. Between these two extremes, the transport process, referred to as intermediate diffusion, will be controlled by both intermolecular and molecule-wall collisions.

Each of the above diffusion processes can be described analytically by expressions relating a characteristic diffusion coefficient to experimentally measurable diffusion fluxes and driving forces. A fundamental development of these equations is based on the momentum-transfer method of Maxwell and Stefan. This method was reviewed by Present (9) for the case of normal diffusion; it

will be discussed here in regard to intermediate diffusion. The momentum-transfer developments of the normal and Knudsen diffusion equations are embodied in the derivation of the intermediate diffusion equation (7, 10).

Diffusion coefficients for normal and Knudsen diffusion will be defined in terms of established relations between the flux vector and the concentration gradient. For purposes of orientation and definition of terms, it is convenient to consider first the diffusion of gases in capillary tubes. Some terms are then redefined in order to apply the equations for diffusion through capillary tubes to porous media. In this regard, particular attention should be paid to both the units and the reference frame used for the diffusion flux.

NORMAL DIFFUSION

For the normal diffusion of Gas A in a binary mixture of A and B, the transport of Gas A is governed solely by the exchange of z-momentum between Gas A and Gas B. The z-momentum communicated to the walls can be neglected, as far as the resistance to diffusion is concerned. Equation (1), which is a form of Fick's first law of diffusion (11), defines the normal diffusion coefficient.

$$\vec{J}_A^* = -cD_{AB} \nabla y_A \qquad (1).$$

$\vec{J}_A^*$ is the molar flux of A relative to the molar average velocity $\vec{v}^*$, c is the molar density of the gas mixture, y_A is the mole fraction of A, and D_{AB} is the normal diffusion coefficient. This coefficient will be referred to as the true normal diffusion coefficient to distinguish it from the effective coefficient which will be used in regard to porous media. To a first approximation, D_{AB} is given in terms of molecular quantities by the following Chapman-Enskog formula (12):

$$D_{AB} = 0.001858 \left[T^3(1/M_A + 1/M_B)\right]^{1/2} / (P\sigma_{AB}^2 \Omega_{D,AB}) \qquad (2);$$

where T is the absolute temperature, M_A and M_B are molecular weights, P is the total pressure, σ_{AB} is the collision diameter, and $\Omega_{D,AB}$ is the so-called collision integral for diffusion. D_{AB} is independent of the composition of a mixture of gases, and it should be noted that it is inversely proportional to pressure.

For this study, it is desirable to relate D_{AB} to the molar flux relative to stationary co-ordinates, $\vec{N}_A$. $\vec{J}_A^*$ is defined by the following expression (11):

$$\vec{J}_A^* = c_A (\vec{v}_A - \vec{v}^*) \qquad (3).$$

where c_A is the molar concentration of A, $\vec{v}_A$ is its diffusion velocity with respect to stationary co-ordinates (11), and

$$\vec{v}^* = (c_A\vec{v}_A + c_B\vec{v}_B)/c \qquad (4).$$

$\vec{N}_A$ is defined by (11)

$$\vec{N}_A = c_A\vec{v}_A \qquad (5).$$

Combination of Equations (1), (3), (4), and (5) leads to the desired relationship.

$$\vec{N}_A - y_A(\vec{N}_A + \vec{N}_B) = -cD_{AB} \nabla y_A \qquad (6).$$

In binary counterdiffusion, the flux vectors $\vec{N}_A$ and $\vec{N}_B$ at a given point are directed along the same line but in opposite directions.

The flux ratio r_{AB} is defined as the ratio of the magnitude of the fluxes and is taken to be negative for counterdiffusion.

$$r_{AB} = N_B/N_A \qquad (7).$$

For one-dimensional diffusion along the z-direction, Equation (6) reduces to

$$N_A = -cD_{AB}(\partial y_A/\partial z)/(1 - \alpha y_A) \qquad (8),$$

where $\alpha = 1 + \underline{\underline{r}}_{AB}$. In the development of Equation (8), it is assumed that the concentrations and diffusion velocities are functions of the axial co-ordinates only and that transverse diffusion velocities are negligible.

For a partially saturated porous medium, Equation (8) would be applicable at a given point in the gas phase. However, to apply this equation at a given plane in such a medium, accurate allowance must be made for the effects of the solid particles and the liquid phase on the geometry of the void space. At the present time, this is not possible. To circumvent this problem, the molar flux can be based on the over-all cross-sectional area of the porous medium, and Equation (8) can be written in the form:

$$N_A = -c(D_{AB})_e(\partial y_A/\partial z)/(1 - \alpha y_A) \qquad (9).$$

$(\underline{\underline{D}}_{AB})_{\underline{e}}$ is the effective normal diffusion coefficient and embodies all of the structural effects of the porous medium on the diffusion resistance, as well as the molecular properties of the gases. It represents the diffusion rate per unit over-all area per (unit driving force/unit medium length).

Since $\underline{c}$ is the moles of gas mixture per unit volume of gas, $\underline{N}_A$ in Equation (9) should be based on the void area. However, the fraction of the total area which is void area is not accurately known, especially for a partially saturated porous medium. Therefore, this factor also is embodied in the effective normal diffusion coefficient.

By the law of conservation of mass, $\underline{N}_A$ and $\underline{\underline{r}}_{AB}$ are independent of $\underline{z}$. Since the temperature and total pressure are uniform, $\underline{c}$ is constant. Integration of

Equation (9) from $z=0$ to $z=L$ leads to

$$N_A = \left[(D_{AB})_e P/(\alpha RTL)\right] \ln \left[(1 - \alpha y_{AL})/(1 - \alpha y_{AO})\right] \qquad (10),$$

where L is the thickness of the porous medium, and R is the gas constant.

KNUDSEN DIFFUSION

Knudsen diffusion of Gas A will be governed almost entirely by collisions of the gas molecules with the walls and is practically unaffected by intermolecular collisions (9). For a binary gas mixture, the component gases will diffuse through a porous medium independently of each other. The treatments of free-molecule flow, the momentum-transfer method and the so-called diffusion method, depend, among other things, upon a knowledge of the effect of molecule-wall collisions on the path of the molecule. Both methods lead to essentially the same expressions for the diffusion flux. The momentum-transfer method is discussed below in relation to intermediate diffusion. The diffusion treatment will be discussed briefly here.

Since most wall surfaces are highly irregular on the molecular scale, the direction of reflection of a molecule from the wall would be expected to bear little if any relation to the direction of incidence. As pointed out by Present (9), this would be the case if the molecule were temporarily adsorbed and later evaporated. Available evidence (6, 9, 13) supports this concept of diffuse reflection. For this case, the reflected molecules have a Maxwellian distribution of speeds corresponding to the temperature of the wall.

With the concept of diffuse reflection as a basis, the diffusion treatment of free-molecule flow consists of developing an expression for the number of molecules crossing a given section of a long capillary tube due to reflection

from an element of surface of the tube wall. For one-dimensional diffusion of Gas A along the z-direction in a capillary tube, the resulting expression for the diffusion flux defines a Knudsen diffusion coefficient (14).

$$N_A = -cD_{KA}(\partial y_A/\partial z) \qquad (11).$$

D_{KA} is the "true" Knudsen diffusion coefficient and is given by the expression (14)

$$D_{KA} = (2/3)\bar{u}_A R_T \qquad (12),$$

where $\bar{u}_A$ is the mean molecular speed of A, and R_T is the radius of the capillary tube. As defined above, the Knudsen diffusion coefficient is independent of both gas concentration and total pressure.

For a porous medium, integration of Equation (11) yields

$$N_A = \left[(D_{KA})_e P/(RTL)\right](y_{AO} - y_{AL}) \qquad (13),$$

where $(D_{KA})_e$ is the effective Knudsen diffusion coefficient. As before, N_A is based on the over-all cross-sectional area of the porous medium.

INTERMEDIATE DIFFUSION

When the effective pore size of a porous medium is approximately equal to the mean free path of the gas molecules, the nature of the diffusion process will be intermediate between that of normal diffusion and that of Knudsen diffusion. Qualitatively, this region of intermediate diffusion has been considered to extend over a hundredfold range of values of the pore size-mean free path ratio (0.1 to 10). However, it now appears that the upper limit of this range is much larger than ten (5).

In this region both molecule-wall collisions and intermolecular collisions will govern the diffusion resistance. The momentum-transfer treatment of intermediate diffusion must account for both mechanisms of momentum exchange. This method was utilized by Scott and Dullien (5) and by Rothfeld (10) with apparent success and will be discussed here. As before, one-dimensional diffusion of Gas A in a binary mixture of A and B along the z-direction will be considered.

The momentum-transfer method of treating diffusion is based on the concept of the pressure as the flux of momentum across a plane. Rothfeld (15) rigorously analyzed this problem in terms of the kinetic theory of gases. Assuming that the diffusion velocities were very small compared to the mean molecular speeds of the gases, i.e., $v_A \ll \bar{u}_A$, Rothfeld showed that the partial pressure of a species in a nonuniform multicomponent gas is equal to the flux of normal momentum carried by that species across a fixed plane. In counterdiffusion experiments, it is generally the case that $v_A \ll \bar{u}_A$ (16).

For steady ordinary counterdiffusion of Gases A and B in a capillary tube, a momentum balance for the molecules of Type A between two parallel planes perpendicular to the z-axis separated by a distance dz may be written as (15)

$$-dp_A/dz = M_{AB} + (2/R_T)M_{Aw} \qquad (14),$$

where p_A is the partial pressure of A, M_{Aw} is the axial momentum lost by Species A per unit time by collisions with the wall per unit area, and M_{AB} is the axial momentum lost by Species A per unit time per unit volume by collisions with Species B.

Providing that $v_A \ll \bar{u}_A$, M_{Aw} and M_{AB} may be readily evaluated for the limiting cases of Knudsen and normal diffusion, respectively. For these cases, the Maxwell distribution law is applicable in a form modified for the translational

motion of the whole gas and corrected for the presence of the second gas and the nonuniform composition of the mixture (16). On this basis, an expression for $\underline{\underline{M}}_{Aw}$ at the limit of Knudsen diffusion was developed by Pollard and Present (14). Similarly, Present (16) derived an expression for $\underline{\underline{M}}_{AB}$ at the limit of normal diffusion.

Assuming that these limiting expressions for the momentum transport processes were applicable to the intermediate region of diffusion, Rothfeld (10) and Scott and Dullien (5) developed an intermediate diffusion equation. The details of a derivation of this equation similar to that of the latter workers are outlined in Appendix I. As applied to a porous medium, the integrated expression for the intermediate diffusion flux of Gas A is

$$N_A = \left[(D_{AB})_e P/(\alpha RTL)\right] \ln \left[\frac{(1 - \alpha y_{AL}) + (D_{AB})_e/(D_{KA})_e}{(1 - \alpha y_{AO}) + (D_{AB})_e/(D_{KA})_e}\right] \qquad (15).$$

Investigations of steady, ordinary counterdiffusion of gases through consolidated porous media were made by Scott and Dullien (5) and by Rothfeld (10). Their measurements were well within the intermediate region of diffusion. Excellent agreement was obtained between experimental values of the diffusion fluxes and values calculated by means of equations equivalent to Equation (15).

Various definitions of a diffusion coefficient for the intermediate region of diffusion have been proposed or developed (5, 17). The definition which appears to be in agreement with several theoretical developments and the limited experimental data available is the Bosanquet interpolation formula (6, 10, 14).

$$1/(D_{NA})_e = 1/(D_{AB})_e + 1/(D_{KA})_e \qquad (16).$$

$(\underline{\underline{D}}_{NA})_e$ is the effective intermediate diffusion coefficient. The Bosanquet interpolation formula was developed originally from a random-walk description of diffusion (14).

THE FLUX RATIO

In order to determine effective normal diffusion coefficients from steady counterdiffusion experiments in an open system, both diffusion fluxes must be known. Measurements of both fluxes may generally be made quite readily. When only one flux is or can be measured, it is necessary to assume a relation between $\underline{N}_A$ and $\underline{N}_B$. In the past, it was frequently assumed that

$$N_A = -N_B \tag{17}$$

for normal diffusion (9, 18). This assumption appears to be valid for counterdiffusion in a closed system only (6). For steady, ordinary counterdiffusion in an open system, equimolal counterdiffusion has not been observed.

Unfortunately, the assumption of equimolal counterdiffusion has led to some confusion in the literature. The flux ratio was used frequently as a criterion for differentiating between normal and Knudsen diffusion. By means of Equations (12) and (13) for Knudsen diffusion and the fact that $\underline{\bar{u}}_A/\underline{\bar{u}}_B = (\underline{M}_B/\underline{M}_A)^{1/2}$, it can be shown that

$$N_B/N_A = -(M_A/M_B)^{1/2} \tag{18}.$$

When the flux ratio was found to satisfy Equation (18), it was often concluded that Knudsen diffusion was taking place. However, use of the flux ratio as a criterion for choosing the diffusion mechanism no longer appears valid.

From momentum-transfer arguments, Hoogschagen (19) asserted that Equation (18) should apply throughout the entire range of ordinary diffusion from Knudsen diffusion to and including normal diffusion. Later, the same conclusion was reached by Evans, et al. (6) from their "dusty gas"-model treatment of diffusion. Experimental verification of this hypothesis has been reported by several

investigators from their measurements of steady counterdiffusion through various consolidated porous media.

Although his data were far outside the region of Knudsen diffusion, Hoogschagen (19) found that the flux ratio was equal to the value predicted by Equation (18). Similar findings were reported by Scott and Cox (20) and Evans, et al. (6, 21) for the region of normal diffusion. Hoogschagen's hypothesis has been supported also by Scott and Dullien (5), by Rothfeld (10), and by Robertson and Smith (22) whose measurements were well within the intermediate region of diffusion.

Theoretically, the ratio of the diffusion fluxes is related to the collisions of the gas molecules with the walls of the porous structure and the momentum exchange resulting from these collisions (7, 19). This appears to be the case even for normal diffusion, for which molecule-wall collisions do not contribute significantly to the diffusion resistance. In his development of Equation (18), Hoogschagen considered steady isothermal counterdiffusion in a cylindrical tube with the gas molecules diffusely reflected after colliding with the walls. He assumed also that the diffusion velocities and mean molecular speeds of the gases were independent of radial position.

As indicated in Appendix II, in the absence of total pressure gradients and surface transport, the net axial momentum transferred to the walls is approximately zero for the above process. Under the assumption of diffuse reflection, the average axial momentum carried off by a given species after impact with the wall is zero. From the kinetic theory of gases, it has been shown (14) that the average axial momentum transferred to the wall per unit area per unit time by Species A, $\underline{\underline{M}}_{Aw}$, is for unidirectional diffusion

$$M_{Aw} = (n_A \bar{u}_A / 4)\,(m_A v_A) \qquad (19),$$

where n_A and m_A are the molecular concentration and molecular mass of Species A, respectively.

In terms of molar quantities, Equation (19) becomes

$$M_{Aw} = N_A \bar{u}_A M_A / 4 \qquad (20).$$

Since the net axial momentum transferred to the pore walls is zero,

$$N_A \bar{u}_A M_A / 4 + N_B \bar{u}_B M_B / 4 = 0 \qquad (21).$$

Equation (18) is obtained directly from Equation (21) since the mean molecular speed is inversely proportional to the square root of the molecular weight.

The weakest assumption in the above development is that of the radial independence of the diffusion velocities. In the intermediate and normal diffusion regions, velocity gradients would lead to additional momentum transfer. Dullien and Scott (7) have shown that this assumption cannot be rigorously true. On the other hand, they have shown that the radial variation of the diffusion velocities is negligibly small when the pore size is much less than one centimeter. The essence of their treatment of this problem is included in Appendix II.

As the pore size becomes larger and larger with respect to the mean free path of the gas molecules, Evans, et al. (6) have indicated that the flux ratio should depart from the value predicted by Equation (18). On the basis of negligible molecule-wall collisions, McCarty and Mason (23) showed, from the one-dimensional equations of motion and continuity of the gas, that the mass average velocity of the gas is zero. For a binary gas mixture, the mass average velocity, v, is defined as (11)

$$v = (\rho_A v_A + \rho_B v_B)/\rho \qquad (22),$$

where ρ is the mass density of the gas mixture and ρ_A and ρ_B are the mass concentrations of Species A and B, respectively. With $\underline{v} = 0$, Equation (22) leads to

$$N_B/N_A = -M_A/M_B \qquad (23).$$

Equation (23) probably represents an unattainable limiting case in practice. Results of experiments with capillaries of diameters of a few tenths of a millimeter were reported (6) to have given flux ratios intermediate between the values represented by Equations (18) and (23).

Until recently, the effect of varying the pore size on the flux ratio had been neglected. Using the fundamental principles of fluid mechanics and the kinetic theory of gases, Dullien and Scott (7) analyzed this problem. They considered the steady-state normal counterdiffusion of two ideal gases at constant total pressure and temperature through a cylindrical capillary in an open system. The details of this development are presented in Appendix II. As a result of their analysis, Dullien and Scott found that

$$(M_A/M_B)^{1/2} < \left| N_B/N_A \right| < (M_A/M_B) \qquad (24),$$

where $(\underline{M}_A/\underline{M}_B) > 1$. They showed further that as the pore size approached zero the flux ratio would approach $-(\underline{M}_A/\underline{M}_B)^{1/2}$, and as the pore size became larger the flux ratio would depart from this value and approach $-(\underline{M}_A/\underline{M}_B)$. Qualitatively, the results of this analysis would be expected to apply also to porous media.

In summary, for the steady ordinary counterdiffusion of gases under uniform pressure and temperature conditions through a porous medium, the flux ratio may have a value within the limits given by Equation (24). For small pores, the flux ratio will be approximately equal to $-(\underline{M}_A/\underline{M}_B)^{1/2}$ for normal, intermediate, and

Knudsen diffusion. In the normal region of diffusion, as the pore size increases the flux ratio will depart from that value and approach $-(\underline{M}_A/\underline{M}_B)$. This transition appears to be related to a decrease in the molecule-wall collisions. The pore size-mean free path ratio corresponding to this transition has not been defined, as of now.

DIFFUSION RESISTANCE OF POROUS MEDIA

Aside from the effects of pore size on the diffusion mechanism, the net effects of the complex geometry of a porous medium is manifested in a reduction of the rate of diffusion as compared with the rate through an equivalent free space. In general, the following factors are considered to be the structural characteristics of porous media primarily responsible for this effect: (1) the reduced area of available cross section, (2) the tortuosity of the paths through the medium, (3) constrictions along the pore length, and (4) dead-end pores, i.e., gas-filled pores through which diffusion does not take place. Although less explicitly than the above factors, the type and degree of interconnection of pores appear to have a bearing on the effects of porous media on the diffusion resistance (24, 25).

The relative importance of each of these factors will depend upon the particular type of porous medium involved. In this regard, there appear to be basic differences between consolidated and unconsolidated media and also a dependence on the shape of the particles composing the medium. There appears to be additional differences between two-phase systems (solid-gas) and three-phase systems (solid-liquid-gas).

Consolidated media appear to exhibit much higher resistances to diffusion than unconsolidated media. The higher resistances of consolidated media have been attributed to pore constrictions and dead-end pores (8). However, Rothfeld (10) has contended, justifiably so, that these high resistances might be due, in part, to incorrect evaluations of the diffusion mechanism. Unconsolidated media, in the dry state, generally exhibit a totally interconnected pore structure. Therefore, little or no contribution of dead-end pores to the diffusion resistance of such media would be expected. Particle shape governs, to a large extent, the

pore shape, which will depend also on the packing of the particles and on the uniformity of the particle size. The Knudsen diffusion coefficient would be expected to be a relatively strong function of pore shape.

Introduction of a liquid into a porous medium will appreciably alter the geometry of the gas-filled pores and will presumably affect all of the above-mentioned pore structure characteristics.

It would be desirable to evaluate quantitatively the effects of each of these factors on the diffusion resistance independently of those of the molecular properties of the gases. Since this is presently not possible, the "true" diffusion coefficient has been related to the effective diffusion coefficient by empirical methods in terms of certain parameters which are presumed to be characteristic of the porous medium.

Most studies of gaseous diffusion through porous media have been made with dry, consolidated or unconsolidated, granular-type materials, such as catalyst pellets, porcelains, soils, and sands. Studies concerned with fibrous networks and/or three-phase systems are virtually nonexistent. Although there would probably be significant differences between diffusion in dry granular porous media and that in partially saturated fiber beds, the results of investigations on the former systems would certainly serve to orient analysis of the diffusion resistance of the latter systems.

Only those studies for which the diffusion mechanism was correctly evaluated will be considered. Unless otherwise noted, normal diffusion was the prevailing mechanism. Further insight into the effect of the structure of porous media on gaseous diffusion has been contributed by studies of electrical conduction. The equivalence of this process and normal diffusion has been relatively well verified

(5, 26, 27). Somewhat more indirectly, the results of gas and liquid permeability studies also have been instructive, particularly in regard to three-phase systems.

TWO-PHASE SYSTEMS

The difference between the true and the effective diffusion coefficients has been characterized in terms of porosity functions, functions of porosity and pore tortuosity, and functions of all of the above-mentioned structural characteristics of porous media.

POROSITY

The porosity, ϵ, of a porous material is that fraction of the over-all volume occupied by void space. Two classes of porosity have been defined, the absolute porosity, which was defined above, and the effective porosity (28). Effective porosity is that fraction of the geometric volume constituted by interconnecting pores. When a porous medium is composed of porous particles, it may be necessary to distinguish between the micropore porosity of the particles and the macropore porosity of the medium. Unless otherwise noted, future use of the word porosity should be taken to be indicative of interconnected macropores.

In assessing the influence of variations in porosity on the diffusion of gases through porous media, most investigators have correlated their data in terms of the diffusibility, δ, which has been defined as the ratio of the effective diffusion coefficient of the true diffusion coefficient* (19). The diffusibility is dependent only on the properties of the porous medium and appears to be independent of the type of ordinary diffusion taking place (5, 20).

*The true diffusion coefficient may be thought of as that coefficient obtained for the same process of diffusion through a straight tube whose radius is equivalent to that of the porous medium and is uniform along the length of the tube.

A variety of empirical diffusibility-porosity correlations have been presented. In all instances, however, the diffusibility decreased as the porosity decreased. In other words, the diffusion resistance increased with decreasing porosity.

Equations of the form

$$\delta = a\epsilon + b \qquad (25),$$

where $b \geq 0$, were obtained by several groups of investigators for a variety of dry, unconsolidated, granular-type porous materials of porosities less than about 0.8 (29-32). For similar types of materials, both consolidated and unconsolidated, other workers arrived at equations of the form

$$\delta = \epsilon^m \qquad (26),$$

where $m > 1$ (19, 27, 33-36).

The differences among the exact forms of the diffusibility-porosity correlations undoubtedly reflect the differences in the porous structure of the media used, as well as the differences in the changes of the porous structure brought about by the imposed porosity variations. The effect of the nature of the porous structure on the δ-ϵ relation is somewhat more evident in the limited number of expressions which have been developed theoretically.

Maxwell (37) considered the conduction of electricity in a bed of uniform spheres separated by distances large compared to their diameter. The expression resulting from his development may be written in the form

$$\delta = 2\epsilon/(3 - \epsilon) \qquad (27).$$

Rayleigh (38) indicated that this equation was applicable also to an array of spheres in cubic order. In general, experimental values of diffusibility were less than the values predicted by Maxwell's expression.

Bruggeman (39) extended Maxwell's treatment to a random distribution of uniform spheres and arrived at the expression

$$\delta = \epsilon^{1.5} \qquad (28).$$

From his treatment of gaseous diffusion in a model porous system, Millington (40) found that the diffusibility was proportional to the 4/3 power of the porosity. The model system consisted of solid spheres which interpenetrated one another, separated by spherical pores which also interpenetrated.

As suggested by Hashin and Shtrikman (41), Weissberg (42) formulated an expression for the effective diffusion coefficient of an idealized bed of spherical particles using a statistical approach. This type of treatment involves describing the random geometry of the pores in terms of certain statistical parameters. Bliesner (43) recently reviewed the application of such an approach to the permeability of porous media.

Weissberg considered a bed of spheres in which their centers were randomly situated without restricting the spheres to nonoverlapping locations. The resulting expression was applicable to such a system of spheres of both uniform and nonuniform sizes. The upper limit for the diffusibility was given as

$$\delta = \epsilon/(1 - \ln \epsilon/2) \qquad (29).$$

This expression was identical to Maxwell's formula, Equation (27), when $\epsilon \rightarrow 1$, to first order in $(1 - \epsilon)$. While Weissberg's expression represents an improvement

over Maxwell's equation, it still overestimates diffusibilities of real granular-type porous materials.

Conduction of electricity through an array of infinitely long cylinders was examined mathematically by Rayleigh (38). The cylinders were arranged in square order and the distance between cylinders was large relative to their diameter. Flow of electricity was perpendicular to the axes of the cylinders. Expressed in terms of the diffusibility, the equation derived by Rayleigh is

$$\delta = \epsilon/(2 - \epsilon) \qquad (30).$$

No applicable experimental data were available for evaluating the above equation. In view of the ideal nature of the system considered by Rayleigh, little agreement between Equation (30) and experimental observations would be expected.

The porosity of a porous medium is a macroscopic property which yields no information concerning the structure of the medium. Diffusibility-porosity correlations are in reality, therefore, indices of the variation with porosity of all of the structural parameters of a porous medium that affect the diffusion process. In this sense, such correlations mask the contribution of these parameters to the diffusion resistance of a particular medium.

It would, of course, be desirable to assess quantitatively the contribution of each of the pore structure parameters to the diffusion resistance. Such a task is difficult, to say the least. Nevertheless, some progress has been made in this direction and will be reviewed in the following section.

PORE TORTUOSITY, CONSTRICTIONS, AND INTERCONNECTIONS

In general, the pores of a porous medium are not straight. Therefore, the path length for diffusion will be greater than the thickness of the porous material.

The retarding influence of this increased path length on the diffusion rate is generally accounted for by a tortuosity factor, τ. In regard not only to gas diffusion but also to liquid and gas permeability, the tortuosity factor has been well established to be of major importance in accounting for the resistance presented by porous media to these processes (8). The tortuosity factor is a function of the ratio of some average pore length L_e to the thickness of the medium L. For electrical conduction and diffusion, it is generally considered that $\tau = L_e/L$ (8, 44).

Many investigators have referred to ϵ/δ as the tortuosity factor. Assuming that this is so, the diffusibility-porosity relationships indicate that the tortuosity factor may be independent of porosity or inversely proportional to some function of the porosity. Carman (8) has contended that a slow variation of the tortuosity factor with porosity seems more probable, since τ should approach unity as the porosity approaches unity. A summary of the results of gas diffusion and electrical conductivity experiments for dry unconsolidated beds of granular materials was presented by Carman. A gradual change of the tortuosity factor with porosity in the expected direction was indicated.

For dry, unconsolidated, granular porous materials, values of the tortuosity factor in the range of 1.4 to 3.0 have been reported (8). Physically, such values are quite reasonable. However, values ranging from ten to twenty have been cited for the so-called tortuosity factor of consolidated media (8). It seems highly unlikely that such values are physically meaningful.

In unconsolidated media, the fractional free area is uniform throughout the medium and equal to ϵ (8), particularly for media with a narrow pore size distribution. However, constrictions along the length of the pores would further reduce the diffusion rate since the fractional free area would be reduced by

such constrictions. Failure to account for this effect, where important, would lead to fictitiously high tortuosity factors. In recognition of the probable importance of pore constrictions, it appears no longer justifiable to refer to ϵ/δ as the tortuosity factor.

Introduction of the pore shape factor, P_s, into the diffusion equation has been used to indicate the contribution of pore constrictions to the diffusion resistance (26, 32, 45). Like the tortuosity factor, the pore shape factor is an empirical macroscopic parameter representative of the net effect on the diffusion resistance of a physically meaningful pore structure characteristic. The pore shape factor has been represented by the expression $P_s = A_e'/A_e$, where $A_e = \epsilon A$ and A_e' is an effective free cross-sectional area (32). Experimental attempts to assess quantitatively the effects of both pore constrictions and pore tortuosity have met with little success. Several workers have evaluated theoretically the effect of only pore constrictions on the diffusion resistance.

Peterson (46) treated, mathematically, the effect of periodic pore constrictions on the effective normal diffusion coefficient. The assumed pore model was a hyperbola of revolution giving a pore constriction at the vertex of the hyperbola. The rate of diffusion through this pore was compared with that through an equivalent cylindrical pore. Solutions of the steady-state normal diffusion equation were obtained for various values of the ratio of the maximum to the minimum cross section of the model pore. Considering only the effects of constrictions in the pore cross-sectional area, an expression was derived for the diffusibility. In this instance, the diffusibility would be the pore shape factor. For porosities greater than about 0.4, it was indicated that the pore shape factor would be unity.

From the geometry of model pore systems, Currie (32) calculated pore shape factors based on the expression $\underline{P}_s = \underline{A}'_e/\underline{A}_e$. An expression for $\underline{A}'_e$ was derived for a porous medium consisting of tubes for which the cross-sectional area varied sinusoidally. Various values of the ratio of maximum to minimum cross-sectional area were considered. $\underline{A}_e$ was calculated for a system of straight tubes of cross section corresponding to a volume equal to that of a given sinusoidal tube. Pore shape factors for this model ranged from 1.0 to 0.218 for ratios of maximum to minimum cross section ranging from 1.0 to 100.

When both pore tortuosity and pore constrictions are important to the diffusion resistance, quantitative evaluation of each of these factors has not yet been achieved. Qualitatively, however, it may be possible to evaluate the relative importance of these factors if ϵ, τ, and $\underline{P}_s$ can be related to the diffusibility. Assuming, for the present, that dead-end pores are absent and that pore interconnections do not significantly affect the diffusion resistance, a simplified relationship between the above parameters can be deduced from purely geometric considerations (32, 46).

As defined by Equation (10), the effective normal diffusion coefficient represents the diffusion rate per unit over-all area per (unit driving force/unit medium length). Similarly, the true coefficient would represent the diffusion rate per unit void area per (unit driving force/unit void length). In terms of the net characterizations of the dimensions of the pore space of a porous medium, the true diffusion coefficient can be related to the effective coefficient by the expression

$$(D_{AB})_e/D_{AB} = \delta = \epsilon P_s/\tau \qquad (31).$$

When the porous medium contains dead-end pores, the effective porosity ϵ_F is used instead of the absolute porosity ϵ. While the exact nature of the effects of

pore interconnections on the diffusion resistance is somewhat uncertain, the type and degree of pore interconnections do appear to be important to the dynamic properties of porous media.

Using the model of interpenetrating solid spheres and interpenetrating spherical pores referred to previously, Millington and Quirk (48) analyzed the pore area resulting from such an interaction model of a porous medium. They concluded that the fractional pore area resulting from interaction would be between ϵ and ϵ^2 since part of ϵ itself would be the resultant of pore interaction. It was further concluded that the minimum fractional pore area for this model system would be approximately $\epsilon^{4/3}$.

Fatt (24) and later Rose (25) considered the problem of pore interconnections in terms of various network models of porous media. "A network model may be defined as the mathematical representation of a system of interconnected pore spaces in which there is an element of point-to-point identity with the reservoir (real) prototype as regards pore shapes, lengths, widths, and orientation" (25). The models consisted of cylindrical tubes of various sizes interconnected according to regular geometric patterns.

For convenience of manipulation, Fatt found it necessary to reduce three-dimensional network models to two dimensions. Fatt stated that "This is equivalent to assuming that the change produced by making the porous medium thin, and thereby eliminating a number of cross-connections in the third dimension, may be compensated by introducing additional channels within the two-dimensional network." Several regular geometric networks were considered and each one was characterized by only a single parameter referred to as the β-factor. The β-factor is the number of tubes connected to each tube in the network.

Using analog computer methods, Fatt investigated the effects of network type and tube size distribution on the capillary pressure curves and dynamic properties of the models. In all cases, the predicted capillary pressure curves were similar to those observed for real porous media and were determined largely by the assumed tube size distribution. Unless the tube size distribution was extremely broad, the model network structure did not influence the shape of the capillary pressure curves.

In relation to the dynamic properties of porous media, such as permeability and electrical resistivity, Fatt's studies showed that these properties were strongly influenced by the network structure assumed and were affected relatively little by the tube size distribution. In other words, the dynamic properties of the network models were determined primarily by the branching and interconnecting of the tubes in the models. Recently, Bliesner (43) studied the porous structure of fibrous sheets using permeability techniques. He found that ".... the pore size distribution of a sheet of paper (as measured by the gas-drive technique) has relatively little effect on the permeability properties of the sheet over the range of pore size distribution studied."

Fatt's work was extended to three-dimensional network models by Rose (25). In addition to the β-factor, the path characterization number was used to describe the network structure. The path characterization number defines the possible number of single, double, triple, and quadruple pore path interconnections between adjacent mesh points in the network. Mesh points represent the relative positions of pore interconnections. Rose introduced the concept of assigning zero pore sizes to some of the tubes in the three-dimensional model. The effect of this was to reduce the β-factor and alter the path characterization number. In this way, Fatt's two-dimensional models could be simulated.

Among other things, Rose's analysis emphasized the importance of the pore tortuosity concept and indicated the effect of pore interconnections on the tortuosity. In this regard, Rose pointed out that network form, type and degree of pore interconnection, and pore size distribution will determine the tortuous path followed during the transport of a fluid through a porous medium. Rose stated:

> As the distribution of pore sizes is broadened, however, tortuosity should increase for all network forms when these various pore sizes are randomly distributed in space. This is because it is likely that the most conductive paths through the randomly located larger pores will tend not to be the shortest-distance paths. Likewise, decreasing the β-factor and/or the path characterization number....will also cause the tortuosity to be increased.

An adequate evaluation of the diffusion resistance of a porous medium must certainly include the effects of pore interconnections. Concerning the area of a porous medium available for diffusion, the effect of pore interconnections is such that the fractional free area may be more correctly represented by $\epsilon^{\underline{m}}$ rather than by ϵ, where $\underline{m}$ is greater than unity. Externally or internally induced changes in the structure of a porous medium will generally affect the tortuosity factor. An evaluation of the change in τ must consider the related factors of pore branches and interconnections. In real porous media, increasing the type and degree of pore interconnections does not necessarily require that the altered or additional pore paths be less tortuous than the previous ones.

It appears that an improved representation of the diffusibility in terms of the pore structure parameters used before would be

$$\delta = \epsilon^{m} P_s/\tau \qquad (32).$$

Unfortunately, at present, there appear to be no satisfactory methods for characterizing the various facets of the structure of pores within porous materials.

Nevertheless, use of the diffusibility will permit some insight into the effects of porous media and associated variables on the diffusion of gases through such materials.

THREE-PHASE SYSTEMS

The resistance to diffusion through three-phase porous systems will be affected by all of the pore structure characteristics discussed above. In addition, the distribution of the liquid phase and its effect on these characteristics must be considered. Porous media partially saturated with a liquid wetting phase and a gaseous nonwetting phase will be the three-phase systems considered here.

According to basic capillary theory, the wetting liquid in a partially saturated porous medium will distribute itself in the smallest pores and crevices in a way such that all of the liquid-gas interfaces will have the same curvature. Real porous media, including fiber beds, have a distribution of pore sizes. As a completely saturated medium is desaturated, liquid is removed from void spaces which are progressively smaller in size, and the curvature of all of the liquid-gas interfaces increases.

Three regimes of saturation have been distinguished (28). In the saturation regime, all of the voids of the medium are completely filled with liquid. When gas permeates the medium, the funicular regime is entered, in which the liquid phase is a continuous network of interconnected channels. Over most of this regime, the gas phase will be continuous also. In the pendular regime of saturation, the liquid phase is no longer continuous and is retained in discrete isolated pockets throughout the porous medium. For beds of glass fibers, the pendular regime was observed to occur at a degree of saturation with respect to water of about 2% (49). In sand beds and sandstone, it occurred at degrees of saturation

of about 10% and 30%, respectively (8). The present discussion will be concerned primarily with the funicular regime of saturation.

Assuming that the liquid is uniformly distributed throughout the medium, the absolute fraction of the void volume occupied by gas at any section in the medium will be (1-s). The fraction of the void volume representing free area for diffusion may be less than (1-s) due to the effects of probable pore interaction and dead-end pores.

In dry unconsolidated porous media, such as beds of glass, nylon, etc. fibers, the occurrence of dead-end pores seems highly improbable. The probability of their occurrence might be expected to increase when such media are partially saturated with a liquid phase. By virtue of the distribution of pore sizes in real porous materials, it is highly plausible that some of the gas-filled pores of a partially saturated medium may not be part of a continuous gas-flow channel. Therefore, in regard to transport of the gases, such pores would, in effect, be dead-end pores.

Concerning pore tortuosity of partially saturated porous media, Carman (8) has pointed out that the wetting phase has the effect of increasing the tortuosity of the channel system occupied by the nonwetting phase. As a partially saturated porous medium is progressively desaturated, the effective pore size decreases and the pore size distribution will, in effect, become broader. When the various pore sizes are randomly distributed, it has been indicated by Rose (25) that the tortuosity should increase as the distribution of pore sizes becomes broader.

In addition, an increase in the tortuosity factor with decreasing degree of saturation has been associated with the fact that during desaturation the wetting

liquid retreats into the smaller void spaces and smaller crevices. Likewise, the radius of curvature of the liquid-gas interfaces decreases. It has been reasoned that fluid following in the crevices and small pores will travel a more tortuous path than fluid flowing through the large pores (28).

Parker (49) determined capillary pressure-saturation curves for beds of 3-micron diameter glass fibers partially saturated with water. In terms of hydraulic radius concepts, his data indicated less than a twofold change in effective pore radius as the degree of saturation decreased from about 0.7 to 0.1. This type of behavior appears to be characteristic of unconsolidated porous materials (24). For such materials, the difference between effective pore sizes from one degree of saturation to another will decrease as the degree of saturation decreases. Therefore, the contribution of pore constrictions to the diffusion resistance would very probably decrease with decreasing degree of saturation.

In his network model studies, Fatt (24) considered primarily porous media partially saturated with a liquid wetting phase. The nonwetting phase was either a gas or a second liquid immiscible with the first. His analyses of the dynamic properties of such media were concerned chiefly with the relative permeability and relative resistivity of the wetting phase. The relative resistivity is defined as the ratio of the resistivity of the porous medium at a given degree of saturation of the conducting phase to the resistivity of the medium completely saturated with the conducting phase. The relative permeability is similarly defined. Both of these characteristics were found to be determined almost entirely by the branching and interconnecting of tubes in the model, with the pore size distribution having little or no effect. Experimentally observed curves of these characteristics versus wetting-phase degree of saturation were quite similar to the derived curves.

To a limited extent, Fatt analyzed the behavior of the nonwetting-phase relative resistivity in terms of network models. Conclusions like the ones for the wetting phase were applicable. Unfortunately, no experimental data were available for comparison with the theoretical results.

For all of the models studied, the nonwetting-phase relative resistivity increased as the nonwetting-phase degree of saturation, (1-s), decreased. On a logarithmic scale, all of the curves were linear over a portion of the saturation range (10-100%) but deviated from linearity below a certain value of (1-s). This transition did not appear to correspond to a change in saturation regime. With increasing β-factor, the extent of the linear region of the curves increased, and the absolute values of the slopes of the curves decreased. These curves are shown in Fig. 1, and the corresponding network models are shown in Fig. 2.

Assuming that the equivalence of electrical conduction and gaseous diffusion in two-phase porous media can be extended to three-phase systems, the results of Fatt's studies of the nonwetting-phase relative resistivity can be treated in terms of diffusibility. The nonwetting-phase relative resistivity would be equivalent to the ratio of the diffusibility of a dry porous medium to the diffusibility of the medium partially saturated to some degree s. In view of Fatt's results, the reciprocal diffusibility of a partially saturated porous medium would be expected to increase as (1-s) decreased. In other words, the diffusion resistance of such a medium would be expected to decrease as s, the wetting-phase degree of saturation, decreased.

From immiscible two-phase flow studies, the nonwetting-phase relative permeability has been found to increase as the wetting-phase degree of saturation decreased (8). In general, these curves were S-shaped. As pointed out by Carman

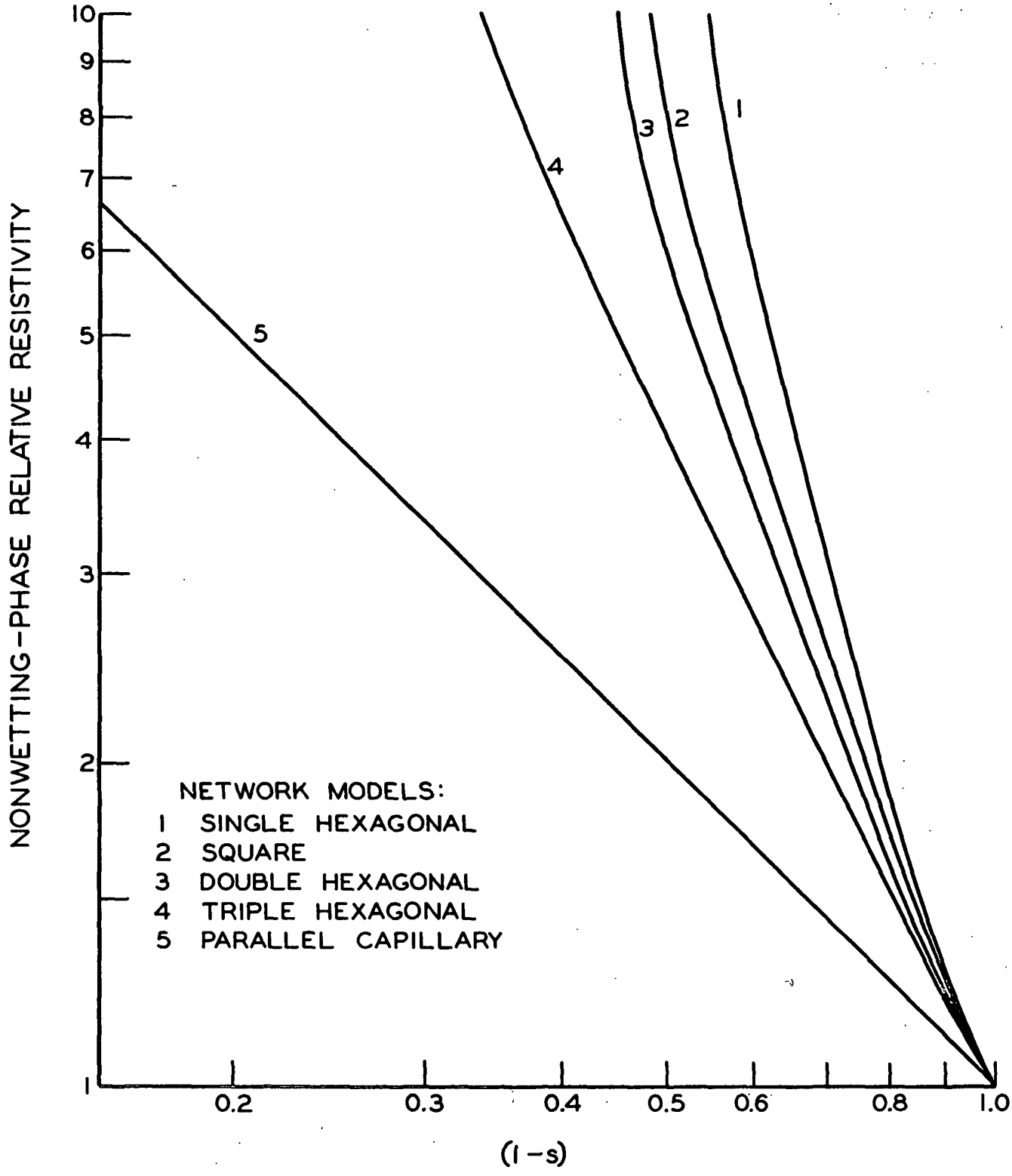

Figure 1. Relative Resistivity Curves Derived by Fatt (24)

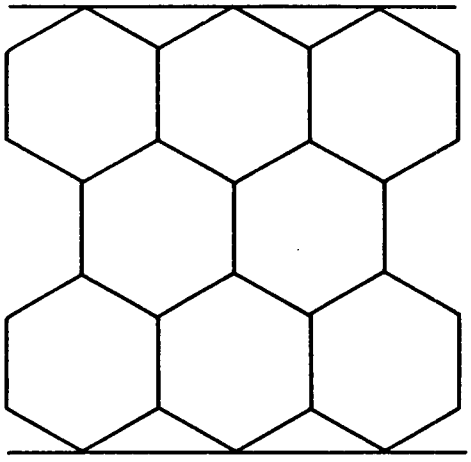

SINGLE HEXAGONAL NETWORK

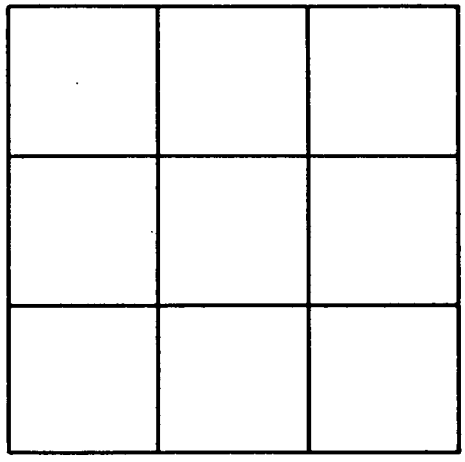

SQUARE NETWORK

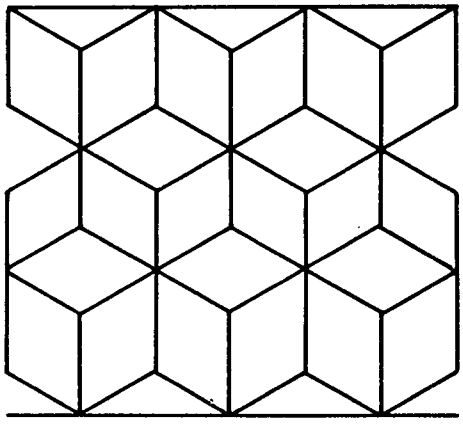

DOUBLE HEXAGONAL NETWORK

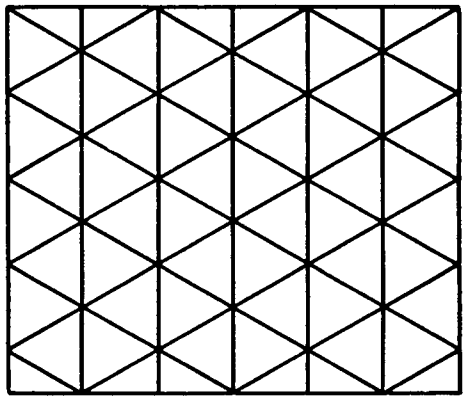

TRIPLE HEXAGONAL NETWORK

Figure 2. Network Models Studied by Fatt (24)

(8), the relative permeability appeared quite sensitive to pore structure. These observations lend support to the preceding arguments.

For partially saturated porous media, Equation (32) must be modified to account for the liquid present. Since the degree of saturation, s, is based on the absolute void volume, the absolute fraction of the total volume of a porous medium occupied by gas will be $\epsilon(1-s)$. Because the effects of pore interaction and dead-end pores may be significant, an improved expression for this property would be $\epsilon(1-s)^n$, where $n > 1$. Considering the results of Fatt's network studies, the exponent n may be a function of s and would be expected to be characteristic of the particular medium studied. In terms of the geometric model used previously, for a partially saturated porous medium

$$\delta = \epsilon(1-s)^n(P_s/\tau) \qquad (33).$$

EXPERIMENTAL EQUIPMENT AND TECHNIQUES

PRELIMINARY CONSIDERATIONS

As indicated previously, the complexly interrelated phenomena occurring during the drying of fiber beds inhibited the use of a drying system for studying clearly the ordinary diffusion of gases in partially saturated fiber beds.

DIFFUSION MEASUREMENTS

There are essentially three basic methods which have been used to study the diffusion of gases through porous media. A method originated by Loschmidt (50) involves the transient interdiffusion of two gases in a closed system. Evaporation of a liquid and the steady-state diffusion of its vapor through the porous medium to a flowing stream of inert gas is a technique devised by Stefan (51). The third method, attributable to Buckingham (52), is steady counterdiffusion in an open system. This last method has been used with porous media most extensively and most successfully.

The obvious advantage of the Loschmidt method would be the brief testing times required. However, unsteady-state systems involve the use of assumed or only partially valid boundary conditions. Another more serious objection to the use of this method is that diffusion in a closed system appears to be accompanied unavoidably by transport due to a small pressure difference (6).

Although the Stefan method involves diffusion in an open system, the inert gas through which the vapor diffuses is stagnant, and, therefore, the transport process is not one of counterdiffusion. In addition, as pointed out by Rothfeld (15), there may be an appreciable pressure difference across the porous medium for this process. These factors rendered the evaporation technique of studying gaseous diffusion unsuitable for the purposes of the present study.

For the steady counterdiffusion of two gases through a porous medium in an open system, the pressures at the opposite faces of the medium can be maintained exactly equal by sweeping the faces with the pure component gases. As a consequence of the equality of pressure at the opposite faces of the medium, the total pressure will be uniform throughout the medium (15). Therefore, the process of ordinary counterdiffusion of gases through partially saturated fiber beds may be examined most clearly by this method.

Determination of the ordinary diffusion mechanism also may best be made using a steady-state open system. The Knudsen diffusion coefficient is independent of pressure, whereas the normal diffusion coefficient varies inversely with pressure. Consequently, the diffusion mechanism may be evaluated for a given test specimen by determining diffusion fluxes at varying total pressures. As the ordinary diffusion process changes from Knudsen to normal diffusion, the diffusion rate as a function of pressure varies typically in the manner shown in Fig. 3.

The linear part of the curve corresponds to Knudsen diffusion, the curved region to intermediate diffusion, and the approximately horizontal portion to normal diffusion. These data were obtained by Scott and Dullien (5) for the steady counterdiffusion of oxygen and argon through a microporous porcelain and represent the variation of the oxygen diffusion rate with total pressure.

GASES

In addition to the requirement of eliminating undesirable adsorption phenomena from the system, the choice of gases which could be used was influenced by the variable total pressure aspect of the experimental program. Selection of a method for analyzing the binary gas mixtures resulting from the diffusion process

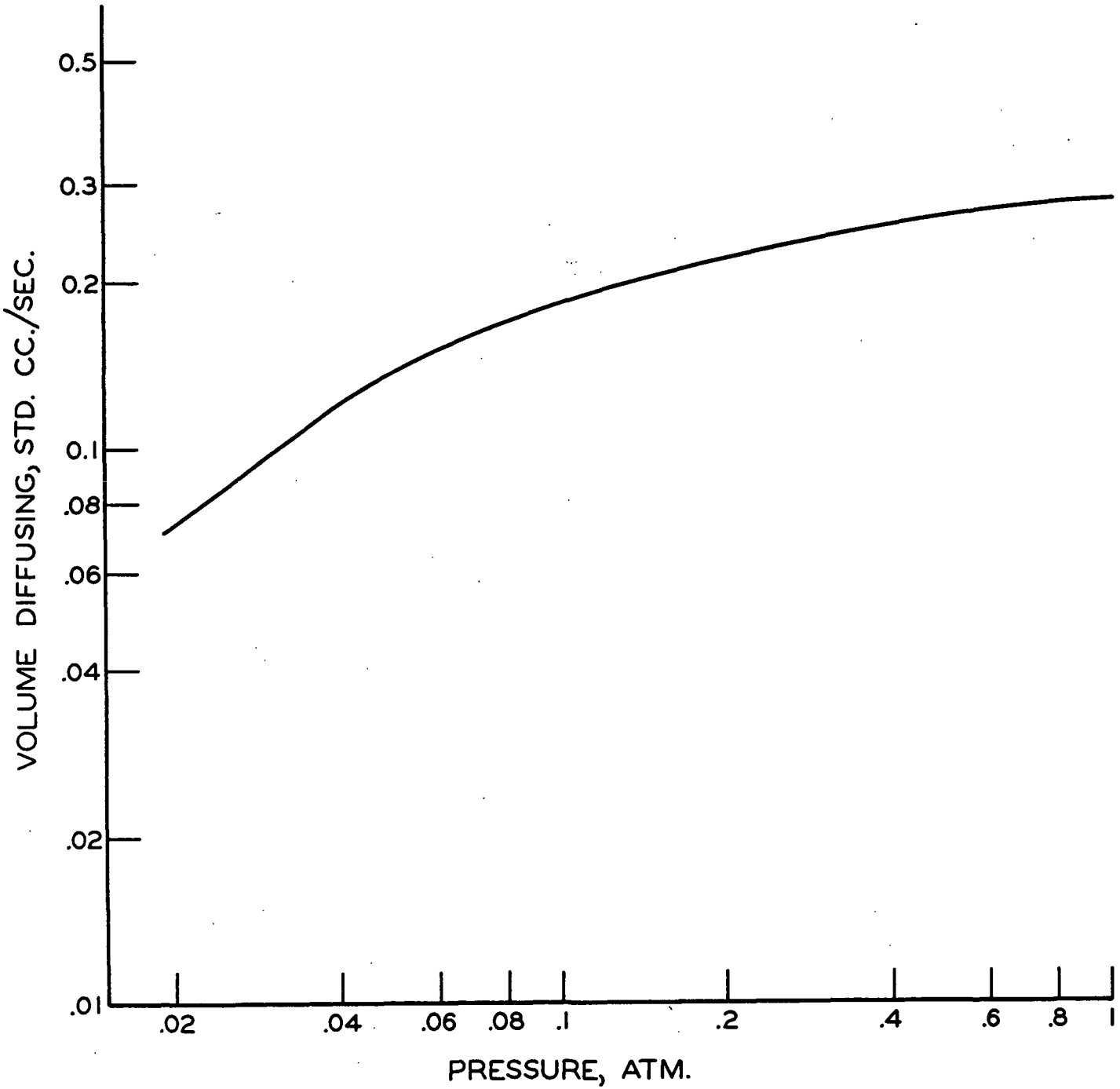

Figure 3. Variation of Diffusion Rate with Pressure (5)

was another important factor in this regard. Because of these and other factors, water vapor was considered unsuitable for use in this study.

In selecting a gas to replace water vapor, it was desirable for the ordinary diffusion behavior of the gas to be similar to that of water vapor. The major factor affecting this behavior is the mean free path of the molecules. Carbon dioxide has a mean free path almost identical to that of water vapor (53). Because of this and the above-mentioned factors, carbon dioxide was used in place of water vapor for this study. In order to facilitate control of the composition of the other gas stream and gas analysis, pure nitrogen was used instead of air.

Calculation of the diffusion fluxes depends upon knowing the steady-state compositions of the effluent gas streams. Therefore, either a continuous analysis or at least an intermittent analysis of the effluent streams was required. In addition, it was desirable for the method of analysis to be rapid, accurate, precise, and insensitive to total pressure changes. Gas analysis by means of thermal conductivity cells most aptly fulfilled all of these requirements. The suitability of this method of gas analysis for diffusion studies has been well established (5, 10, 22, 35). The thermal conductivities of nitrogen and carbon dioxide are sufficiently different to permit the use of this technique for analyzing binary mixtures of these gases.

Carbon dioxide was obtained from the Pure Carbonic Company with a purity of 99.85%. According to the manufacturer, the percentage of nitrogen in the carbon dioxide was too small to measure. The nitrogen used was a prepurified grade produced by the Matheson Company and reportedly had a minimum purity of 99.996%.

FIBER BED SYSTEMS

Although studies concerned with wood pulp fiber beds would be directly applicable to the problem of paper drying, beds of nonporous synthetic fibers of uniform geometry were used for this study. This further idealization of the working system was considered essential (1) to provide for a more basic system than a wood pulp fiber system which includes intrafiber pores, variable fiber dimensions, and inter- and intrafiber bonds among other things, and (2) to restrict diffusion to the interfiber pores.

Some early experiments of the present study indicated that relatively high compacting pressures were required to make satisfactory diffusion measurements and to effect a certain desired degree of bed porosity variation. Beds of nylon fibers best fulfilled all of the above-mentioned requirements and so were used for the major portion of this study.

The fibers were prepared from a continuous, multifilament, Dupont nylon yarn. The diameter of the fibers was 42.64 $\pm$ 1.03 microns (54), and the fiber density was 1.14 g./cc. (55). This fiber diameter was selected in an attempt to obtain beds for which the diffusion mechanism would vary with degree of saturation.

Fibers of about 1.76 mm. in length were prepared from the continuous filament yarn by means of a razor blade gang cutter. This technique has been described adequately by Jones (56) and has been shown to result in a relatively narrow fiber length distribution (4, 56). Use of this fiber length allowed beds to be formed from a water suspension within a reasonable period of time, while avoiding flocculation of the fibers.

The other nongaseous component of the fiber bed systems was the saturating liquid. Dioctyl phthalate, di-(2-ethylhexyl) phthalate, was selected because it is relatively nonvolatile, is fluid enough to saturate the beds conveniently, and is not hygroscopic. According to the manufacturer (FMC Corp.), this liquid has a vapor pressure of less than 0.06 mm. Hg at 150°C., a viscosity of 80 centipoises at 20°C., and a specific gravity of 0.986 $\pm$ 0.003. In addition, dioctyl phthalate was predicted to have little or no effect on the properties of the nylon fiber (57).

PREPARATION OF TEST SPECIMENS

FORMING OF FIBER BEDS

In order to ensure that the formation of the fiber beds would be uniform and reproducible, the beds were formed by constant-rate filtration of dilute fiber suspensions using the equipment and techniques described by Bliesner (43). Using fibers of appropriate dimensions and extremely dilute suspensions, this technique results in beds with the fibers randomly oriented primarily in the x-y or horizontal plane of the bed (56).

The beds were formed from a suspension of the fibers in deaerated distilled water with an initial consistency of about 0.002%. The fibers were deposited on a septum consisting of a drilled brass plate over which a 150-mesh brass screen had been clamped. All of the beds formed were 5 inches in diameter. Throughout the forming process, the flow rate was 4 g.p.m., which is within the laminar flow region for the system used, and the water was recycled back to the supply tank.

From preliminary experiments, it was found that 2.1 grams of fiber were deposited in ten minutes from a slurry of the above consistency for the above

rate of flow. On this basis, the consistency was maintained approximately at its initial value by 2-gram additions of fiber at ten-minute intervals until the desired weight of fiber had been added to the supply tank.

Ten minutes after the last addition of fiber had been made, the water was pumped to the sewer. After the water level had passed below the septum, the pump was shut off, and the septum together with the bed was removed from the forming apparatus. The bed was then removed from the septum and allowed to air dry overnight, after which it was dried in an oven at 105°C. for about 4 hours. After it was weighed, the bed was stored in a desiccator over Drierite until it was partially saturated and/or used for diffusion studies.

PARTIAL SATURATION TECHNIQUE

Partial saturation of a dry bed with dioctyl phthalate (DOP) was carried out by desaturation of the bed from a completely saturated condition. This procedure would simulate more closely a drying process than would an imbibition technique.

Before saturation of the bed, the DOP was evacuated in a vacuum oven at 60°C. for about 16 hours to remove air and any volatile impurities. The bed itself was evacuated in a vacuum desiccator at room temperature for 16 hours. To prevent liquid from flowing out of the bed during its saturation, the bed was placed within a 5-inch diameter, 1-inch deep plexiglas ring. The bottom of the bed was covered with Saran film, and the entire assembly (bed-ring-film) was placed in one-half of a culture dish. The bed, uncompressed, was saturated under vacuum by dropwise addition of the DOP at the edge of the bed.

Desaturation of the saturated bed was accomplished by the blotter technique used by McMaster (4). The saturated bed was placed on top of several standard pulp blotters, and the liquid was allowed to flow into them.

In an attempt to minimize any discontinuity between the diffusion resistance of the dry bed and that of the partially saturated bed, as the degree of saturation approached zero, the initial desaturation of the bed was carried out in two stages. First of all, the bed was desaturated in an uncompressed condition (thickness > 1.19 cm.) until the degree of saturation of the uncompressed bed corresponded to complete saturation of the bed, as it would exist in the diffusion chamber (thickness = 1.1907 cm.). Further removal of the liquid was carried out with the bed compressed to this thickness in a Williams hand-press. All subsequent desaturations were carried out using the latter technique.

DIFFUSION STUDIES

To carry out the objectives of this thesis, the steady-state ordinary counterdiffusion of carbon dioxide and nitrogen through fiber beds was studied under conditions of uniform temperature and pressure in an open system. These measurements were made at several levels of total pressure primarily with nylon fiber beds partially saturated with dioctyl phthalate to varying degrees. A constant temperature of 40°C., which was sufficiently above expected ambient temperatures, was maintained throughout this study. The systems developed for making these diffusion measurements will be described in the following sections.

DIFFUSION CHAMBER

A properly designed apparatus for containing the test specimen is one of the more important components of the over-all diffusion system. Eliminating leakage of gas around the edge of the test specimen and minimizing the thickness of stagnant gas films at the specimen's faces are the major design problems encountered.

The design of the diffusion chamber constructed for this study was influenced also by the relatively large diameter and characteristically high compressibility and high permeability of the fiber beds which were to be used. To minimize the complications due to edge effects arising from the formation of the fiber beds and from the air space between the bed and the wall of its retaining ring, the guard ring principle described by Carson (58) was employed.

Basically, the diffusion chamber consisted of three parts: two identical half-cells for entrance and exit of the gases and a retaining ring (E) for the fiber bed. A photograph of the assembled chamber is shown in Fig. 4. The entire apparatus was constructed from brass to provide for good heat conduction, small thermal expansion, and good machinability. Gas tightness at all joints of the chamber was insured by using solder for permanent joints and, where necessary, rubber O-rings at the nonpermanent joints.

A sectional view of the top half-cell is shown in Fig. 5. Photographs of it are shown in Fig. 6 and 7. Each cell consisted of two concentric cylinders. The inside diameter of the inner cylinder was 3.00 inches and that of the outer cylinder was 5.00 inches. The diffusion measurements were concerned only with the area within the inner or test cylinder. The space between the cylinders constituted the guard area.

Gas entered each cylinder through manifolds (A and A') and sets of 12 circumferential holes. The inlet ports were placed as close as possible to the faces of the bed. Exit of the gas streams took place through similar sets of circumferential holes and manifolds (B and B'). This type of entrance-exit system was used to eliminate stagnant gas films and minimize radial variation in the composition of the gas mixture resulting from diffusion.

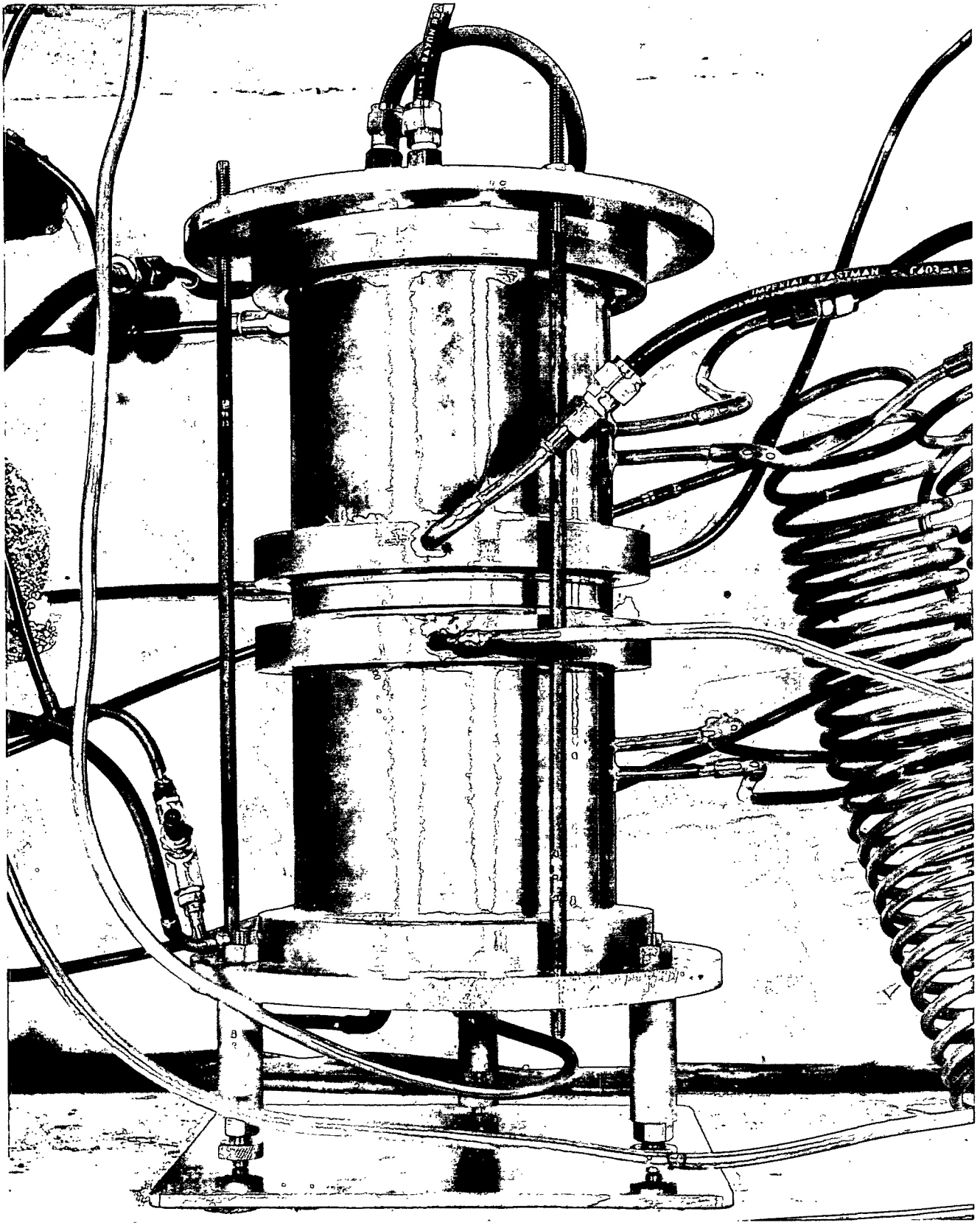

Figure 4. Diffusion Chamber

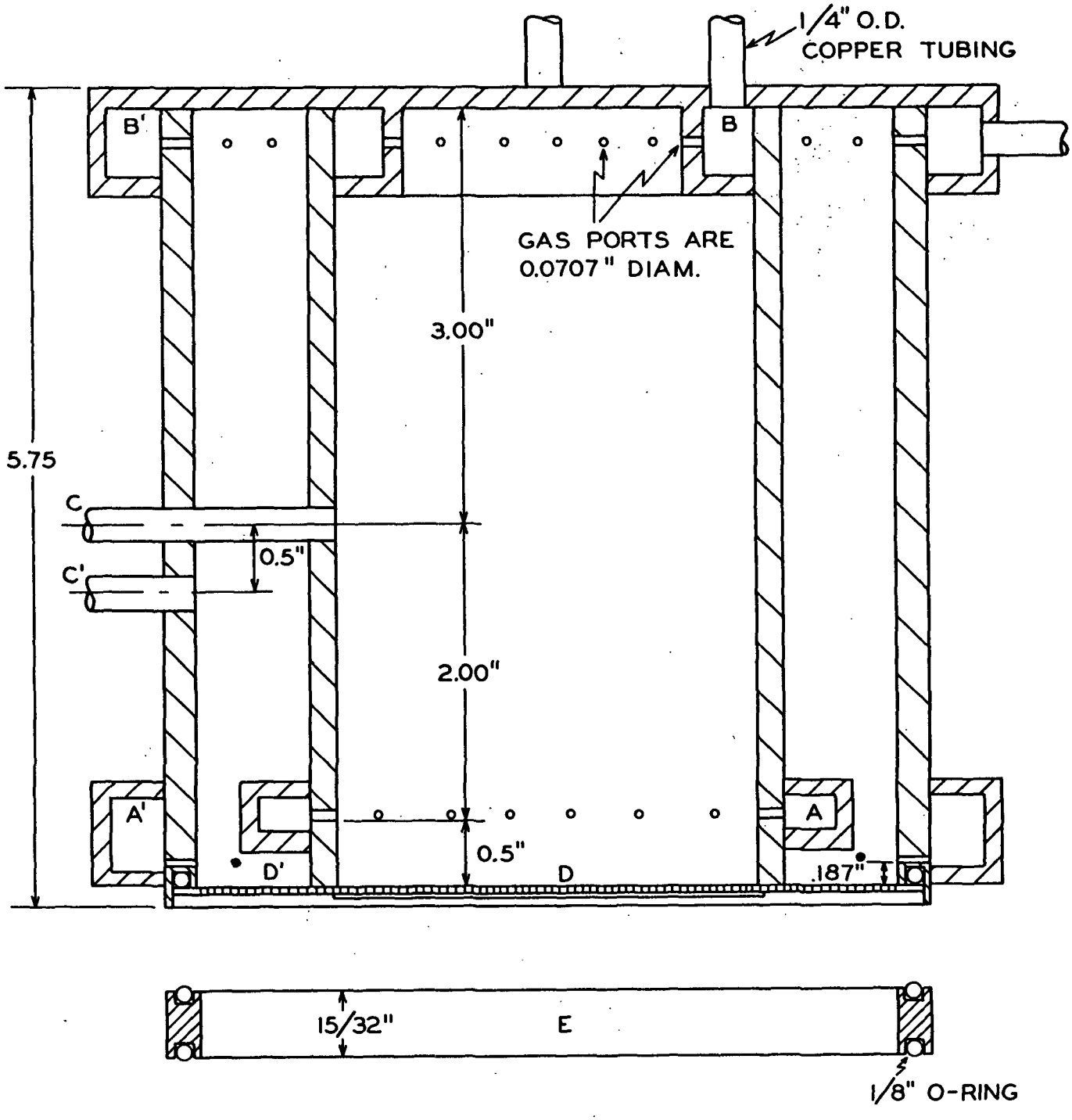

Figure 5. Top-Half Cell of Diffusion Chamber (Full Scale)

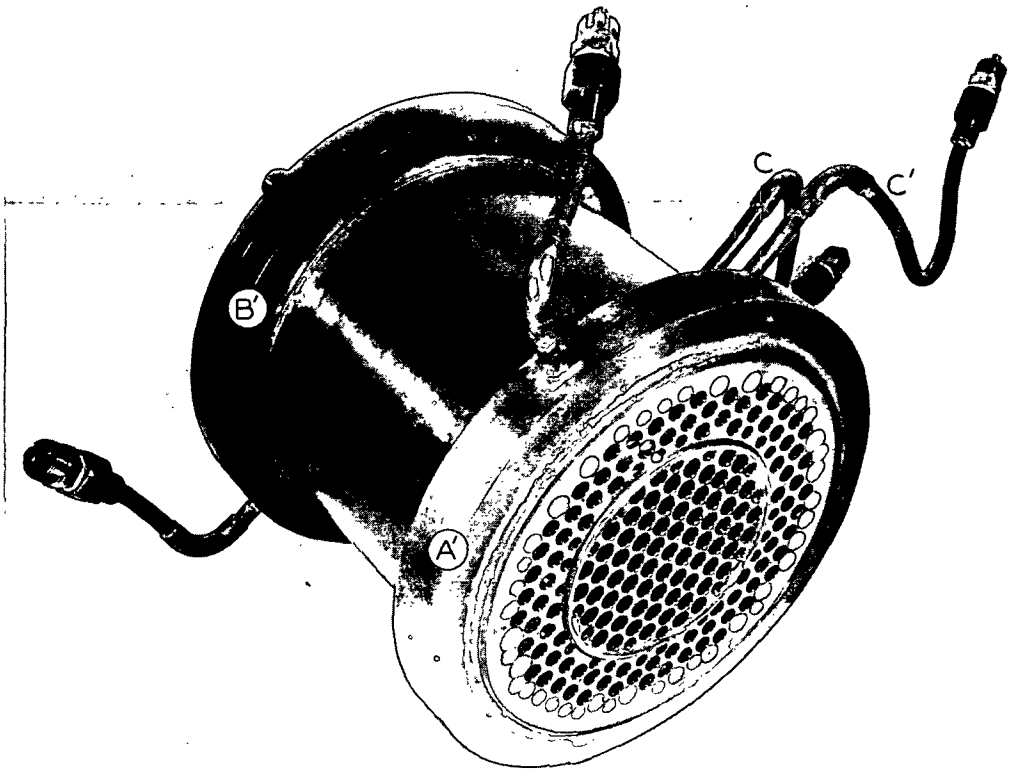

Figure 6. Top Half-Cell, Septum in Place

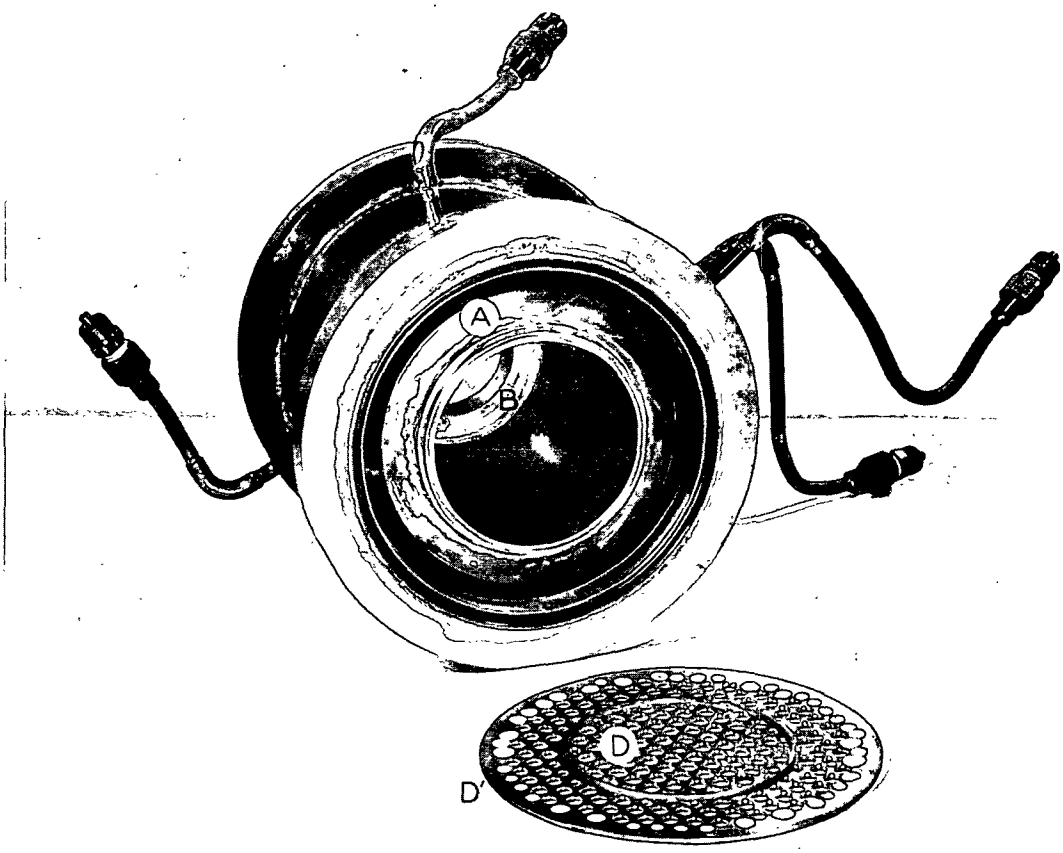

Figure 7. Top Half-Cell, Septum Removed

Uniformity of total pressure throughout the entire diffusion chamber is one of the most important factors in the operation of the diffusion system. Pressure taps (C and C'), located on both gas cells, were connected to draft gages in order to monitor the balance of pressure between cylinders and between half-cells. A measure of the pressure in the chamber was obtained with an absolute manometer connected to the inner cylinder of the top half-cell. Equality of pressure between cylinders was essential also for satisfactory performance of the guard ring arrangement.

In addition to a 5-inch inside diameter, brass retaining ring (E), the fiber beds were confined between brass septums located just below the gas entrance ports in each cell. These septums were made from brass sheetstock by drilling 1/4-inch holes on 5/16-inch centers with interspersed 0.1800-inch holes to give an open area of about 55%. The septum for each cell consisted of two separate components; viz., a septum (D') for the annulus and a septum (D) for the inner cylinder. The annular septum was 1/16-inch thick, as was the inner septum. A 1/16-inch extension, which was 1/16-inch thick, around the outer edge of the inner septum was the guard ring which served to define the test area.

The entire chamber rested on a three-legged stand, provided with leveling screws. Clamping together of the three parts of the chamber was provided for by three steel rods which extended from the bottom plate of the stand to a removable plate on top of the chamber. This type of clamping arrangement facilitated insertion and removal of the fiber beds and provided for a uniform distribution of clamping pressure.

The main criterion for effective use of the guard ring arrangement to minimize edge leakage is that the thickness of the test specimen be less than the width of the guard space (58). All of the diffusion measurements were made

with the fiber beds compressed to a thickness of 1.191 cm. The width of the guard space was more than twice that value.

In addition to the above requirement, there are other important requisites for applying the guard ring principle to studies of gaseous diffusion through fiber beds. Since these studies were concerned with determining average z-directional diffusion fluxes, radial diffusion to or from the test section of the bed should be negligible. Uniformity of total pressure throughout the chamber will eliminate any forced flow. In a small section of the guard section adjacent to the test section of the bed, the axial concentration gradients of the counter-diffusing gases should approach those prevailing within the test section in order to minimize radial diffusion effects. For a bed of finite diameter and for uniform pressure diffusion, satisfaction of this requirement will depend upon the difference between the porous structure of the bed in the test section and that in the guard section and also upon the width of the air space between the edge of the specimen and the wall of the retaining ring.

Since the beds used in this study were formed by constant rate filtration of extremely dilute suspensions of uniform synthetic fibers to a diameter of five inches, the above structural requirements were fairly well satisfied. Therefore, use of the guard ring principle hinged mainly on obtaining and maintaining uniform pressure conditions. In order to equalize the total pressures in the four cylinders of the diffusion chamber, one had to be able to observe pressure differences initially. These pressure differences were quite small but could be sensed with suitable draft gages. From preliminary experiments, it was found that satisfactory operation of the system in this regard was achieved when the uncompressed beds of high porosity ($\epsilon > 0.90$) were compressed to the extent that their porosity was reduced to about 0.85.

FLOW SYSTEM

To carry out the proposed diffusion studies, the over-all system had to contain facilities for controlling and monitoring temperature, flow rates, pressures, and pressure differences, and provisions for proper operation of the thermal conductivity (TC) cells. The flow system and its various components are schematically illustrated in Fig. 8 and are shown photographically in Fig. 9.

Nitrogen flowed through two pressure regulators (PR1 and PR3) to the feed valve (NV1) and was heated up to the temperature of the air bath after passing through the heat exchanger (H1). The stream then divided. Part of it flowed directly to the guard cylinder, and the rest flowed indirectly to the test cylinder of the top half-cell of the diffusion chamber. The flow rates to these cylinders were adjusted by the flow control valves (MV3 and MV5) so that the pressure difference between these cylinders was zero, as indicated by the oil-filled draft gage D1. The flow rate of only the stream which flowed to the test cylinder was measured. After passing through the rotameter (R1), this stream flowed first through the reference side of the Top TC cell and then through the three-way valve (TWV1) into the test cylinder. For diffusion runs, the toggle valve TV17 was open.

The flow sequence for the carbon dioxide stream was identical to the nitrogen sequence. Draft gage D3 was used in equalizing the gas pressures of the cylinders of the bottom half-cell of the diffusion chamber. Draft gage D2 was used in equalizing the gas pressures of the two test cylinders.

From the test cylinders of both half-cells, the effluent streams flowed through the sample passages of their respective TC cells and then to the surge tank, a 5-gallon bottle. The effluent streams from the two guard cylinders flowed

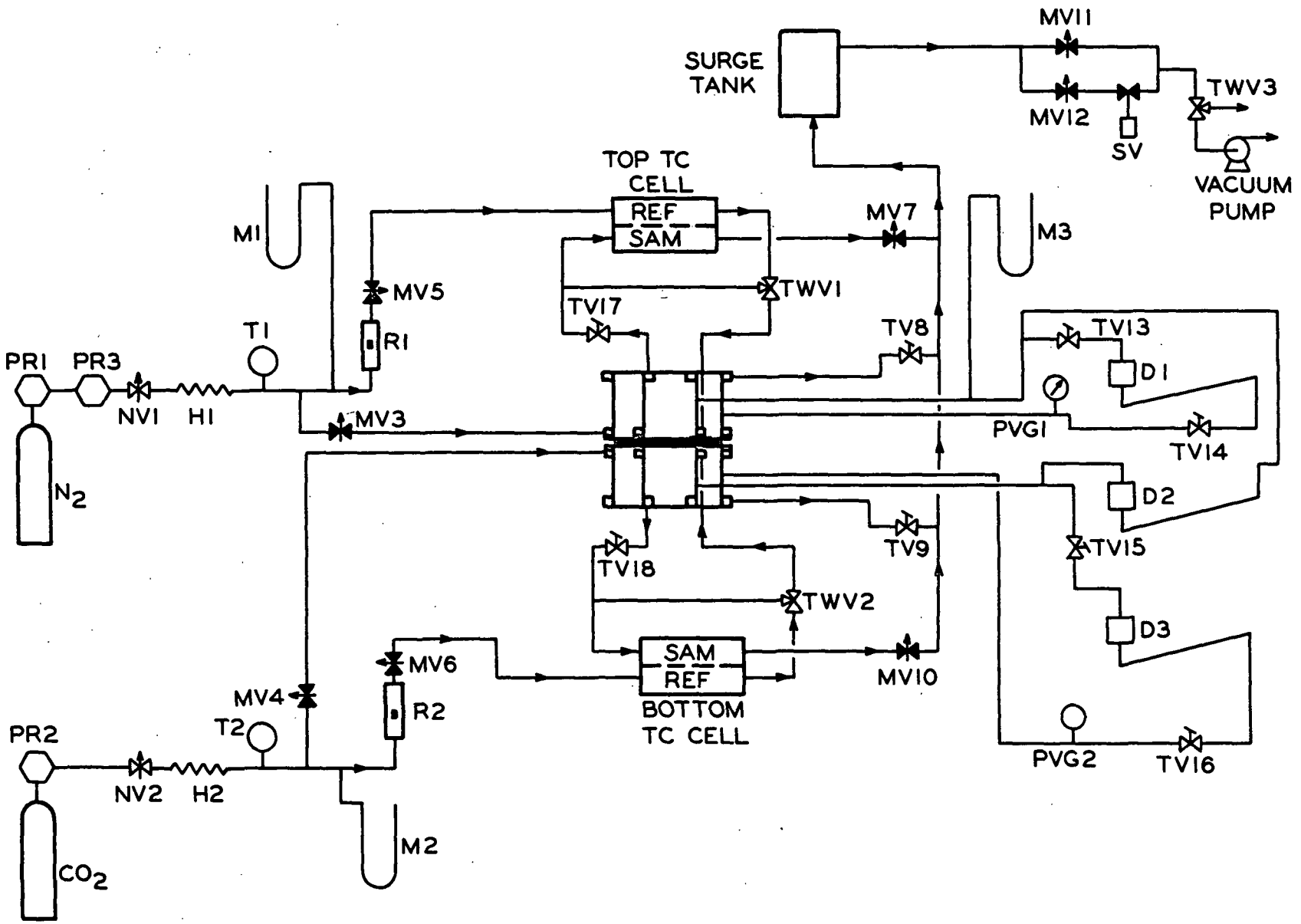

Figure 8. Flow Diagram of Diffusion System

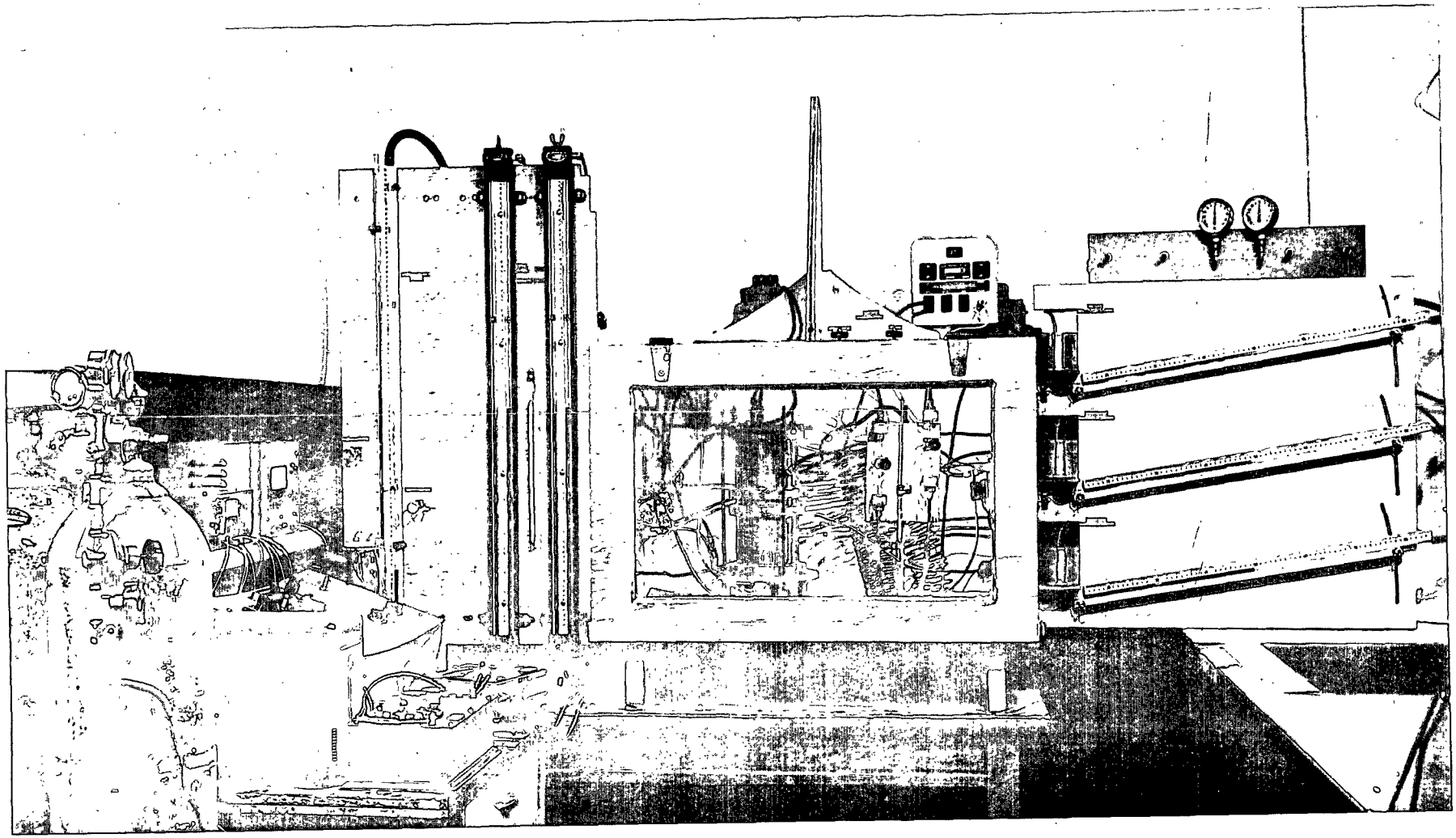

Figure 9. Diffusion Apparatus

directly to the surge tank. The combined streams then flowed through the pressure control system and into the atmosphere, either directly or indirectly through the vacuum pump. Metering Valves MV11 and MV12 were components of the pressure control system.

During diffusion runs, Valves MV7, TV8, TV9, and MV10 were open. They were used in conjunction with prerun operation of the TC cells. Toggle Valves TV13 through TV16 were normally open but could be closed quickly to prevent the draft gages' liquid from being blown out as a result of excessive pressure differences. In such a situation, the pressure-vacuum gages (PVG1 and PVG2) could be used to obtain coarse pressure balances; the draft gages could then be used for finer balancing.

Except for short spans of lines connected to the top half-cell of the diffusion chamber, all flow lines were 1/4-inch copper tubing. Metal-metal connections were made with solder-joint fittings. Connections of the various parts of the flow system with the top-half cell of the diffusion chamber were made using 1/4-inch, rubber-covered, rayon braid hose (Imperial C403-1) together with standard brass hose fittings and female adapter solder fittings. Such connections were used to facilitate removal of this half-cell from the air bath.

Operation of the system under uniform temperature conditions was provided for by a thermostatically controlled air bath. The air bath itself was constructed from 1/2-inch plywood with an interior lining of 1/2-inch fiberboard and a "Thermopane" window in the door. The inside dimensions of the cabinet were 34 by 22 by 22 inches. Air circulation was provided by a 100 c.f.m. blower mounted outside the cabinet but connected to its back face by 2-inch inside diameter Tygon tubing lagged with hair felt. The temperature was controlled by a Fenwal thermoregulator in conjunction with a Precision Scientific electronic relay that activated the heater circuit.

The primary heating element, which was located around the periphery of the bottom of the cabinet, was a lead-lined nichrome wire rated at 385 watts. This heating element was connected to the 110-volt circuit through a variable transformer. Heat losses were partly compensated for by a 75-watt incandescent bulb that operated continuously through another variable transformer. With this heater and control circuit, the temperature of the flowing gases was maintained within $\pm$ 0.02°C. of the set point, which was about 40°C. The maximum point-to-point variation of the air bath temperature was found to be about 0.5°C.

Both gas streams were heated to the temperature of the air bath by passage through twenty-foot coils of 1/4-inch copper tubing.

The temperatures of the gas streams were measured by means of thermocouples (T1 and T2), which were constructed from 28-gage iron and constantan wires. The thermal wires were insulated with enamel and cotton braid. Hot junctions were formed by twisting the two wires together and dipping in molten silver solder; excess solder and wire ends were removed. Cold junctions were formed by twisting the two wires together and immersing the junctions in mercury wells submerged in an ice-distilled water bath.

Calibration of both thermocouples was conducted against a thermometer calibrated by the National Bureau of Standards. The thermometer and both thermocouples were immersed in an oil bath which had previously been heated to about 70°C. and placed in a Dewar flask. The thermocouples were attached to a double-pole-double-throw switch which was attached to a potentiometer circuit, in which were utilized a Leeds-Northrup 2430-a galvanometer and a Leeds-Northrup student potentiometer. Emfs could be measured to $\pm$ 1 microvolt. Both thermocouples were calibrated over a temperature range of 35 to 65°C. After calibration the thermocouples were sealed into the flow systems by means of an epoxy adhesive.

Two Fischer-Porter triflat rotameters were used for measuring flow rates and were located within the air bath. They were calibrated against a wet-test meter. The pressure upstream from the rotameters was measured by mercury-filled manometers (M1 and M2) and was regulated by two-stage pressure regulators (PR1 and PR2). In the case of the nitrogen stream only, a relief-type pressure regulator (PR3) was used in addition to the two-stage regulator. Barometric pressure was measured by a Cenco aneroid barometer. The rotameters were connected into the system by means of Cenco glass-to-metal vacuum couplings.

Throughout the calibration of both rotameters, the upstream pressure was maintained at 1000 $\pm$ 1 mm. Hg absolute; the control point of the thermoregulator was not altered from that cited above. For these conditions, the rotameters were found to have the following useful flow ranges:

carbon dioxide: 0.500 - 19.8 std. cc./sec.
nitrogen : 0.500 - 23.5 std. cc./sec.

Duplicate flow rate determinations differed by 1% or less. At the conclusion of the calibration runs, random flow rate determinations indicated that the calibration could be reproduced to within 1% or less of the initial calibration.

During a diffusion run, any pressure differences between the test cylinders of the diffusion chamber and between the guard cylinder and the test cylinder of each half-cell had to be eliminated and maintained at zero. Draft gages were selected as the monitoring devices. This type of gage provides a relatively high multiplication factor but does not require the elaborate precautions associated with micromanometers (59).

Three draft gages were constructed. The wells were made from 2.75-inch lengths of brass pipe, 3.50-inch O.D. by 0.125-inch wall thickness. The face plates, which were cut from 1/4-inch brass plate, were press fitted into the

pipe and then soldered into place. The distance between the inside faces was 2.5 inches. Short lengths of copper tubing, which were soldered into place in the center of the face plates, were used to connect the wells to the system and to the inclined legs. Precision bore glass tubing, 0.25 $\pm$ 0.0002 inch inside diameter by 0.030-0.050 inch wall, was used for the inclined legs. All three draft gages were mounted on a hardwood board. The glass tubing and its associated meter stick were mounted in a way such that the angle of inclination could be set at any value ranging from 0 to 20 degrees, as shown in Fig. 9.

For most of the diffusion studies, the legs of the gages were inclined with respect to the horizontal at an angle of 10 degrees. Dioctyl phthalate (DOP), tinted with a brown dye, was used as the gage liquid. For the above angle of inclination, calculations indicated that a pressure difference of 1 mm. Hg corresponded to a scale reading of 79.2 mm. DOP. Since the location of the zero point of the meniscus could be determined to the nearest 0.2 mm. DOP, balancing of the pressures to less than a pressure difference of 0.005 mm. Hg was possible.

A small number of diffusion runs were made with the legs of the draft gages inclined at an angle of 15 degrees. For this angle of inclination, a scale reading of 53.2 mm. DOP corresponded to a pressure difference of 1 mm. Hg. This multiplication factor was confirmed experimentally.

In order to investigate the mechanisms governing the diffusion of gases through fiber beds, an accurate and precise means for controlling the total pressure in the diffusion chamber and downstream from it was required. Control of the pressure both above and below atmospheric pressure was necessary. In addition, the capacity of the control system had to be at least 1000 cc./min. The operating differential of the control system was required to be about 0.2 mm. Hg. The error introduced into the calculation of the diffusion coefficient

by this amount of pressure variation would be negligible at all pressures above 0.01 atmosphere, compared to that introduced by the limited accuracy of the flow rate measurements.

The desired control of pressure was achieved with the system schematically illustrated in Fig. 10. Solenoid valve (SV) was the final control element, which was actuated by a "Thermocap" relay (R). Operation of this relay was brought about by a change in capacitance between its input post and ground. The pressure under control was measured by a sealed-tube mercury-filled manometer, which measured absolute pressure directly. A metallic pick-up clip was attached to the open leg of the manometer at the desired set point and to the input post of the relay. Slight movement of the mercury column away from the set point (bottom of pick-up clip) caused the change in capacitance necessary to operate the relay.

The normally closed, solenoid valve had a 1/4-inch orifice. Depending on the gas flow rate and the pressure set point, flow through the solenoid valve had to be throttled by Valve MV12 in order to minimize surging of the pressure about the set point. As the flow rate was increased for a given set point, Valve MV11 had to be adjusted to allow part of the flow to by-pass the solenoid valve. The desired set point and to a certain extent the operating differential of the control system were regulated by the adjustments made to Valves MV11 and MV12. Fine regulation of the set point and operating differential were made by means of the controls of the "Thermocap" relay. Two balance controls permitted precise setting of the point at which the relay operated. Controls were provided also for adjusting the sensitivity and operating differential of the relay. In addition, a three-position toggle switch varied the response speed of the instrument.

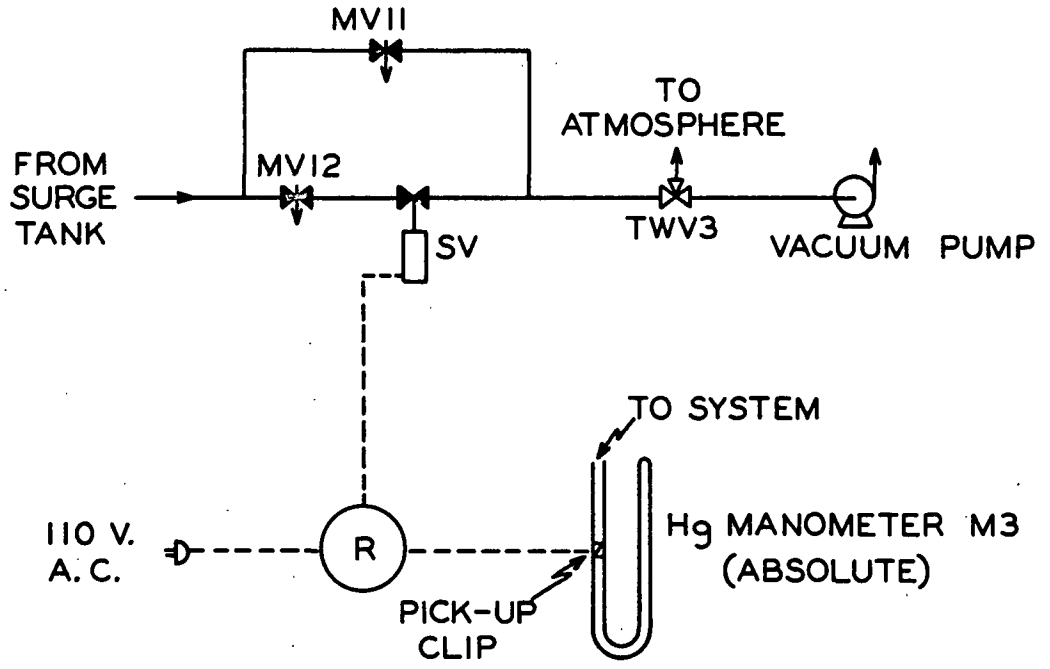

Figure 10. Pressure Control System

Satisfactory operation of the control system for set points of 499.0, 98.0, and 9.0 mm. Hg absolute and for flow rates of about 30, 500, and 1200 std. cc. N_2/min. at each set point was realized. For the first two set points and at all three flow rates, the pressure was maintained to within 0.2% of the set point. An operating differential of $\pm$ 1% was achieved for the third set point.

THERMAL CONDUCTIVITY CELLS

Thermal conductivity gas analyzers detect changes in the thermal conductivity of a gas and therefore changes in its composition as a function of the change in resistance of an electrically heated wire or thermistor.

Two model 30-S thermal conductivity (TC) cells were purchased from the Gow-Mac Instrument Company. Each cell, which was a 2-inch cube of brass, had two reference cavities and two sample cavities, each of which contained a filament of coiled bare tungsten wire. Each pair of cavities was located perpendicular to a passage through which the gas flowed. Gas entered the cavities primarily by diffusion. The filaments were arranged to form the four arms of a Wheatstone bridge in such a way that two opposite arms of the bridge were filaments surrounded by reference gas and the other two were filaments surrounded by the gas to be analyzed. As received from the manufacturer, these units required connection of only the associated electrical components.

Operation of the TC cells depended, first of all, on balancing the Wheatstone bridge circuits with all of the filaments surrounded by the carrier or reference gas. This operation is referred to as zero balancing. When the sample filaments were then exposed to a binary mixture of the carrier gas and another gas of sufficiently different thermal conductivity, an out-of-balance potential was developed. Measurement of this voltage in conjunction with an appropriate

calibration curve resulted in a determination of the composition of the binary gas mixture.

According to several sources (60-62), certain precautions must be observed in designing and using TC cells: (1) the cavities and filaments of the cell must have a high degree of geometric and physical symmetry, (2) the temperature must be maintained constant to within ± 0.1°C., and (3) the heating current should be kept constant. The manufacturer of the TC cells indicated that flow rates outside the range of 50 to 1000 cc./min. could be used only at the expense of stability and/or sensitivity of the instruments. Unless heat transfer by convection were minimized in the design of the instrument, as well as asymmetry among the filaments, variation of pressure could affect the operation of the TC cells (62).

Since it was desired to operate both TC units simultaneously and with a common power source, the cells were connected in parallel and operated at a constant voltage of 4.00 volts. The schematic wiring diagram of the TC cells and associated components is shown in Fig. 11.

Power was taken from a regulated d.c. power supply (Model ABC 18-0.5M, Kepco, Incorporated). Regulation of the voltage at the load was specified as less than 0.05% or 1 mv. output voltage change, whichever was greater, for no load to full load change at any output voltage within the range of 0-18 volts. The output was connected for remote error sensing, by which the power supply regulated for voltage drops in the load connecting wires and thereby maintained specified regulation directly at the load. The bridge outputs from the cells were measured by means of the potentiometer circuit described previously. Connection of the TC cells, as well as the thermocouples, to the potentiometer circuit was made through a multijunction rotary switch (SW).

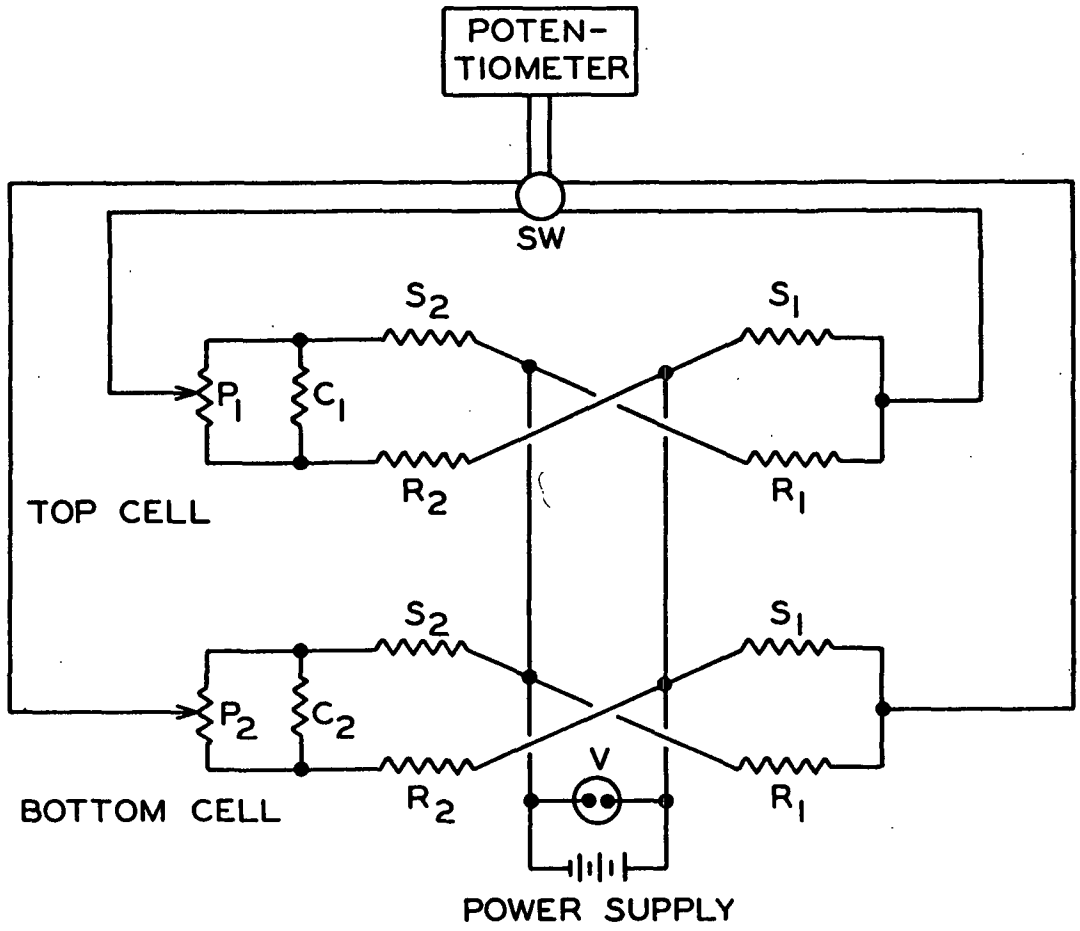

R_1, R_2, S_1, S_2 - 18 ohms (cold), Tungsten filaments

C_1, C_2 - 0.5 ohm, Constantan shunts

P_1 - 10-turn, 500 ohms Helipot, zero-control potentiometer

P_2 - 10-turn, 1000 ohms Helipot, zero-control potentiometer

SW - rotary switch

V - voltmeter

Figure 11. TC Cells' Electrical Circuit

From preliminary studies, it was found that optimum operation of the TC cells was achieved using a steady-state flow technique. This technique simulated the conditions of the analyses made during diffusion measurements. The Top TC cell was used with mixtures rich in nitrogen and lean in carbon dioxide and the Bottom TC cell with mixtures rich in carbon dioxide. Therefore, it was found best to zero balance the Top TC cell with pure nitrogen and the Bottom TC cell with pure carbon dioxide.

Before zero balancing a given TC cell, the sample and reference passages were evacuated for about one hour. During this time, the power supply was turned on and the output voltage was adjusted to 4.00 volts. After this period of time, which provided a sufficient warm-up period for the TC cell, flow of pure gas was started through the reference and sample passages of the unit. The diffusion chamber was by-passed by having the three-way valve (TWV1 or TWV2) opened to the by-pass line and the toggle valve (TV17 or TV18) closed.

Zero balances were made always with the gas flowing at a rate of about 6 std. cc./sec., which was approximately the flow rate used for most of the diffusion studies. This flow rate was not critical, however, since it was found that the zero balances of both cells were not significantly affected by flow rate changes as large as twentyfold.

From preliminary studies it had been found that for pressures above 100 mm. Hg absolute, the stability of the zero balances of both cells was relatively independent of pressure. The gas pressure, downstream from the sample passage of the TC cell, used most conveniently for all zero balancing operations was 760 mm. Hg absolute.

After the flow rate, pressures, and bridge voltage had been adjusted, about thirty minutes was allowed for the system to come to steady state. The TC unit's

bridge was then balanced by means of the zero-control potentiometer (P_1 or P_2) in conjunction with the galvanometer. The balance was considered to be stable when two successive checks of the balance at ten-minute intervals indicated negligible drift away from the balance point.

The above procedure, used for both units, resulted in extremely stable zero balances. Day-to-day drift away from the balance points was less than five microvolts.

During the calibration of the TC cells, it was considered necessary to investigate the dependence of the bridge outputs on pressure and composition. When a given TC cell was being calibrated, the sample passage of the other TC cell was removed from the flow system (see Fig. 8).

After the TC cell had been zero balanced, the entire flow system, excluding the inlet flow lines, was evacuated for about an hour. Nitrogen and carbon dioxide were then introduced simultaneously into the test or inner cylinders of the empty diffusion chamber where they mixed. For calibration operations, the inner cylinders of the diffusion chamber were isolated from the outer cylinders. The gas mixture then flowed through the sample passage of the TC cell. About thirty minutes was allowed for steady state to be reached. Bridge outputs were recorded at ten-minute intervals until the values were steady. The pressure or composition was then changed, and the above sequence was repeated. The compositions of the gas mixtures were calculated from the known values of the mass flow rates of the individual gases.

The bridge outputs for the mixtures used were not affected significantly by changes in pressure above about 100 mm. Hg. Typical results obtained for the Top TC cell are shown in Table I. Bridge outputs of the Bottom TC cell showed a similar independence of pressure.

TABLE I

EFFECT OF PRESSURE ON TOP TC CELL

CO_2, %	Absolute Pressure, mm. Hg	Bridge Output, mv.
14.2[a]	46	-28.1
	100	-27.2
	400	-27.0
	760	-26.7
16.4[a]	40	-32.6
	100	-32.4
	760	-32.1

[a]Typical compositions for diffusion runs.

For the calibration factors of the TC cells to be independent of the composition of the gas mixture, the thermal conductivity of the mixture should be approximately a linear function of its composition in the range concerned. This condition is generally fulfilled by relatively dilute mixtures (62). For mixtures of carbon dioxide and nitrogen, Dye (35) found that the bridge outputs of model 30-S Gow-Mac TC cells with platinum filaments were independent of composition.

To check on the fulfillment of this condition for the system used in this study, the bridge outputs of both TC cells for several gas mixtures were measured using the procedure described above. In all instances, the measurements were made at an absolute pressure of 760 mm. Hg.

The results obtained for the Top TC cell are shown in Table II. For the composition range shown, which is the range pertinent to the diffusion studies, the calibration factor of the Top TC cell was independent of composition.

TABLE II

EFFECT OF COMPOSITION ON TOP TC CELL

CO_2, %	Bridge Output, mv.	Calibration Factor, mv./% CO_2
24.06	-45.5	-1.89
19.44	-38.1	-1.96
16.40	-31.8	-1.94
14.24	-26.4	-1.85
11.77	-23.4	-1.99
Mean		-1.93
Standard deviation		0.0559
Coefficient of variation		2.90%

Similar results were found also for the Bottom TC cell. For three mixtures containing 22.93, 26.23, and 29.75% N_2 in CO_2, the calibration factor was +2.343 $\pm$ 0.009 mv./% N_2.

The accuracy of the flow rate measurements was better than 1%. Since the bridge outputs could be measured to the nearest 0.1 mv., determinations of the compositions of the gas mixtures were accurate to better than 0.1 mole per cent of the gas involved.

OPERATING PROCEDURE

After a fiber bed had been placed in the diffusion chamber, it was assembled and the flow lines were connected. The part of the flow system downstream from the flow control valves (see Fig. 8), which will be referred to as the CAPS, was then slowly evacuated. If a pressure of at least 1 mm. Hg could not be attained, leaks were indicated. When the leaks had been eliminated, the evacuation was

continued for about 18 hours. The temperature control elements of the air bath were activated, and an overnight period of thermal equilibration was allowed.

Before a series of diffusion runs was started, the TC cells were zero balanced. The power supply was turned on, the output voltage was adjusted to 4.00 volts, and a warm-up period of one hour was allowed. The diffusion chamber, in an evacuated condition, was then isolated from the rest of the system by opening the three-way valves (TWV1 and TWV2) to the by-pass lines and closing the toggle valves (TV17 and TV18). The TC cells were zero balanced simultaneously in the manner described previously, the Top cell with pure nitrogen and the Bottom cell with pure carbon dioxide.

After the zero balancing procedure had been completed, the CAPS was evacuated for an hour. With the CAPS still under vacuum, nitrogen and carbon dioxide were introduced slowly and simultaneously into the guard and test cylinders of both half-cells. While the pressure was gradually increasing to the desired value, the pressures in the various cylinders were maintained as equal as possible by adjustment of the flow control valves. When the pressure had increased to a value slightly above the value desired, the elements of the pressure control system were adjusted to maintain the desired pressure. Flow rates, pressures, and pressure balances were adjusted as required, and about thirty minutes was allowed for the system to reach steady state. The bridge outputs from both TC cells were recorded at ten-minute intervals until their values were steady. At this point, the following data were recorded: room temperature, barometric pressure, rotameter readings and pressures, thermocouple outputs, and the diffusion chamber pressure. The draft gages were monitored periodically to be sure that all pressure differences were zero.

When a run was completed, the diffusion chamber pressure was changed to the next desired level. Flow rates, pressures, and pressure balances were adjusted as necessary, and about thirty minutes was allowed for the system to reach steady state. At the conclusion of a series of runs, the CAPS was evacuated for an hour and left in an evacuated condition. The inlet flow lines were left under a positive pressure of their gases.

Several series of variable pressure runs were made with each test specimen in the range of 0.264 to 1.0 atmosphere. With dry beds, runs were made generally over a period of 2-3 days, to ensure that the structure of the beds was not changing with time. For the partially saturated beds, a test period of 3-4 days was used to ensure that the distribution of the liquid was at equilibrium.

EXPERIMENTAL RESULTS

Preliminary diffusion studies were concerned with clarifying the physical characteristics of the diffusion system and the mechanical manipulations needed for conducting the proposed studies. As a result of these experiments, the systems and operating procedure described above were developed. Included in these studies were evaluations of the effects of sweep stream flow rate variation and axial total pressure differences on the ordinary diffusion process.

Subsequent studies were concerned with characterizing the mechanisms governing the counterdiffusion of carbon dioxide and nitrogen through dry and partially saturated nylon fiber beds.

For all of the studies, the thickness of the beds in the diffusion chamber was 1.191 cm. The cross-sectional area of the test section of the beds was 45.60 sq. cm.

From the results of a material balance made over the test section of the beds, the carbon dioxide and nitrogen diffusion fluxes were calculated as shown in Appendix III. In reference to the diffusion equations presented previously, for this study Gas A will be carbon dioxide and Gas B will be nitrogen.

As mentioned above, diffusion measurements on a given test specimen were made over a period of several days. Only the time-independent results are reported here.

DRY FIBER BEDS

PRELIMINARY STUDIES

For the initial studies, diffusion runs were made with commercial pads of cotton fiber at atmospheric pressure (0.971-0.996 atm.). These cotton pads were

used to facilitate determining the degree of bed compression required to utilize the guard ring arrangement effectively.

Using a thick brass plate, which had been machined to a diameter of five inches, and razor blades, a number of 5-inch diameter pads were cut from a continuous web of commercial-grade cotton fiber. The uncompressed thickness of the pads was about 0.5 inch.

A pad composed of six of these 0.5-inch layers was used. Compression of this pad to 1.191 cm. in the diffusion chamber corresponded to decreasing the macropore porosity from about 0.97 to 0.87.

Effect of Flow Rate

This study permitted an evaluation of the effectiveness of the inlet flow system (manifold and ports) of the diffusion chamber in eliminating stagnant gas films, since the thickness of such films would be expected to depend on the flow rates of the sweep streams. Because of the turbulence and divergence of the gas jets being discharged from the 0.07-inch diameter ports (63), the existence of any stagnant gas films at the faces of the beds was considered highly improbable.

A series of diffusion runs was made on the cotton pad under apparently uniform pressure conditions at atmospheric pressure. Variation of the sweep streams' flow rates was made in a random order. For comparative purposes, it was assumed that the diffusion process was normal diffusion. In view of the results obtained for the dry beds of nylon fibers, this assumption proved to be a valid one.

The results of the variable flow rate runs are shown in Table III. Effective normal diffusion coefficients were calculated using Equation (10), as shown in Appendix III.

TABLE III

EFFECT OF FLOW RATE

Run No.	Flow Rates, millimole/sec. CO_2	Flow Rates, millimole/sec. N_2	$-N_N/N_C$	$(D_{AB})_e$, sq.cm./sec.
40	0.290	0.208	1.46	0.0533
41	0.302	0.208	1.55	0.0531
42	0.314	0.208	0.51	0.0524
47	0.349	0.208	1.25	0.0527
43	0.415	0.262	1.16	0.0536
25	0.448	0.262	1.10	0.0554
24	0.521	0.262	0.89	0.0531
Mean			1.13	0.0533
Standard deviation			0.354	0.00097
Coefficient of variation, %			31.3	1.82

Analysis of the values for the diffusion coefficient indicated no effect of flow rate in the range covered. Although the mean flux ratio was only 9.6% smaller in magnitude than the theoretical value (1.25) represented by the lower limit of Equation (24), the variation among the values of the flux ratio was quite significant. This variation was not worse than that encountered for runs made at identical flow rates (referring to Table V, Runs 41, 45, and 46 were made with a CO_2 flow rate of 0.302 mmol./sec. and a N_2 flow rate of 0.208 mmol./sec.) and was definitely random in nature. Therefore, the variation among the values of the flux ratio could not be attributed to variation of the flow rates.

Using a large pore graphite which had an effective porosity of 0.22, Evans, et al. (21, 64) studied the counterdiffusion of argon and helium under uniform pressure conditions and in the presence of small pressure differences. Their

measurements were well within the normal region of ordinary diffusion. The pressure differences (argon side minus helium side) ranged from -2.48 to +8.96 mm. Hg.

When runs were carried out with the pressure on the argon side of the specimen 1.43 mm. Hg higher than that on the helium side, a value for the ratio of the helium flux to the argon flux of -2.31 was obtained. The uniform pressure result was -3.29. In both cases, the values of the effective normal diffusion coefficient were essentially the same. Similar results were obtained for the other pressure differences used. Studies like those of Evans, et al. were carried out with a similar graphite specimen by Hewitt and Sharrat (65), whose findings were essentially the same as those reported above.

The results shown in Table III indicated that the values of the diffusion coefficient were not affected significantly by considerable changes in the values of the flux ratio.

It was pointed out above that the uncertainty associated with reading the position of the meniscus of the oil in the inclined legs of the draft gages was ± 0.2 mm. Therefore, when a pressure balance was made, the observed zero point could have been as much as 0.4 mm. away from the true zero point. For an angle of inclination of 15°, such an error would correspond to a pressure difference of about 0.01 mm. Hg. Although such small pressure differences would not a priori be expected to have a significant effect on diffusion, an investigation of the effect of small axial pressure differences was warranted.

Effect of Pressure Differences

Using the cotton fiber pad, a series of diffusion runs was made at atmospheric pressure in the presence of small but measurable pressure differences. A series of ten runs was then made under apparently uniform pressure conditions.

Total pressure differences were established in the axial or z-direction by adjusting the inlet gas flow rates. The pressures of the gas in the guard cylinders were balanced against the gas pressures of their associated test cylinders in all cases. Variation of the pressure differences was made in a random order.

Small pressure differences were desirable so that the molar density of the gas would not vary appreciably along the length of the path through the test specimen. In addition, Evans, Watson and Mason (64) demonstrated that the usual form of the normal diffusion equation was applicable when the pressure differences were small.

The results of the nonuniform pressure study are reported in Table IV. For comparative purposes normal diffusion was assumed.

TABLE IV

EFFECT OF PRESSURE DIFFERENCES

Run No.	$P_{CO_2}-P_{N_2}$, mm. DOP[a]	Diffusion Rates, micromoles/sec. $N_C A$	$-N_N A$	$-N_N/N_C$	$(D_{AB})_e$, sq.cm./sec.
33	-1.1	2.94	165.6	56.3	0.0498
31	-1.0	4.52	137.3	30.4	0.0490
35	-0.7	5.04	149.3	29.6	0.0508
36	-0.3	6.03	120.0	19.9	0.0490
37	+0.2	56.0	31.3	0.56	0.0540
38	+0.4	68.6	28.0	0.41	0.0571
34	+0.9	108.8	9.88	0.09	0.0576
30	+1.0	122.3	6.72	0.05	0.0501
Mean					0.0522
Standard deviation					0.00355
Coefficient of variation, %					6.80

[a]Scale reading for 15° angle of inclination.

An extremely significant dependence of the diffusion fluxes on small axial pressure differences is evident. This dependence is graphically illustrated in Fig. 12. In agreement with the findings of Evans, et al., the diffusion coefficient was independent of the net flux. In contrast to the findings of Evans, et al., the data showed a much larger change in the value of the flux ratio resulting from the application of much smaller pressure differences.

For a pressure-balancing error of $\pm$ 0.4 mm. DOP, the data indicated that the flux ratio could vary from -0.66 to -2.54 with the leg of the draft gage inclined at an angle of 15 degrees. Therefore, the existence of axial pressure differences as small as 0.01 mm. Hg would account for the variation among the values of the flux ratio observed previously.

At zero pressure difference the value of the flux ratio, obtained by interpolation of the data shown in Fig. 12, was -1.45. This value is within the limits represented by Equation (24), which pertains to normal diffusion. For this study, the upper limit of Equation (24) is 1.57.

The differences between the results of this work and those of Evans, et al. may be resolved in terms of the differences between the permeabilities of the porous media used. For the cotton fiber pad, the average value of the effective normal diffusion coefficient was 0.0522 sq. cm./sec.* at 40°C. At a temperature of 100°C., an average value for this coefficient of 0.00485 sq. cm./sec.* was obtained by Evans, et al (64) for their porous graphite; a permeability coefficient of 10^{-10} sq. cm. was reported by these workers for this specimen. For thick mats of bleached sulfite pulp fibers with interfiber porosities of about 0.8, Bliesner (43) reported permeability coefficients of about 10^{-8} sq. cm.

*Pressure was one atmosphere.

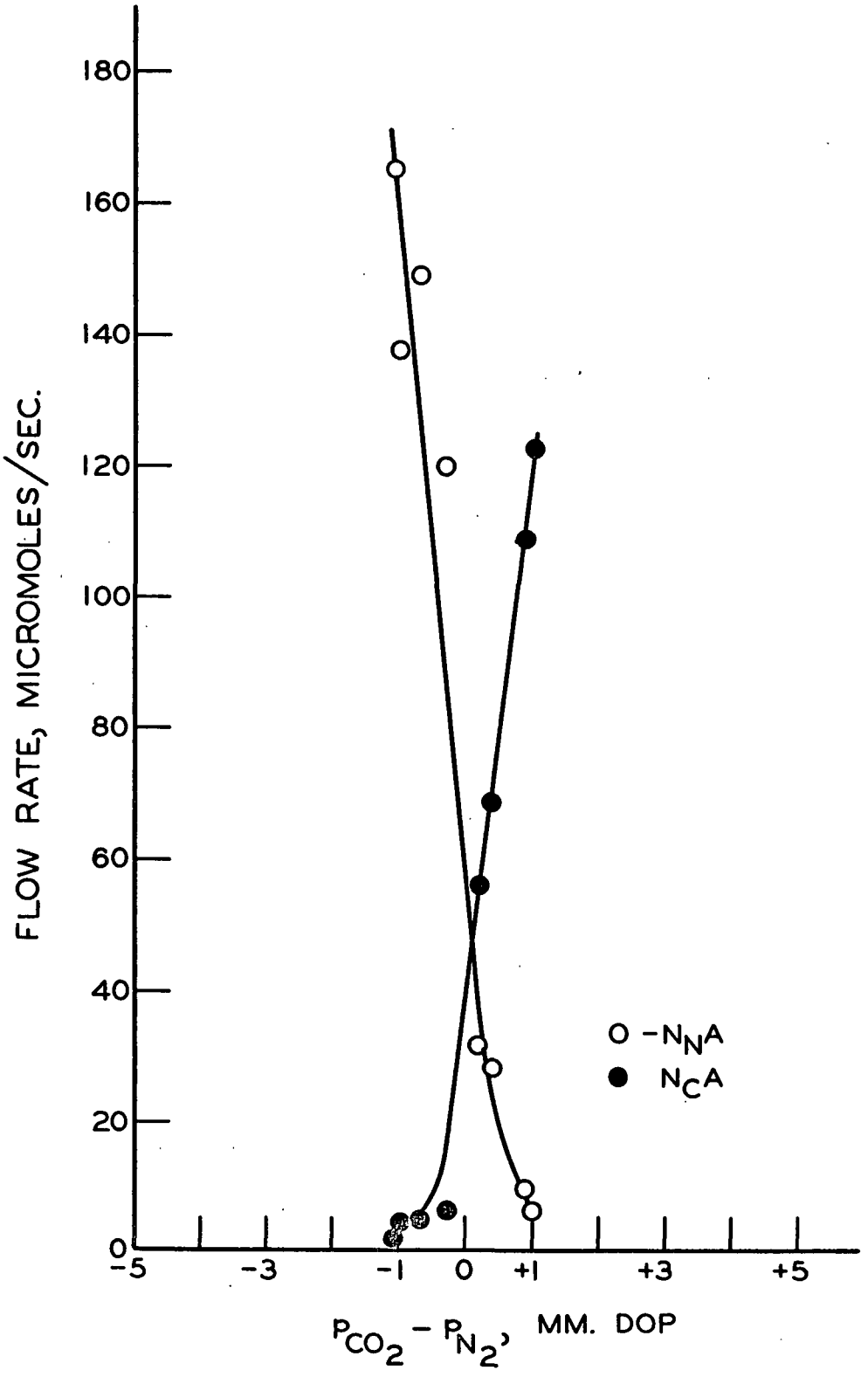

Figure 12. Effect of Pressure Differences

To clarify the effect of random, unobservable pressure differences that might arise from pressure balancing errors, ten runs were made under apparently uniform pressure conditions at atmospheric pressure with the cotton pad. The results of these ten runs are shown in Table V.

TABLE V

"UNIFORM" PRESSURE DIFFUSION

Run No.	$-N_N/N_C$	$(D_{AB})_e$, sq.cm./sec.
39	0.27	0.0552
40	1.46	0.0533
41	1.55	0.0531
42	0.51	0.0524
43	1.16	0.0536
44	0.68	0.0540
45	1.25	0.0524
46	1.17	0.0522
47	1.25	0.0527
48	1.45	0.0519
Mean	1.08	0.0531
Standard deviation	0.437	0.000995
Coefficient of variation, %	40.5	1.87

Even under apparently uniform pressure conditions the standard deviation of the values of the flux ratio was rather large. As was observed for the nonuniform pressure study, the effective diffusion coefficient was independent of the net flux.

The mean value of the effective diffusion coefficient obtained for the uniform pressure study appeared to agree quite closely with that obtained for the nonuniform pressure study. By means of the Student t-Test, the difference between these values was found to be statistically insignificant.

VARIATION OF PRESSURE

In order to determine the maximum pressure range necessary for defining the diffusion mechanism applicable to the nylon fiber beds and to assess the suitability of the system for detecting small changes in diffusion resistance, several series of runs were made with two dry beds of the 43-micron diameter nylon fibers.

The first bed studied, Bed Number N43-1-D, had a porosity of 0.810. The second bed, Bed Number N43-2-D, had a porosity of 0.742. Porosities were calculated from the relation $\epsilon = 1 - \underline{W}/(\rho_{\underline{f}}\underline{L}\underline{A})$, where $\underline{W}$ is the ovendry weight of the bed and $\rho_{\underline{f}}$ is the density of the nylon fiber.

Diffusion Fluxes

The results of the runs made with Bed No. N43-1-D are shown in Fig. 13, in which the nitrogen transport rates, $\underline{N}_{\underline{N}}\underline{A}$, and the carbon dioxide transport rates, $\underline{N}_{\underline{C}}\underline{A}$, have been plotted versus absolute pressure. Below a pressure of about 0.5 atm., the transport rates were approximately independent of pressure. For this pressure region, therefore, the results suggested that normal diffusion was taking place. Above a pressure of 0.5 atm., the carbon dioxide transport rate increased fairly rapidly with increasing pressure, while the nitrogen transport rate decreased. As shown in Fig. 14, similar results were obtained for the diffusion runs made with Bed No. N43-2-D.

To check on the reproducibility of the observed behavior of the diffusion fluxes with pressure, two series of variable pressure runs were made with Bed Number N43-2-D. As may be observed from Fig. 14, the fluxes at a given pressure agreed quite closely, except at a pressure of 1 atm. Previously, it was shown that the observed diffusion fluxes were highly dependent on small, axial,

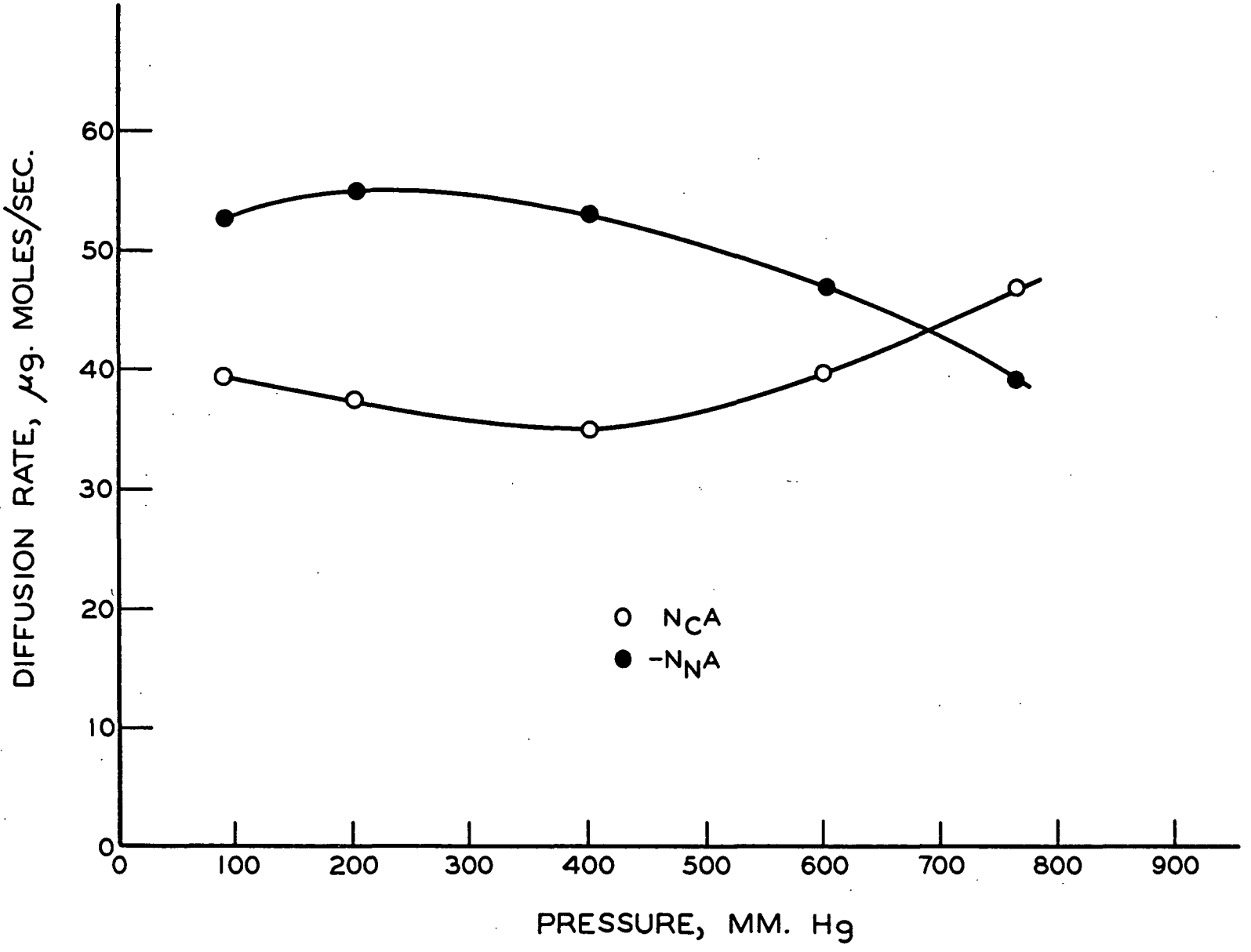

Figure 13. Diffusion Fluxes: Bed No. N43-1-D

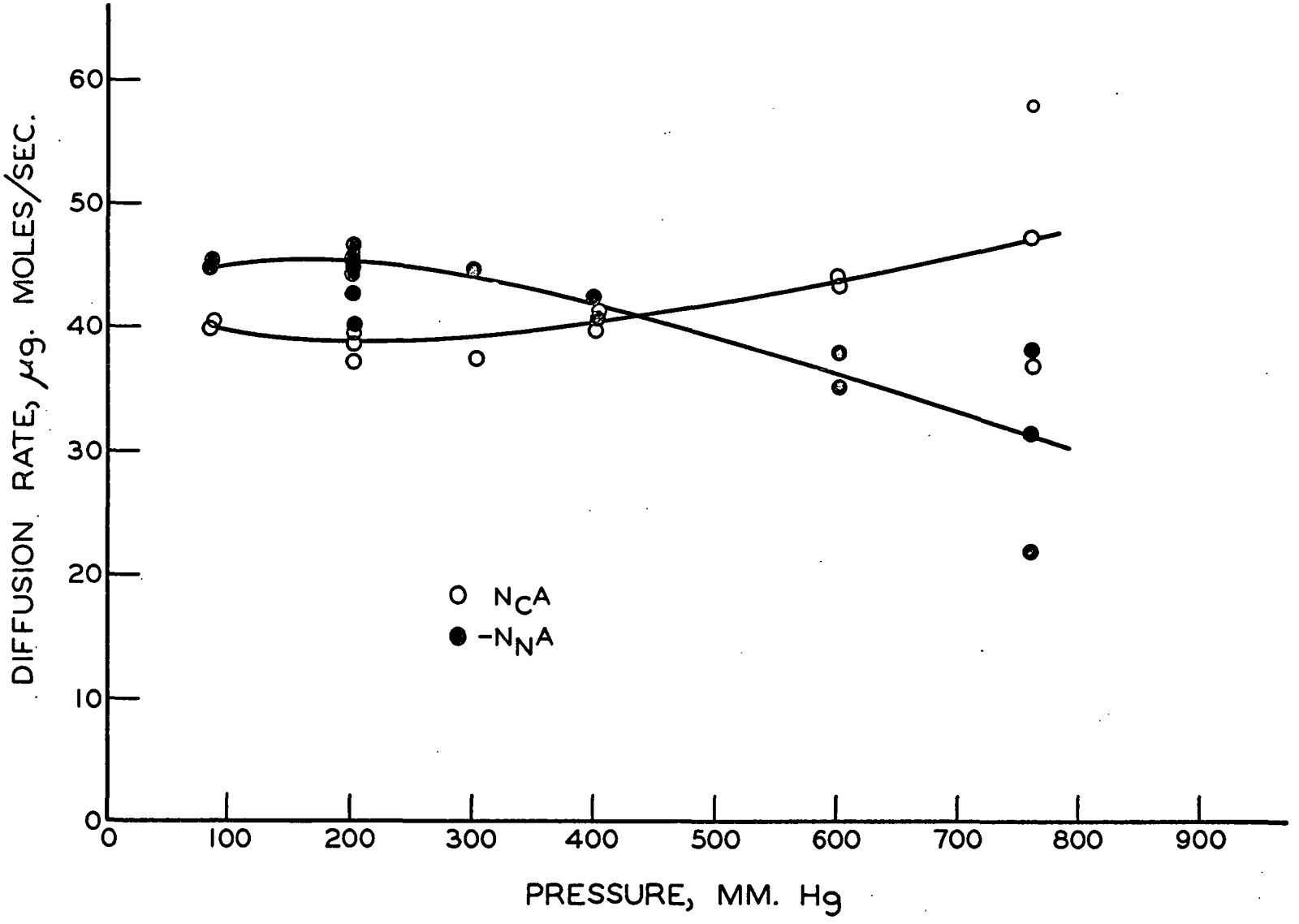

Figure 14. Diffusion Fluxes: Bed No. N43-2-D

total pressure differences. For the isothermal flow of a gas, the mass flow rate is directly proportional to the total pressure for a given pressure difference. Therefore, the effect of small total pressure differences on the observed diffusion fluxes would be expected to become more pronounced as the pressure increased. This would account for the larger scatter of the data at 1 atm. than that at the lower pressures.

The reproducibility of the results obtained in the lower pressure range was checked by making five independent runs on Bed No. N43-2-D at a pressure of 0.264 atm. The mean diffusion rate of carbon dioxide was 38.8 micromoles/sec. The coefficient of variation was 2.86%.

As the pressure increased above about 0.5 atm., the data obtained for both dry beds indicated an apparent departure of the transport process from normal diffusion behavior. Referring to Fig. 3, such behavior could not be attributed to a transition from intermediate to normal diffusion or vice versa. Several combinations of various transport processes were analyzed as possible causes of this behavior: (1) axial normal diffusion accompanied by radial diffusion, (2) radial forced flow superimposed on axial normal diffusion, (3) axial normal diffusion enhanced by axial forced flow, and (4) normal diffusion accompanied by surface transport of carbon dioxide.

Because of the independent manner in which the pressures of a guard cylinder and its associated test cylinder were balanced, the effects of radial diffusion and/or radial flow on axial diffusion would have been quite random in nature, as opposed to the regular behavior shown in Fig. 13 and 14. In consideration of the technique used for forming the nylon fiber beds, the structure of the guard section of a bed was undoubtedly quite similar to that of the test section. Under "uniform" pressure conditions, the axial concentration gradients of the

counterdiffusing gases would be essentially the same in a small region of the guard section adjacent to the test section and in the test section of a given bed. Therefore, radial diffusion to or from the test section of a bed would be expected to be negligible in comparison to axial diffusion.

In view of the results obtained for the nonuniform pressure study, radial forced flow resulting from random pressure balancing errors would have an insignificant effect on the observed gas transport rates in comparison to that of axial forced flow similarly induced. The only conceivable cause of the observed pressure dependence of the gas transport rates, other than surface transport of carbon dioxide, might have been a small, constant, axial pressure difference.

To be consistent with the data, the total pressure on the carbon dioxide-rich side of the bed would have to be greater than that on the nitrogen-rich side of the bed. However, the studies made with the cotton pad indicated that the reverse of this situation was also quite probable. As will be discussed below, all of the data obtained for the dry and all of the partially saturated beds were not consistent with the axial pressure difference hypothesis. On the other hand, these data were consistent with the hypothesis of surface transport of carbon dioxide being responsible for the apparent departure of the transport process from normal diffusion behavior.

When measurable adsorption of a gas by the particles of a porous medium occurs, it frequently has been found that the gas possesses an enhanced rate of flow through the medium (66). In addition to the normal rate of flow in the gas phase, there is a parallel flow due to surface transport.

As stated by Carman (66):

> When an adsorbable gas is caused to flow through a porous septum under a constant pressure gradient, each molecule colliding with the solid surface is adsorbed for a certain average period and then is

> desorbed. After the system settles down to a steady rate of flow, the amount adsorbed is constant, but it is not distributed uniformly. Since the surface concentration of adsorbed molecules depends on the pressure, the pressure gradient must give rise to a corresponding gradient of surface concentration, parallel to the direction of flow .....If the thermal motion of adsorbed molecules does not merely produce vibration about fixed adsorption sites, but endows them also with two-dimensional mobility, they can undergo diffusion along this gradient.

The transport of both physically and chemically adsorbed gases has been well established and has been reviewed by Carman.

When surface transport accompanies bulk phase transport, the moving adsorbed gas would exert a drag force on the bulk phase transport of gas. In this situation, therefore, the diffusion rate of the adsorbed gas would be larger and that of the nonadsorbed gas would be smaller than those found for only bulk phase transport of the gases.

Under the temperature and pressure conditions used in this study, measurable adsorption of nitrogen would not be expected (67). However, such would not be the case for carbon dioxide. Although no information was available concerning the adsorption of carbon dioxide on nylon fiber, a number of investigators have reported measurable amounts of adsorbed carbon dioxide for temperatures as high as 100°C. and for absolute pressures in the range of 0.1 to 1.0 atmosphere on solids such as CaF_2 (68), charcoal (69), porous glass (70), and cotton and bleached sulfite pulp (71).

Evidence for appreciable surface transport of carbon dioxide in activated charcoal was reported by Wicke and Kallenbach (18), who studied the counter-diffusion of carbon dioxide and nitrogen through a porous plug of charcoal. At 0°C. and 1 atm. total pressure, they indicated that about half of the total transport of carbon dioxide was due to surface transport. The amount of surface transport decreased gradually with increasing temperature but was still appreciable even at 200°C.

That appreciable adsorption of carbon dioxide on nylon fiber will take place is indicated by the forces of attraction operative in this system and by the results of the investigations referred to above. The general formula of a nylon monomer is shown below.

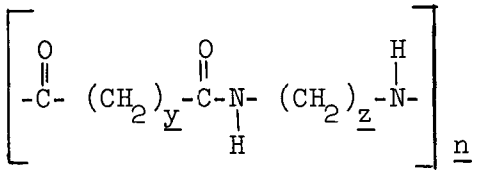

Reyerson and Peterson (72) studied the adsorption of gaseous HCl by nylon yarn at 20°C. They reported that one molecule of HCl was adsorbed per amide group at almost zero pressure. The adsorption appeared to be chemical. Similar results were reported also by Benson and Seehof (73) for HCl and BF_3. Although carbon dioxide is an acidic gas, it is certainly much weaker than HCl or BF_3. Whether or not chemical adsorption of carbon dioxide by nylon fiber occurs, a strong force of attraction would be expected between the amide groups of nylon and the carbon dioxide.

In addition to the above-mentioned force of attraction, a secondary valence force (van der Waals force) of attraction exists between the carbonyl groups of the nylon polymer and the carbon dioxide. The particular attractive force involved here would be the London or dispersion force, which arises because of the relatively high polarizability of the carbonyl groups of both the nylon and the carbon dioxide (74, 75). As a result of the oscillations of the nuclei and electrons with respect to each other, the carbonyl groups will behave as oscillating dipoles (74, 76). When these dipoles are in phase, there will be a resultant attraction between them (76). Therefore, physical adsorption of the carbon dioxide by nylon is quite likely. It is possible for a gas to be physically adsorbed at first, and then enter into a chemical reaction with the surface

of the solid; alternately, additional gas may absorb physically in second or further layers on top of a monolayer of chemically adsorbed material (67).

Haselton (77) studied the adsorption of carbon dioxide on KOH-extracted chlorite holocellulose at -78.6 and -89.3°C. Data pertaining to the differential heat of adsorption indicated that hydrogen bonding occurred between the oxygens of the adsorbed carbon dioxide molecules and the uncombined cellulosic hydroxyl groups. The possibility of forming such bonds or at least the potential for hydrogen bonding would exist between the carbon dioxide and the NH groups of nylon.

In view of the above considerations, it appeared that the departure of the transport of carbon dioxide from normal diffusion behavior above a pressure of 0.5 atm. was due to a parallel surface transport of this gas. The decrease in the nitrogen transport rate may be accounted for in terms of a drag force exerted by the moving adsorbed film on the bulk phase transport of gas. Although adsorption of carbon dioxide would be expected throughout the entire pressure range, it appeared that the contribution to the total observed transport of carbon dioxide by surface transport was negligible below a pressure of about 0.5 atm. These conclusions are supported also by the results presented below.

Flux Ratio

For the five runs made with Bed No. N43-2-D at 0.264 atm., the mean flux ratio, N_N/N_C, was -1.16. The coefficient of variation was 6.30%. This degree of reproducibility represented a very marked improvement over that obtained for the preliminary studies.

For uniform pressure counterdiffusion of nitrogen and oxygen through a pellet of silica gel at 1 atm. and 25°C., Hoogschagen (19) found that the ratio

of the nitrogen flux to the oxygen flux was -1.06. This value compared favorably with the theoretical value of -1.07. For the same pellet and test conditions, the experimental flux ratio of oxygen to carbon dioxide was -0.552, compared to a theoretical value [Equation (18)] of -1.18. This difference was attributed to surface transport of carbon dioxide.

Henry, et al. (78) found similar results for the gas pairs nitrogen-helium and carbon dioxide-helium for counterdiffusion through an alumina catalyst pellet at 1 atm. and 30°C. The experimental value of the helium-nitrogen flux ratio agreed almost exactly with the theoretical value. A value of -2.74 was obtained for the helium-carbon dioxide flux ratio; the theoretical value was -3.32.

Although the flux data of this study indicated that surface transport was not significant compared to the total transport of carbon dioxide at a pressure of 0.264 atm., surface transport, nevertheless, would be taking place even at this pressure. In agreement with the findings of the above workers, this would account qualitatively for the 7% difference between the experimental value of the flux ratio, -1.16, and the theoretical value of -1.25.

In Fig. 15, the flux ratios obtained for Bed No. N43-2-D have been plotted versus total pressure. Similar results were found also for Bed No. N43-1-D. In spite of the scatter of the data, which may be attributed to axial pressure differences, there is a trend for the absolute value of the flux ratio to decrease with increasing pressure. The solid line represents the result of a least squares analysis of all the data. A correlation coefficient of -0.796 was obtained. The zero-pressure intercept is -1.29.

Another least squares analysis of the data, excluding the data pertaining to a pressure of 1 atm., gave the dashed line. For this line the correlation

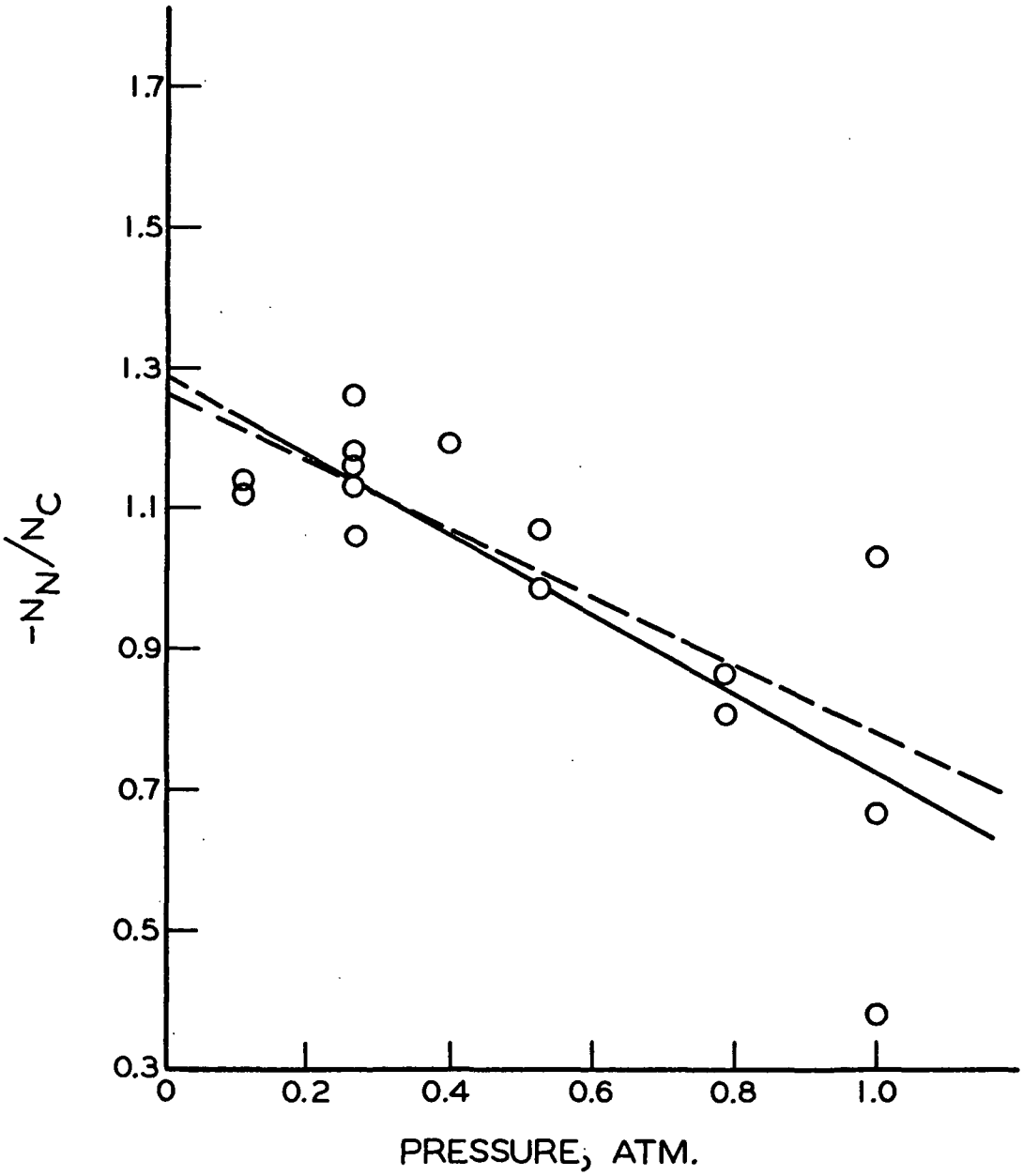

Figure 15. Flux Ratio: Bed No. N43-2-D

coefficient is -0.827, and the zero-pressure intercept is -1.26. In both instances, the zero-pressure values of the flux ratio agreed quite closely with the theoretical value of -1.25.

It would appear then that the bulk phase counterdiffusion process was not equimolal. The pressure dependence of the flux ratio was most probably the result of adsorption and surface transport of carbon dioxide.

Diffusion Coefficient

For both beds, the observed transport rates were approximately independent of pressure below a pressure of about 0.5 atmosphere. These results indicated that the bulk phase transport process was normal counterdiffusion. Since a departure from normal diffusion behavior in the bulk phase would not occur with increasing pressure, the bulk phase transport process would be normal diffusion over the entire pressure range of 0.1 to 1.0 atm.

As a means of affirming this conclusion, the ratio of the effective normal diffusion coefficient to the effective Knudsen diffusion coefficient was estimated from the intermediate diffusion equation, Equation (15). Using the results obtained for Bed No. N43-2-D at pressures of 0.110 and 0.264 atm., this equation was solved by a trial and error procedure for the group $(\underline{\underline{D}}_{AB})_e P/(\underline{\underline{D}}_{KA})_e$. The value obtained for this ratio was approximately 0.001.

At a pressure of 1 atm., $(\underline{\underline{D}}_{KA})_e$ would be a thousand times larger than $(\underline{\underline{D}}_{AB})_e$. At a pressure of 0.1 atm., the former coefficient would be a hundred times larger than the latter coefficient. Within this pressure range, the bulk phase diffusion process for both beds was in the normal region of ordinary diffusion.

For the five runs made with Bed No. N43-2-D at a pressure of 0.264 atm., the mean value of $(\underline{\underline{D}}_{AB})_{\underline{e}}$ was 0.177 sq. cm./sec. The coefficient of variation was 0.63%.

According to theory, a plot of $1/(\underline{\underline{D}}_{AB})_{\underline{e}}$ versus total pressure should be a straight line passing through the origin. The curves obtained for Beds N43-1-D and N43-2-D are shown in Fig. 16 and 17, respectively.

For Bed No. N43-2-D, the curve is linear up to a pressure of about 0.7 atm., at which point there is a pronounced curvature upward. Such curvature is not as evident for the curve obtained for Bed No. N43-1-D. In agreement with theory, both curves extrapolate quite closely to the origin.

When gaseous diffusion along the channels of a porous medium is accompanied by surface transport, Damköhler (79) pointed out that the transport coefficient for this combined process should be larger than the coefficient expected in the absence of surface transport. The results presented here agree with this concept.

For the normal counterdiffusion of gases in a porous medium, molecule-wall collisions do not contribute significantly to the diffusion resistance. The flux ratio is, however, controlled by molecule-wall collisions and the related momentum exchange. When normal diffusion is accompanied by surface transport, the momentum exchange between the bulk phase gas molecules and the moving adsorbate must be considered.

In the present instance, nitrogen moves in the -z direction and carbon dioxide in the +z direction. The net flux in the bulk phase will be in the -z direction. The moving adsorbate will transfer +z momentum to the bulk phase, which is equivalent to the removal of -z momentum from the bulk phase. To balance this momentum exchange an axial pressure gradient would be required,

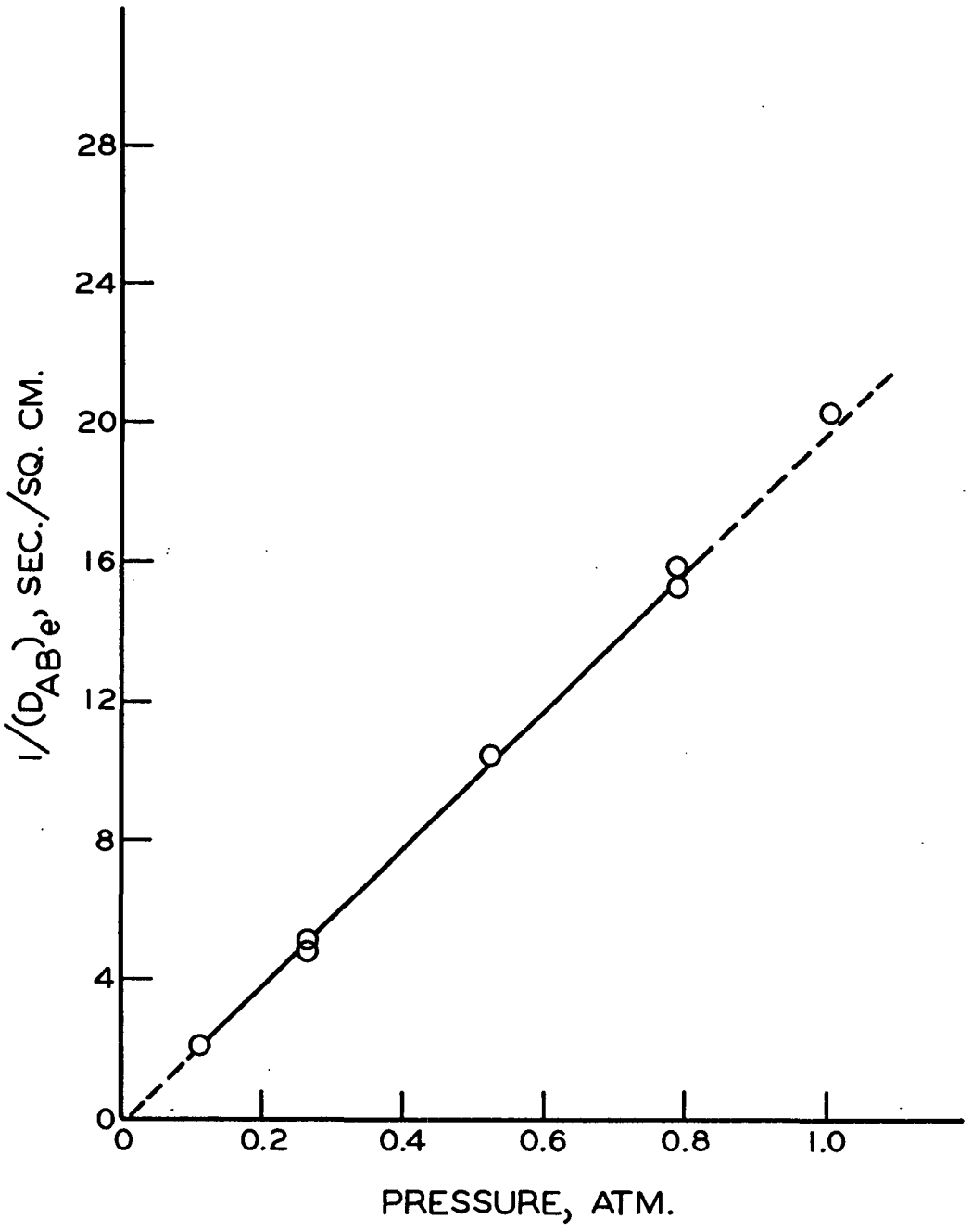

Figure 16. Diffusion Coefficient: Bed No. N43-1-D

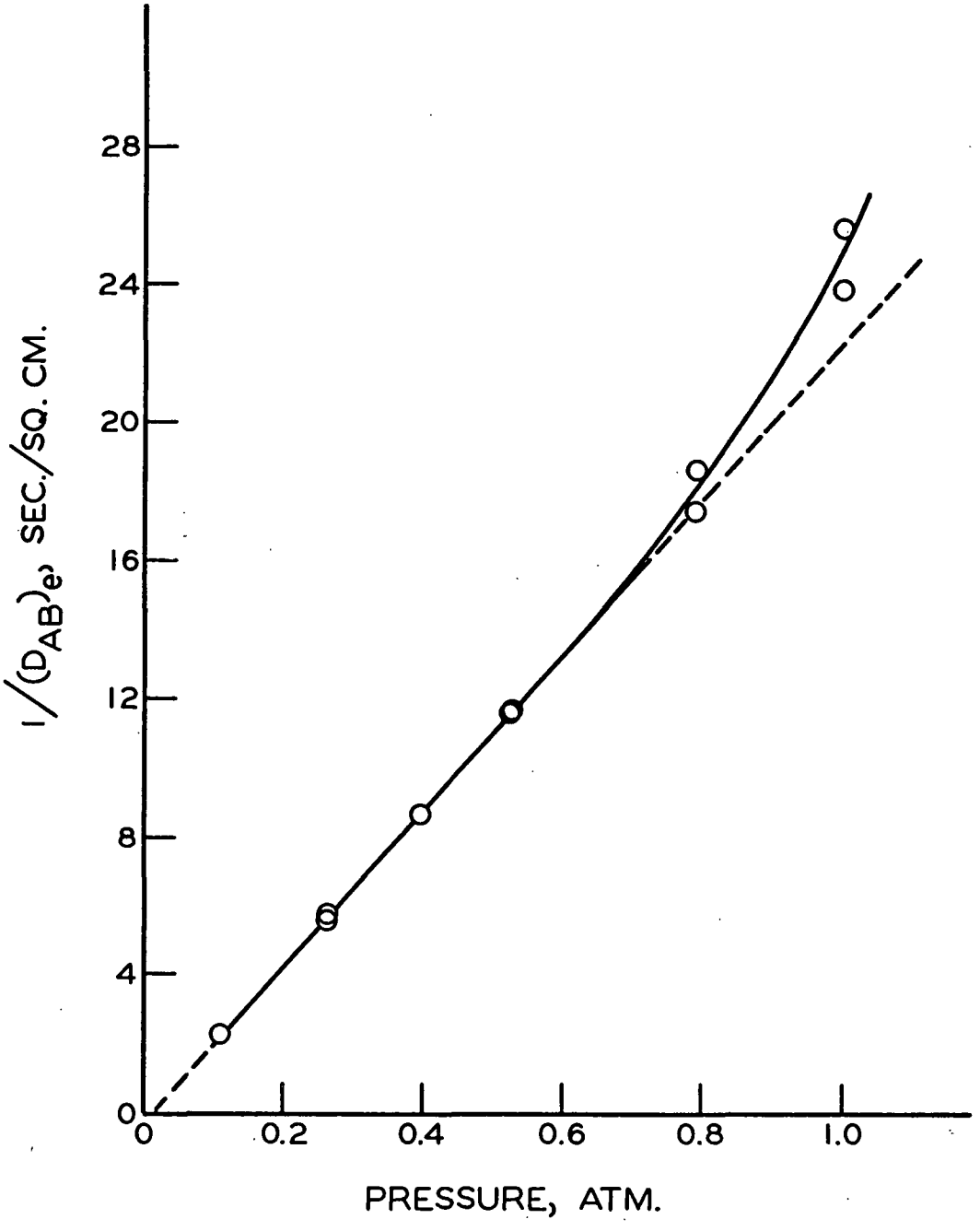

Figure 17. Diffusion Coefficient: Bed No. N43-2-D

the direction of which would be such as to further enhance the transport of carbon dioxide.

Consequently, the diffusion resistance in this case would appear larger than that which would be obtained for normal diffusion in the absence of surface transport of carbon dioxide. Below a pressure of about 0.5 atm., surface transport of carbon dioxide appeared negligible, and the calculated diffusion coefficient apparently was the effective normal diffusion coefficient.

At a pressure of 0.264 atm., the effective normal diffusion coefficient decreased from 0.2078 sq. cm./sec. for a porosity of 0.810 to 0.1770 sq. cm./sec. for a porosity of 0.742. This behavior agreed with the findings of previous investigators.

PARTIALLY SATURATED FIBER BEDS

Ordinary diffusion measurements were made with another bed formed from the 43-micron diameter nylon fibers, Bed No. N43-3-PS which was partially saturated with dioctyl phthalate to varying degrees. Several series of variable pressure runs were made at each of the following degrees of saturation: 0.701, 0.495, 0.407, 0.295, 0.195, and 0.108.

The degree of saturation was calculated from the weight of DOP in the bed, the absolute void volume of the dry bed as it would exist in the diffusion chamber ($\epsilon = 0.710$), and the density of DOP at 40°C. To determine whether there was an appreciable loss of liquid from the bed due to handling, the degree of saturation was determined before and after a series of diffusion runs. The absolute difference between these values never exceeded 0.003. The final degree of saturation will be used here.

For each degree of saturation, the results presented were generally obtained over a period of 2-3 days. The reproducibility exhibited by these data gives evidence for the fact that the distribution of the liquid was at equilibrium.

DIFFUSION FLUXES

A plot typical of the variation of the nitrogen and carbon dioxide diffusion rates with total pressure is shown in Fig. 18, for the bed which had a degree of saturation of 0.295. These curves are quite similar to those obtained for the dry beds. It should be noted, however, that the reproducibility of the fluxes is quite good, not only at the lowest pressure but also at the highest pressure used. This improvement over the dry bed results pertained to all of the partially saturated beds tested and was primarily a consequence of a decrease in the effect of small axial pressure differences on test specimens of decreased permeability.

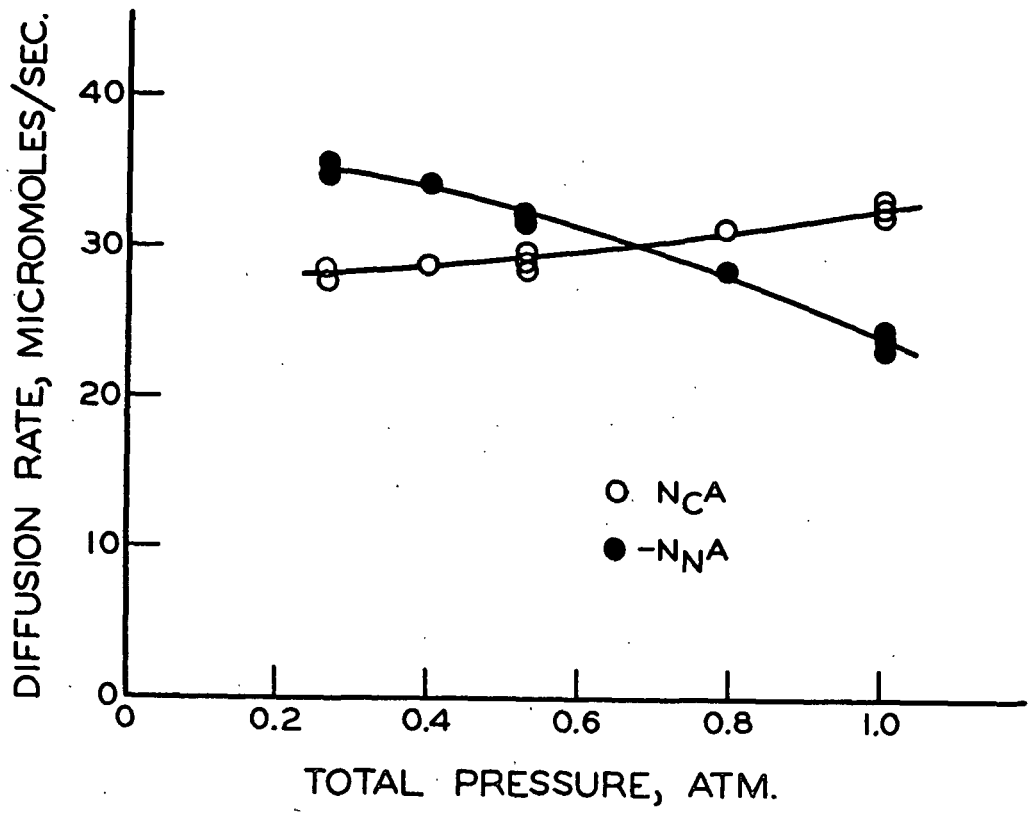

Figure 18. Diffusion Fluxes, $\underline{s}$ = 0.295.

The increase in the carbon dioxide diffusion rate and the decrease in the nitrogen diffusion rate with increasing pressure are consistent, as before, with the hypothesis of transport of adsorbed carbon dioxide. This departure of the transport rates from apparent normal diffusion behavior was less pronounced for the partially saturated beds than for the dry beds, as may be seen in Fig. 19.

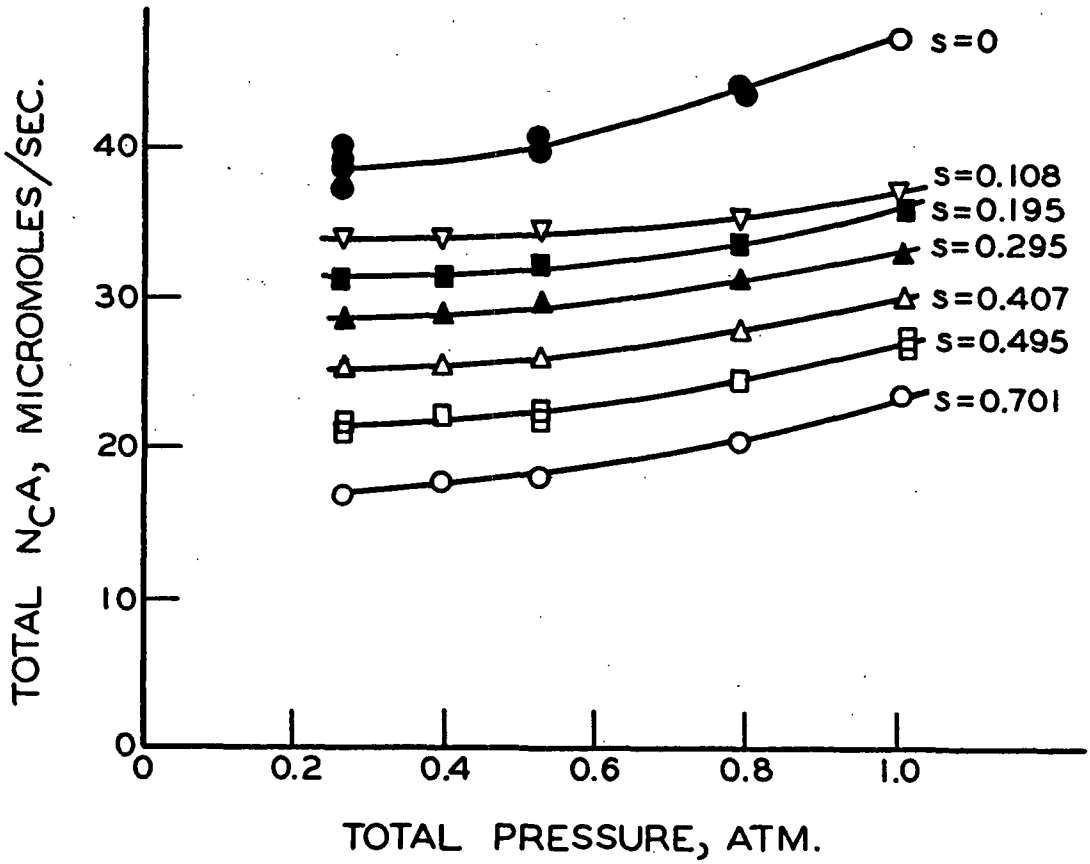

Figure 19. CO_2 Diffusion Rates

With degree of saturation as the parameter, the carbon dioxide diffusion rates were plotted against pressure in Fig. 19. The curve for zero degree of saturation pertains to Bed Number N43-2-D (ϵ = 0.742). At any given pressure, the diffusion rate increased with decreasing degree of saturation. The measured

driving force was observed to be proportional to the degree of saturation. Therefore, the resistance to diffusion in the bulk phase must have decreased with decreasing degree of saturation.

As was observed for the dry nylon fiber beds, the diffusion rates were relatively independent of pressure below a pressure, in this case, of about 0.6 atmosphere. Above this pressure, a curvilinear increase (increasing slope) in the carbon dioxide diffusion rate with increasing pressure persisted at all degrees of saturation. Previously, it was deduced that such behavior was caused by the effect of surface transport of carbon dioxide superimposed on a transport of the gas by normal diffusion.

The London force of attraction discussed previously would exist also between the carbon dioxide and the dioctyl phthalate, which has the formula shown below.

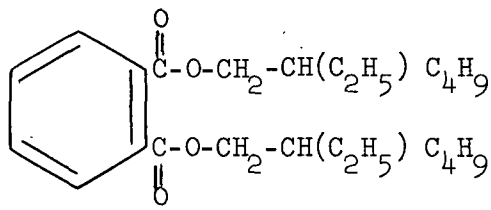

Therefore, physical adsorption of the carbon dioxide by the DOP is quite likely to occur and in turn surface transport of carbon dioxide in the partially saturated beds.

In terms of the postulated surface transport process, the data shown in Fig. 19 indicated a decrease in the surface transport rate of carbon dioxide as the degree of saturation decreased, with the exception of the dry bed. Since the bulk phase concentration gradient decreased with decreasing degree of saturation, the driving force for surface transport also would decrease. In addition, the

resistance to surface transport would increase as the degree of saturation decreased, since the average tortuosity of the liquid channels appears to increase as a porous medium is desaturated (8, 49).

Below a degree of saturation of about 0.4, the data indicated further that the contribution to the total observed transport of carbon dioxide by surface transport was greater for the dry bed than for the partially saturated beds. The measured concentration gradient was smaller for the dry bed than for any of the partially saturated beds. However, the driving force for surface transport could have been greater for the dry bed than for the partially saturated beds due to the adsorption of more carbon dioxide by the nylon than by the DOP. In addition, the path taken by the mobile adsorbed gas might have been less tortuous, on the average, for the dry bed than for the partially saturated beds.

FLUX RATIO

The variation of the flux ratio (nitrogen to carbon dioxide) with pressure was quite similar for all of the partially saturated beds. Figure 20, which shows the data for the degree of saturation of 0.295, typifies this variation. Like the results obtained for the dry beds, the absolute values of the flux ratios for the partially saturated beds decreased with increasing pressure. This behavior is consistent with the surface transport hypothesis.

The value of the flux ratio at a pressure of 0.264 atm. for the partially saturated bed (s=0.295) is -1.23, which differs by only 1.6% from the theoretical value of -1.25. Extrapolation of the curve shown in Fig. 20, as well as the curves for the other partially saturated beds, to zero pressure yielded a flux ratio value which was only a few per cent different from the value at 0.264 atm.

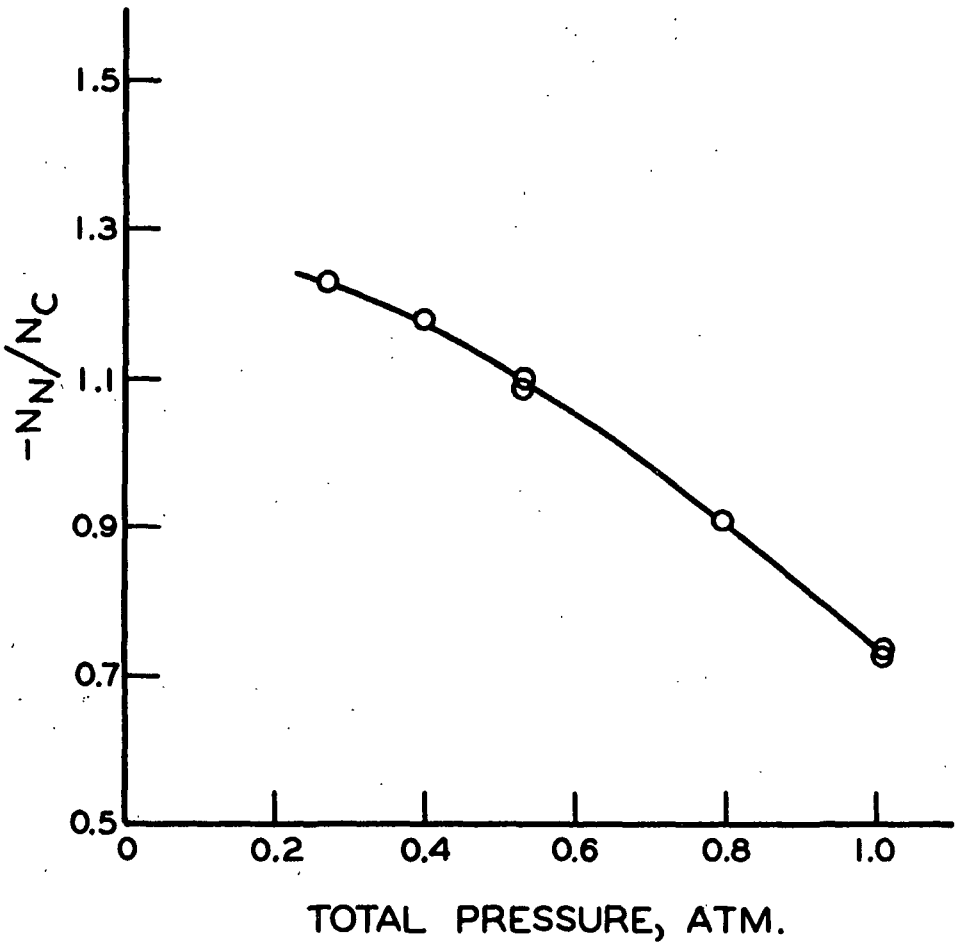

Figure 20. Flux Ratios, $\underline{s}$ = 0.295

For the dry beds, the data indicated that the variation of the flux ratio with pressure was approximately linear, and that the theoretical value of -1.25 was approached as the pressure approached zero. In terms of the surface transport hypothesis, these differences between the dry and the partially saturated beds indicated that the amount of carbon dioxide adsorbed by the DOP was less than that adsorbed by the nylon. In fact, it would appear valid to assume that the adsorption of carbon dioxide below a pressure of 0.264 atm. was negligible in the case of the partially saturated beds.

The values of the flux ratio obtained at a pressure of 0.264 atm. were taken to pertain to normal diffusion in the absence of adsorption of carbon dioxide. These values together with their average numerical deviations are listed in Table VI.

TABLE VI

FLUX RATIOS, $\underline{P}$ = 0.264 ATM.

Degree of Saturation	Flux Ratio $\underline{N_N}/\underline{N_C}$
0.701	-1.34 ± 0.01
0.495	-1.33 ± 0.01
0.407	-1.26 ± 0.02
0.295	-1.24 ± 0.02
0.195	-1.26 ± 0.01
0.108	-1.24 ± 0.08

It was previously established that

$$(M_A/M_B)^{1/2} < \left| N_B/N_A \right| < (M_A/M_B) \qquad (24)$$

where $(\underline{M_A}/\underline{M_B}) > 1$. In the present instance, the lower limit of Equation (24) would be 1.25 and the upper limit would be 1.57.

The data listed in Table VI were in good agreement with the lower limit of Equation (24) for beds in which the liquid occupied less than about half of the void volume. Above a degree of saturation of 0.5, the experimental values of the flux ratio were in between the limits given by Equation (24).

The above variation of the flux ratio with degree of saturation was opposite to the effects expected of phenomena associated with adsorption of carbon dioxide. At a pressure of 1.0 atm., the absolute value of the flux ratio increased from about 0.6 at $\underline{s}$ = 0.701 to about 0.8 at $\underline{s}$ = 0.108.

Small axial pressure differences, of the type postulated previously, could not have been responsible for the behavior shown in Table VI. If such were the

case, the absolute values of the flux ratio would be expected to be less than the theoretical value of 1.25 and to show a continual increase with degree of saturation.

In agreement with the theories of Evans, et al. (6) and of Dullien and Scott (7), however, the marked decrease in the absolute value of the flux ratio below a degree of saturation of about 0.5 was probably related to a significant increase in the frequency of molecule-wall collisions.

DIFFUSION COEFFICIENT

From the low-pressure flux data, it appeared that the bulk phase transport process was normal diffusion in the pressure range of 0.264 to 1.0 atm. for all degrees of saturation. From the data obtained at pressures of 0.264 and 0.396 atm., an estimate was made of the group $(\underline{\underline{D}}_{AB})_e P/(\underline{\underline{D}}_{KA})_e$ using the intermediate diffusion equation. For the bed which had a degree of saturation of 0.108, the value of this ratio was greater than zero but less than 0.001. Similar results were obtained for the other partially saturated beds.

Plots of the reciprocal values of the effective normal diffusion coefficient, calculated from Equation (10), versus total pressure are shown in Fig. 21. All of the curves are linear below a pressure of about 0.5 atm. and have a common zero-pressure intercept, which is quite close to the origin. This fact and the fact that the curves are shifted upward with increasing degree of saturation indicated that the data were internally consistent. The data for $s=0$ pertain to Dry Bed No. N43-2-D ($\epsilon = 0.742$).

Above a pressure of 0.5 atm., all of the curves deviate from linearity and curve upward to varying degrees. The same type of behavior was observed for the dry beds and was related to the effects of surface transport of carbon dioxide.

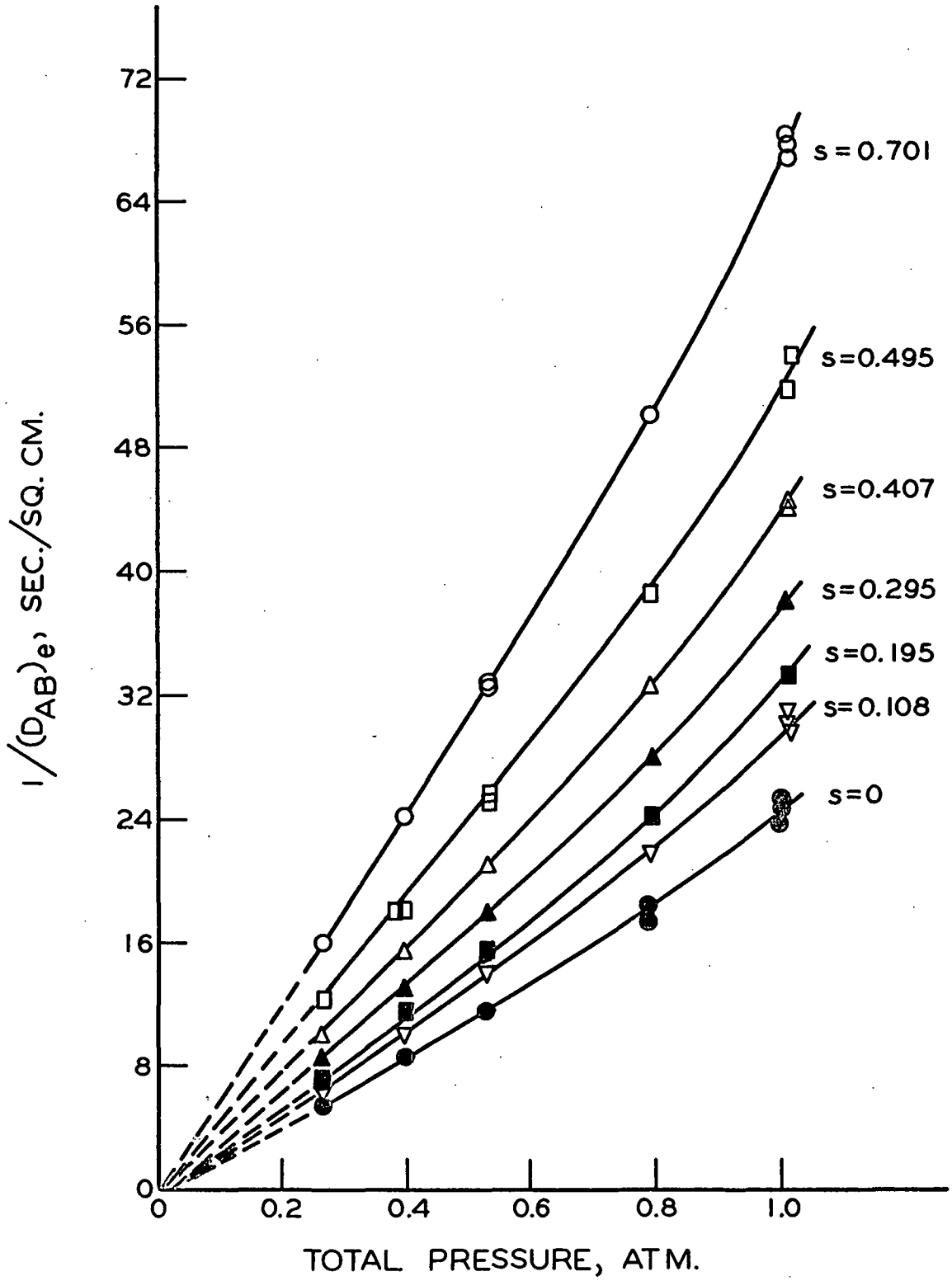

Figure 21. Diffusion Coefficients

The variation of the effective normal diffusion coefficient with degree of saturation is shown in Fig. 22. The data obtained at a pressure of 0.264 atm. were used, since adsorption and surface transport of carbon dioxide appeared to be negligible at this pressure. $(\underline{D}_{\underline{AB}})_{\underline{e}}$ increases quite regularly as the degree of saturation decreases. This behavior must be due in part to the expected increase in area available for diffusion. The variation of the other factors, such as the tortuosity and pore shape factors, with degree of saturation is not as apparent and will be considered later. For the present, it may be concluded that the net resistance of the partially saturated beds to diffusion decreased as the degree of saturation decreased.

The data points at $\underline{s}=0$ in Fig. 22 are for Bed Number N43-2-D, which had a porosity of 0.742. The results of the dry bed studies indicated that the value of the effective normal diffusion coefficient should change only slightly with a decrease in porosity from 0.742 to 0.710. Therefore, the value of this coefficient obtained by extrapolation of the curve in Fig. 22 to $\underline{s}=0$ should differ only slightly from the data points shown at $\underline{s}=0$. Such a result is shown and attested to the internal consistency of the data and indicated a good degree of between-bed reproducibility of the porous structure of the beds. It may be concluded also that these data represented an accurate and precise measure of the variation of the effective normal diffusion coefficient with degree of saturation.

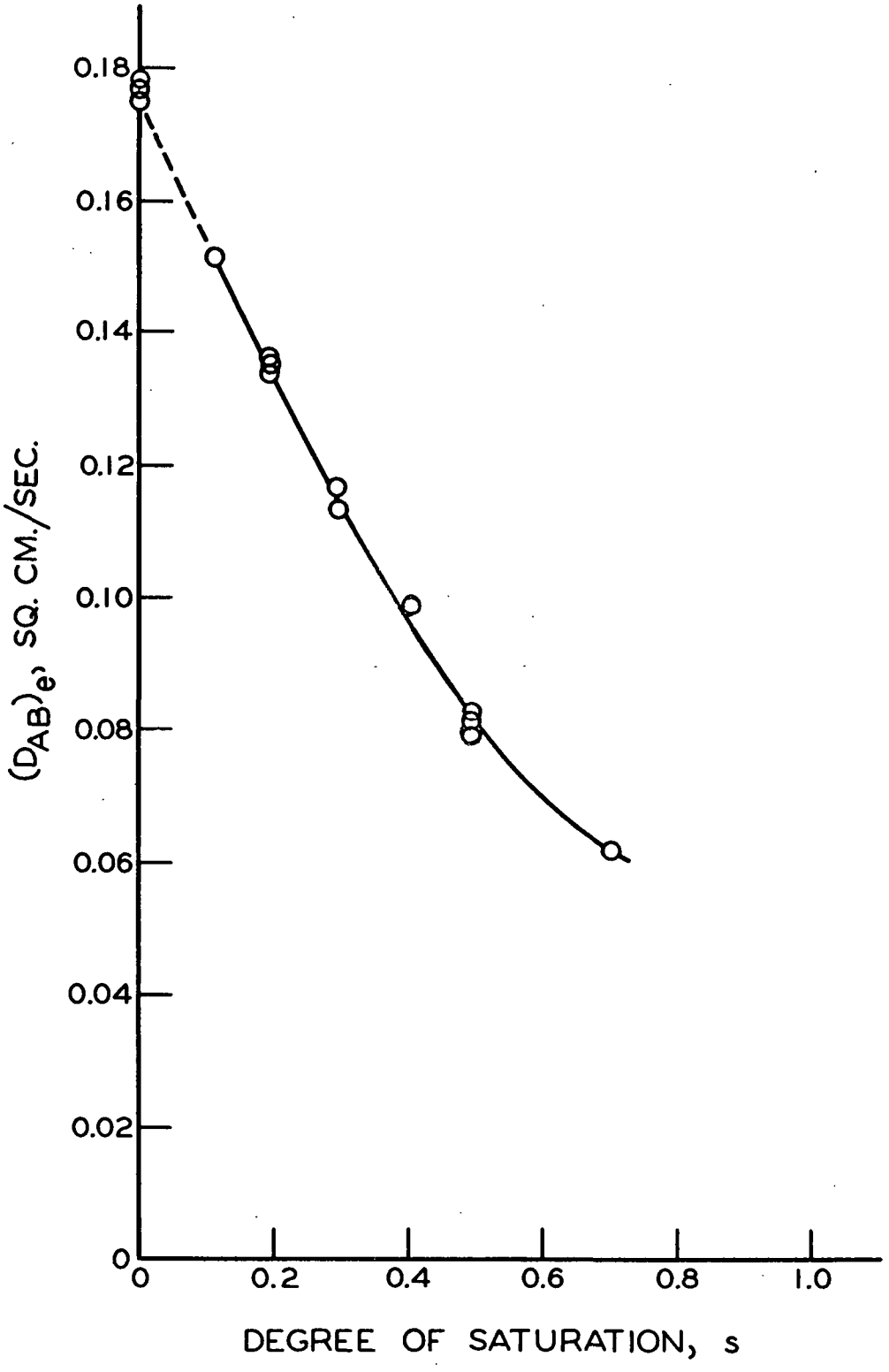

Figure 22. Diffusion Coefficients, $\underline{P}$ = 0.264 atm.

ANALYSIS OF RESULTS

Since surface transport of carbon dioxide was apparently negligible at a pressure of 0.264 atm., the data obtained at this pressure were used to analyze the normal diffusion process. The fundamental momentum exchange processes were examined in relation to the diffusion flux ratio. Using the geometric model expressions for the diffusibility, the diffusion resistance of the partially saturated nylon fiber beds was analyzed.

Further analyses were concerned with (1) estimating the contribution of surface transport of carbon dioxide to the total observed transport of this gas, and (2) evaluating the results of the nonuniform pressure study in terms of a theory developed by Evans, et al. (64).

NORMAL DIFFUSION

FLUX RATIO

Theoretically, the ratio of the nitrogen flux to the carbon dioxide flux for the steady normal counterdiffusion of these gases through a porous medium under uniform pressure conditions in an open system and in the absence of surface transport should lie within the limits given by Equation (24). For small pores, the flux ratio should be approximately equal to -1.25. As the pore size increases, the flux ratio should depart from this value and approach -1.57. According to theory, this transition appeared to be related to a decrease in the molecule-wall collisions and consequently to a decrease in molecule-wall momentum exchange.

When the liquid occupied more than about half of the void volume of the partially saturated beds, the flux ratio was equal to -1.34. Below this degree

of saturation, the flux ratio was approximately equal to -1.25 and was independent of any further decrease in the degree of saturation.

To examine the variation of the axial momentum exchange resulting from molecule-wall collisions with degree of saturation, the ratio of the intermolecular momentum exchange to the molecule-wall momentum exchange was calculated from the data obtained at a pressure of 0.264 atmosphere. The axial momentum transferred to the pore walls by carbon dioxide molecules was estimated from Equation (20).

The momentum exchange resulting from collisions of carbon dioxide molecules with nitrogen molecules was estimated by means of an expression derived by Present (16) for one-dimensional normal counterdiffusion. Present used the Stefan-Maxwell momentum-transfer method in his derivation, which necessarily incorporated the assumptions outlined in Appendix I. As applied to diffusion through porous media, this expression would be

$$M_{AB} = RT(y_B N_A - y_A N_B)/(D_{AB})_e \qquad (34),$$

where $\underline{M}_{\underline{AB}}$ is the axial momentum lost by species A (CO_2) per unit time per unit volume by collision with species B (N_2). $\underline{M}_{\underline{AB}}$ was calculated for a thin cylinder at $z=0$, which is the carbon dioxide-rich side of the bed.

Relative to the molecule-molecule momentum exchange, a marked change in the variation of the molecule-wall momentum exchange with degree of saturation was clearly evident when the ratio of these two momentum exchanges ($\underline{M}_{\underline{AB}}/\underline{M}_{\underline{Aw}}$) was plotted against degree of saturation. As may be observed in Fig. 23, a significant increase in the slope of this curve occurred at a degree of saturation of about 0.5. While this behavior was indicative of a marked increase in the frequency of intermolecular collisions, it indicated also a marked decrease

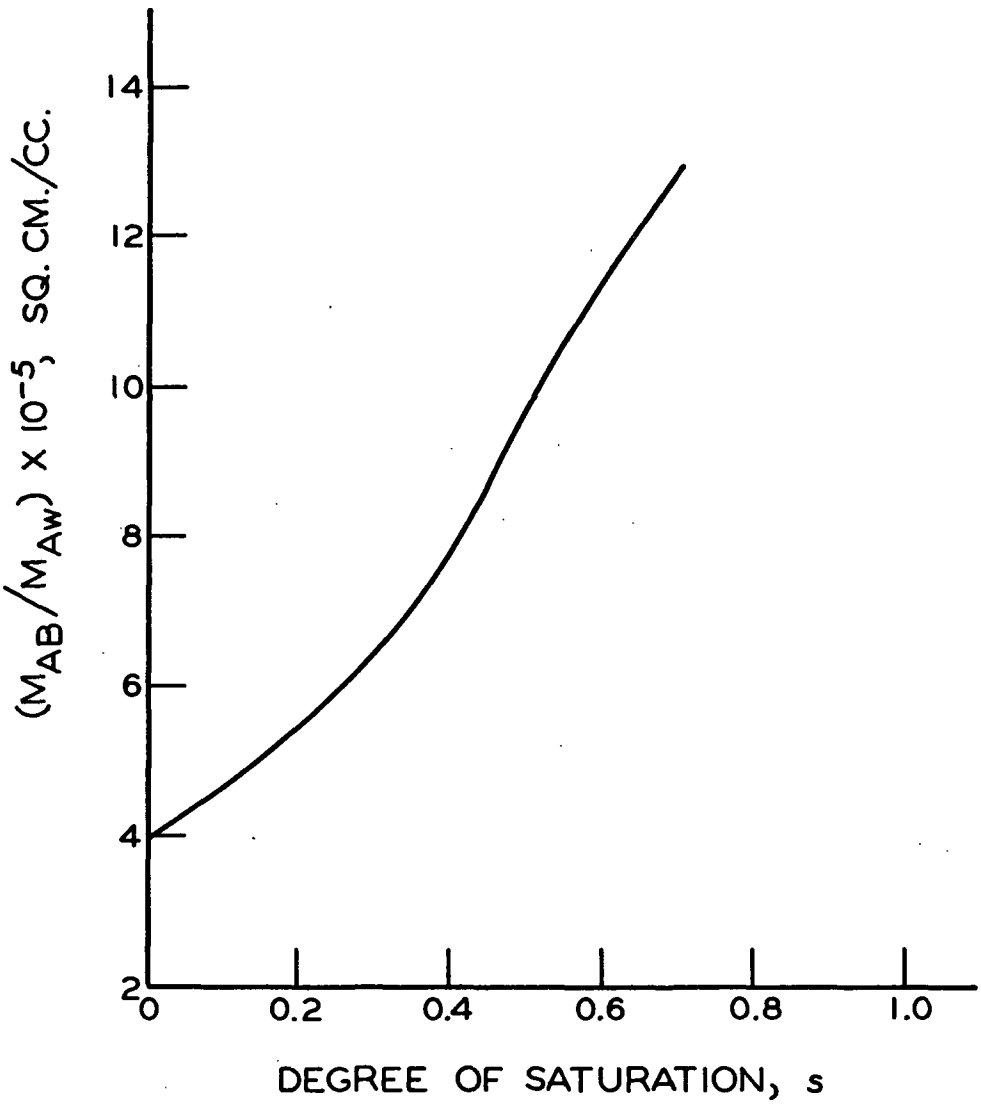

Figure 23. Momentum Flux Ratio, $\underline{P}$ = 0.264 Atm.

in molecule-wall collisions. Previously, it was pointed out that the net axial momentum transferred to the pore walls would be zero providing the pores were small enough so that the radial variation of the diffusion fluxes would be negligible. Satisfaction of these requirements led to the conclusion that the flux ratio would be equal to the square root of the inverse ratio of the molecular weights of the gases involved.

The net axial momentum transferred to the pore walls was estimated from Equation (21) using the data obtained at a pressure of 0.264 atmosphere. This was found to be approximately -0.01 dyne/sq. cm. above a degree of saturation of about 0.5 and was not less than zero nor greater than +0.001 dyne/sq. cm. below this region of saturation.

Inspection of Equation (21) indicated that when the net axial momentum transferred to the pore walls was less than zero,

$$N_B/N_A < -\sqrt{M_A/M_B} .$$

This observation is consistent with the results of this study.

The apparent net transfer of -z-momentum to the pore walls could have arisen from transverse velocity gradients present in the larger pores of the beds in which the liquid phase occupied more than about half of the void volume.

As the degree of saturation decreased, smaller and smaller pores would be opened to diffusion. Consequently, the contribution to the molecule-wall momentum exchange by momentum transfer due to transverse velocity gradients within the pores would be expected to decrease. In agreement with theory it was found that as the net axial momentum transferred to the pore walls approached zero, the flux ratio approached the theoretical value of -1.25.

DIFFUSION RESISTANCE

As the degree of saturation decreased, it was found that the effective normal diffusion coefficient increased. While it was apparent that the area available to the diffusing gases increased as $\underline{s}$ decreased, the variation of the other structural characteristics of the partially saturated beds with $\underline{s}$ was not as apparent. It was not the purpose of this thesis to study the porous structure of partially saturated fiber beds by means of diffusion experiments. However, analysis of the data in terms of the structural characteristics of the partially saturated fiber beds would contribute to understanding the variation of the diffusion resistance of such media with degree of saturation.

Analysis of the diffusion resistance was made in terms of the reciprocal diffusibility, $1/\delta$, which is dependent only on the properties of the porous medium. For normal diffusion, the reciprocal diffusibility is equal to the ratio of the diffusivity, $\underline{\underline{D}}_{AB}$, to the effective normal diffusion coefficient, $(\underline{\underline{D}}_{AB})_e$. The diffusivity for carbon dioxide-nitrogen was calculated from the Chapman-Enskog formula for the diffusivity of gases at low density, Equation (2). At 1.0 atm. and 40°C., the value calculated was 0.1681 sq. cm./sec.

Effect of Liquid Phase

In simplified terms, the reciprocal diffusibility for partially saturated porous media was deduced to be represented by the following expression:

$$1/\delta = \tau/[P_s \epsilon (1-s)^n] \qquad (35).$$

The variation of $\ln(1/\delta)$ with $\ln(1-\underline{s})$ is shown in Fig. 24. As $(1-\underline{s})$ increased, the reciprocal diffusibility decreased. Below a degree of saturation of about 0.5, the curve was apparently linear.

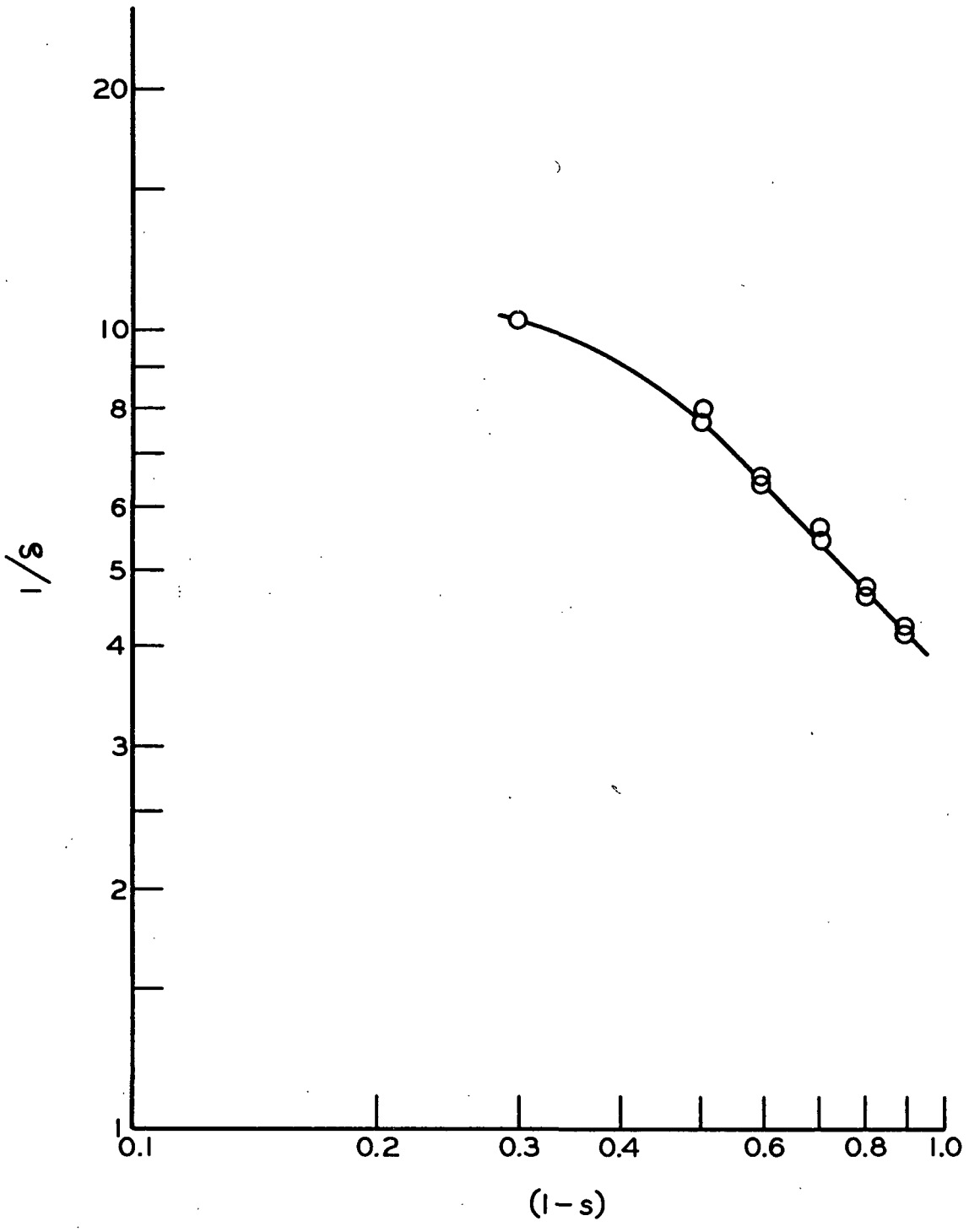

Figure 24. Reciprocal Diffusibility, $\underline{P}$ = 0.264 Atm.

For the linear portion of the curve, the data were fitted to a linear regression equation using the method of least squares. The resulting equation was

$$\ln(1/\delta) = -1.084 \ln(1-s) + 1.312 \qquad (36).$$

A close relationship between these variables was indicated by the correlation coefficient, -0.9986. Equation (36) may be rearranged into a form analogous to Equation (35).

$$1/\delta = 3.714/(1-s)^{1.084} \qquad (37).$$

The fact that the power of $(1-\underline{s})$ was greater than unity could indicate that through some of the gas-filled pores transport of the gases did not take place. It could be indicative also of the effects of pore interaction on the area available for diffusion, as discussed previously. Expressed as a percentage of $\epsilon(1-\underline{s})$, the difference between $\epsilon(1-\underline{s})$ and $\epsilon(1-\underline{s})^{1.084}$ was 4% at $\underline{s}$=0.407 and 1% at $\underline{s}$=0.108. Therefore, the effects of the above factors on the area effective in gas transport were apparently quite small.

Comparing the geometric model expression for $1/\delta$ with the related empirical expression, it may be seen that $\tau/(\underline{P}_{\underline{s}}\epsilon)$ is equal to 3.71. For the bed studied, the porosity was 0.710. Consequently, $\tau/\underline{P}_{\underline{s}}$ would be equal to 2.64 and was apparently constant for the partially saturated beds in which the gas phase occupied more than half of the void volume.

As the bed is progressively desaturated, the larger pores or void spaces will be emptied of liquid before the smaller pores. Below some degree of saturation, the portion of the larger pores occupied by gas will become relatively constant. However, the gas-filled portion of the smaller pores will continue to increase as the degree of saturation decreases. Therefore, the effect of pore constrictions on the diffusion resistance of the partially saturated beds would be

expected to decrease as the bed was progressively desaturated. The pore shape factor would thus be expected to increase with decreasing degree of saturation.

In order for the ratio of the tortuosity factor to the pore shape factor to be independent of degree of saturation, as indicated by Equation (37), the tortuosity factor would be required to increase with decreasing degree of saturation. If at some degree of saturation s the pore shape factor were 0.5, the tortuosity factor would be 1.32, according to Equation (37). For a dry unconsolidated porous medium with a relatively narrow pore size distribution, Carman (8) has indicated that the pore shape factor would be approximately unity. Therefore when $s=0$, the tortuosity factor for the fiber bed studied would be 2.64. In consideration of the values for the tortuosity factor listed by Carman (8), the above values are quite reasonable.

For porous media partially saturated with a conducting solution, which wets the solid, an empirical relationship, usually called "Archie's Law," exists (33). The part of the pore space not filled with wetting-conducting solution is filled with nonwetting, nonconducting fluid. The solid must be nonconducting also. This "law" may be expressed in the following form:

$$R_s/R_0 = s^{-n} \qquad (38),$$

where R_s is the resistivity of the medium at a degree of saturation s, R_0 is the resistivity of the saturated sample, and n is a constant called the saturation exponent. For clean sands n has a value of about two. For other materials, it may be greater than or less than two (33).

A relationship quite analogous to "Archie's Law" appeared to exist for gaseous diffusion in the partially saturated nylon fiber beds if the gas phase degree of saturation, $(1-s)$, were used instead of the liquid phase degree of

saturation, s. As may be observed from Equation (37), the proportionality constant, 3.714, is the reciprocal diffusibility of the dry fiber bed. Therefore, Equation (37) may be expressed in the following form:

$$(D_{AB})_{e_r} = (D_{AB})_{e_s}/(D_{AB})_{e_0} = (1-s)^n \qquad (39),$$

where $(D_{AB})_{e_r}$ is the relative diffusion coefficient.

Fatt's (24) network model studies showed that the exponent in Archie's relation for the wetting phase was a function of the network structure of the porous medium and independent of the pore size distribution. The value of the exponent was 4.0 for a network structure in which only four channels were joined to each channel. As the number of channels joined to each channel approached infinity, the value of the exponent approached unity. Similar conclusions were apparently applicable to the results of Fatt's nonwetting-phase model studies shown in Fig. 1, in which the variation of the nonwetting-phase relative resistivity with nonwetting-phase degree of saturation was illustrated. In Fig. 25, the experimental data of this study are shown along with Fatt's theoretical results for the triple hexagonal and the parallel capillary models which had β-factors of ten and infinity, respectively. Above a nonwetting-phase degree of saturation of about 0.5, the experimental curve was quite similar to Fatt's derived curves and lied close to the curve for the highly branched parallel capillary model.

In consideration of the results of Fatt's network model studies and the results shown in Fig. 25, it is hypothesized that the exponent of Equation (39), 1.084, is a characteristic of the network structure of the partially saturated fiber beds above $(1-s)=0.5$. The void spaces of these beds apparently constituted a highly branched pore structure.

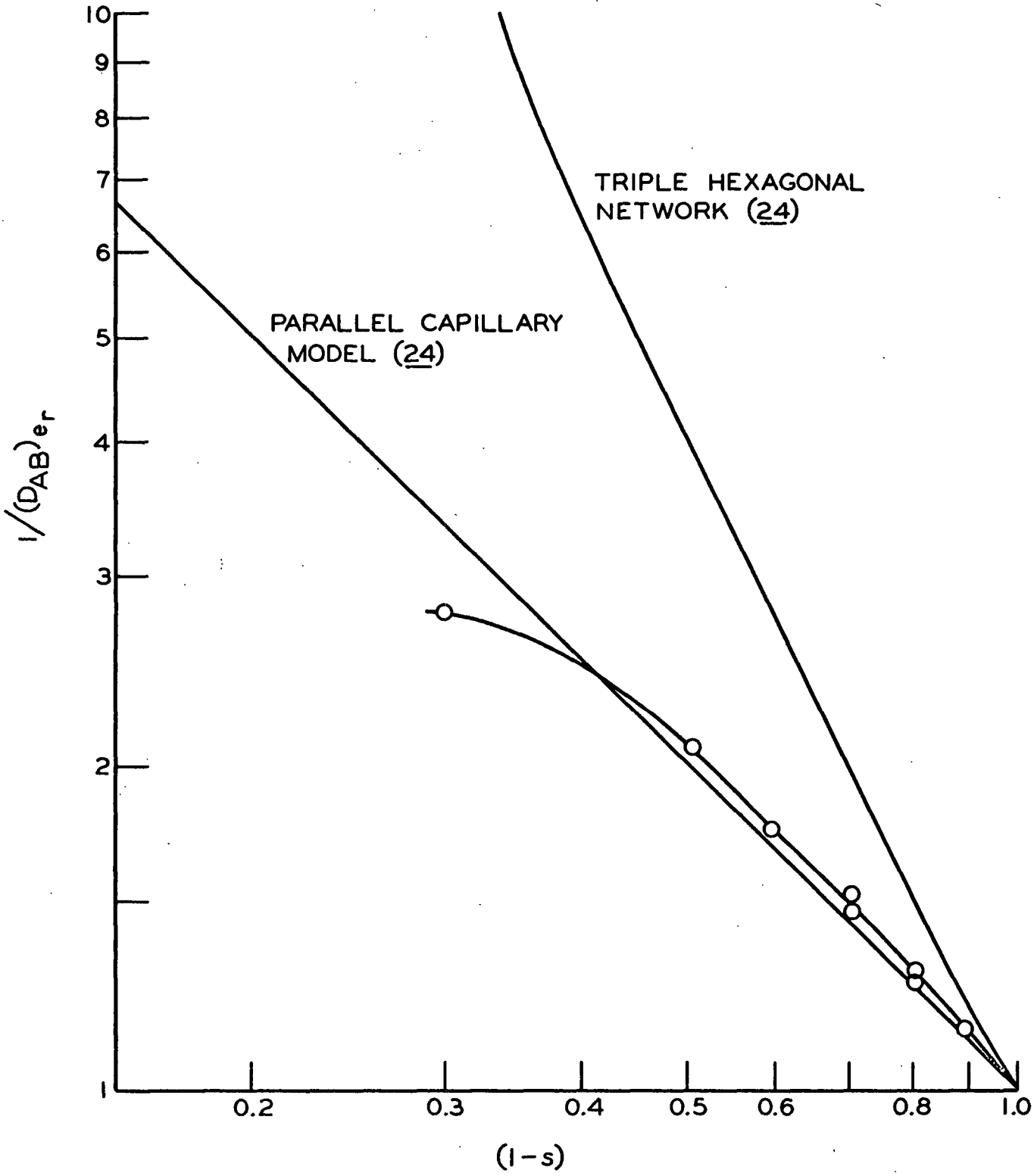

Figure 25. Relative Diffusion Coefficient

Referring to Fig. 24, it may be observed that as the degree of saturation decreased from 0.701 to about 0.5, the decrease in the reciprocal diffusibility was much less than that which took place below a degree of saturation of 0.5. The experimental value of the reciprocal diffusibility at a degree of saturation of 0.701 was about 35% smaller than the value predicted by Equation (37). It would appear then that above $\underline{s}$=0.5 the porous structure of the partially saturated bed and its variation with degree of saturation differed markedly from those below $\underline{s}$=0.5.

Discontinuities in the variation of the dynamic properties of partially saturated porous media with degree of saturation have been observed at the extreme levels of saturation (8, 28, 49). Such behavior was especially marked at the point of transition from the funicular saturation regime to the pendular saturation regime. The degree of saturation at which the behavior observed in this study occurred was about 0.5. It is doubtful that this degree of saturation represented the point of transition from the funicular to the pendular saturation regime.

On the other hand, it was noted previously that there was a significant decrease in molecule-wall collisions above a degree of saturation of 0.5. This behavior was apparently related to a marked increase in the effective size of the pores participating in the diffusion process. Undoubtedly, the pore size distribution was narrower above $\underline{s}$=0.5 than below it. The path through these larger pores may have been markedly less tortuous above than below $\underline{s}$=0.5.

The results shown in Fig. 25 indicated a marked change in the network structure of the partially saturated bed at a degree of saturation of about 0.5. The absolute values of the slopes of Fatt's derived curves shown in Fig. 1 decreased with increasing pore branching. However, it is doubtful that the

pore branching of the partially saturated beds increased with increasing degree of saturation as indicated in Fig. 25. The behavior shown could have resulted from a decrease in pore branching with increasing degree of saturation, the effect of which was masked by a significant decrease in pore tortuosity.

At a degree of saturation of 0.701, the experimental value of $1/\delta$ was 10.27 at a pressure of 0.264 atmosphere. If τ/P_s were to have the same value as that given by Equation (37), the exponent n would have to be less than one, which is not probable. For all values of n greater than one, τ/P_s at a degree of saturation of 0.701 would have to be less than the value given by Equation (37). Therefore, it appeared most likely that as the degree of saturation decreased from 0.701 to 0.5, the ratio of the tortuosity factor to the pore shape factor did not remain constant but increased.

Since the pore shape factor would be expected to increase with decreasing degree of saturation, the tortuosity factor would be required to increase more rapidly than the pore shape factor as s decreased from 0.701 to 0.5. In this saturation region, it appeared probable that the pore structure could have been less highly branched than that below $s=0.5$. Such an effect could have led to and been masked by a less tortuous path through the medium.

In view of the foregoing analysis of the data obtained on the partially saturated beds, it is hypothesized that the following changes in the porous structure of these beds were associated with the observed net decrease in the diffusion resistance with decreasing degree of saturation:

(1) the area available for transport of the gases increased,

(2) the resistance due to pore constrictions decreased,

(3) the branching and interconnecting of pores increased;

and (4) the tortuosity factor increased.

For all degrees of saturation within the range of 0.701 to 0.108, the variation of the reciprocal diffusibility with degree of saturation was found to be represented quite well by the following equation:

$$\ln(1/\delta) = 1.574\ s + 1.254 \qquad (40).$$

The correlation coefficient for this equation was 0.9976. Although there is no apparent theoretical or physical justification for this correlation, it has been presented for its possible practical utility.

Dry Beds

The variation of the reciprocal diffusibility with porosity was analyzed to illustrate the difference between the effects of this type of void space variation and the effects of that brought about by partial saturation on the diffusion resistance of the fiber beds.

For a pressure of 0.264 atm., the average values of the reciprocal diffusibilities obtained for the dry nylon fiber beds are listed in Table VII. The $1/\delta$ value for the 0.710 porosity level was obtained from extrapolation of the partially saturated bed data to $s=0$.

TABLE VII

DIFFUSION RESISTANCE OF DRY BEDS

ϵ	$1/\delta$
0.710	3.71
0.742	3.60
0.810	3.20

In agreement with the findings of previous investigations, $1/\delta$ increased with decreasing porosity. A least squares analysis of the original data, rather

than the average values of $1/\delta$, resulted in the following equation for which the correlation coefficient was 0.892:

$$1/\delta = 2.48/\epsilon^{1.23} \qquad (41).$$

Millington and Quirk (48) theorized that the fractional void area of a porous medium would be between ϵ and ϵ^2 as a result of pore interaction. For the dry nylon fiber beds used in this study, such pore interaction should not be very extensive, as indicated by Carman (8). It is proposed that $\epsilon^{1.23}$ is a realistic measure of the fractional void area of the dry nylon fiber beds available for diffusion.

Evaluation of Equation (41) in terms of the geometric model expression for the diffusibility of dry porous media, Equation (32), showed that τ/P_s would be equal to 2.48. Carman (8) and Petersen (46) have indicated that the pore shape factor for dry unconsolidated porous media is approximately unity. Therefore, the value of the tortuosity factor for the dry nylon fiber beds may be taken to be 2.48. For the porosity range of 0.710 to 0.810, a constant tortuosity factor of this magnitude was quite plausible (8).

Correlations similar to Equation (41) have been reported for dry granular-type porous media. As pointed out previously, the expressions obtained for similar types of unconsolidated materials appeared to be characteristic of the particular medium and the shape of the component particles. It is suggested that Equation (41) is applicable to dry beds composed of cylindrical nonporous fibers and formed in the manner used in this study.

SURFACE TRANSPORT

For the dry and the partially saturated nylon fiber beds, the diffusion process appeared to deviate from normal diffusion above a pressure of about 0.5

atmosphere. In consideration of all of the experimental results, it was concluded that this behavior resulted from surface transport of carbon dioxide, which became increasingly significant as the pressure increased. The surface transport process was analyzed to estimate the contribution it made to the total observed transport of carbon dioxide.

In order to estimate the surface transport rates of carbon dioxide it is not necessary to utilize any mechanistic theories or to know the amount of gas adsorbed. Assuming that any net transport of carbon dioxide between the gas phase and the adsorbed layer is negligible, the surface transport rates can be calculated as the difference between the observed total rates and the values predicted by the equation governing the bulk phase transport of the nonadsorbed gas (80, 81).

It was pointed out previously that the data indicated that surface transport of carbon dioxide was negligible at a pressure of 0.264 atm. for both the dry and the partially saturated nylon fiber beds. It was concluded, therefore, that the effective diffusion coefficient and the flux ratio obtained at 0.264 atm. characterized only the bulk phase transport process which was normal diffusion. For normal diffusion, the flux ratio and $(\underline{D}_{\underline{AB}})_{\underline{e}}\underline{P}$ would be independent of pressure for a given test specimen.

The values of these quantities obtained at a pressure of 0.264 atm. for a given fiber bed were used to calculate the normal diffusion rates of carbon dioxide at all pressures used. The driving force for normal diffusion was taken to be the experimentally observed concentration differences.

If the above method of calculating the normal diffusion rates were valid, the calculated values should be independent of pressure. With degree of saturation as the parameter, the estimated normal diffusion rates of carbon dioxide

as a function of total pressure are shown in Fig. 26. As may be observed, these rates were, indeed, relatively independent of pressure.

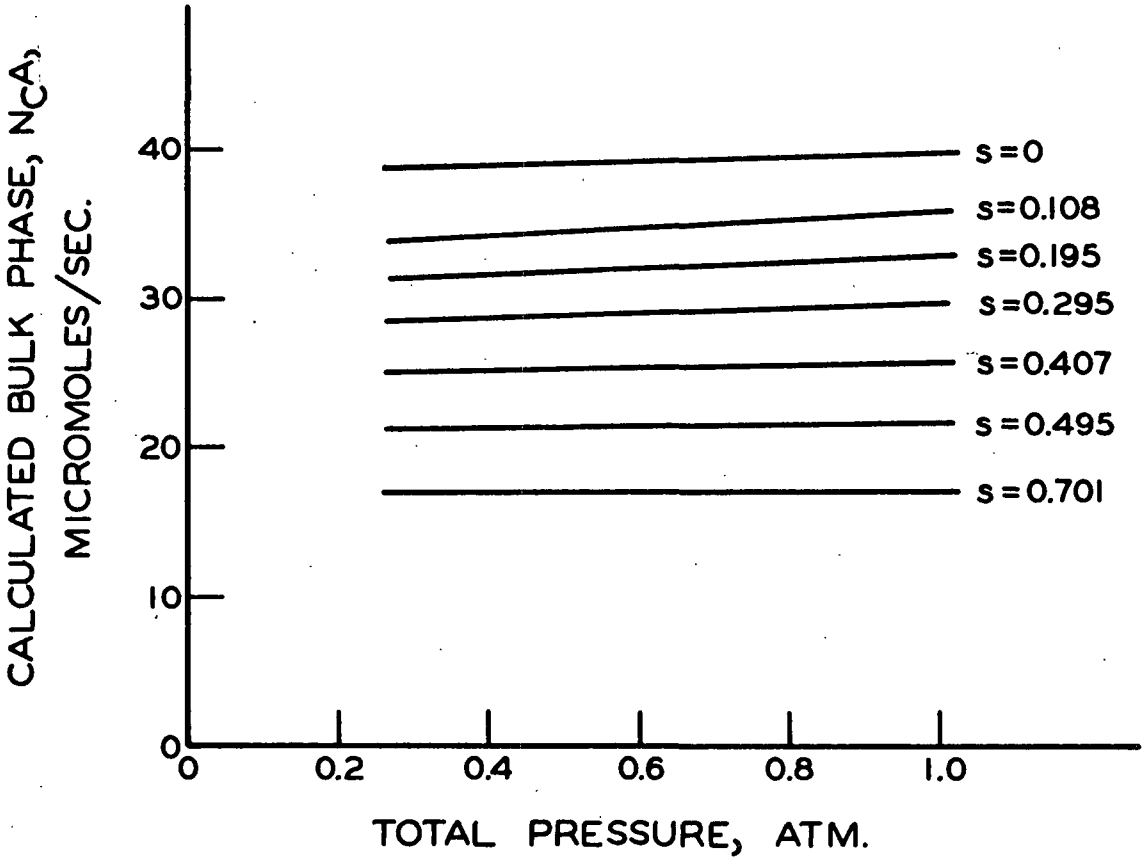

Figure 26. Calculated CO_2 Normal Diffusion Rates

The estimated surface transport rates for a pressure of 1.0 atm., along with the measured concentration differences, are listed in Table VIII.

For the partially saturated beds, the surface transport rate decreased with decreasing degree of saturation. This behavior would be expected in view of the decrease in the gas phase concentration gradient with decreasing degree of saturation. As pointed out previously, the resistance to surface transport would be expected to increase as the degree of saturation decreased, since the tortuosity of the liquid channels has been indicated to increase as a porous medium is desaturated (8, 49).

TABLE VIII

SURFACE TRANSPORT RATES
($\underline{P}$ = 1.0 atm.)

Degree of Saturation	$\underline{y}_{AO}-\underline{y}_{AL}$	Surface Transport Rates, micromoles/sec.	% of total rate
0.701	0.820	6.3	26.8
0.495	0.781	5.4	19.9
0.407	0.753	4.1	13.7
0.295	0.725	3.3	10.0
0.195	0.696	3.1	8.6
0.108	0.676	1.1	3.0
0.0[a]	0.623	7.3	15.4

[a]Data for Dry Bed No. N43-2-D (ϵ = 0.742).

The rate of surface transport for the dry bed was greater than all of the values for the partially saturated beds. More carbon dioxide was probably adsorbed by the nylon than by the DOP, and/or the surface transport resistance was smaller for the dry bed than for the partially saturated beds.

From a comparison of the calculated normal diffusion rates with the total observed rates of transport of carbon dioxide, Fig. 26 and 19, respectively, it may be concluded that the surface transport rates relative to the total rates were negligible for all of the beds below a pressure of about 0.5 atmosphere.

Under the conditions normally employed for the drying of paper and wood pulp fiber beds, appreciable adsorption of water vapor by such fibers has been observed (71, 82). In consideration of the results of this study, surface transport of water vapor would be an important mode of transport during the drying of such materials.

NONUNIFORM PRESSURE DIFFUSION

When diffusion took place in the presence of axial pressure differences of about 0.01 mm. Hg, it was found that the observed transport rates of the gases were appreciably different from the rates obtained under "uniform" pressure conditions. It was observed further that the effective normal diffusion coefficient was unaffected by such pressure differences.

Qualitatively, the above results may be resolved in terms of the momentum transport mechanisms affecting the gas transport process. For normal diffusion in the presence of an axial pressure difference, there will be a net transfer of axial momentum from the gas to the pore walls. Although the normal diffusion resistance is governed primarily by intermolecular momentum exchange, the flux ratio is controlled by molecule-wall momentum exchange. For a positive axial pressure difference (pressure on CO_2 side greater than pressure on N_2 side of the bed), there will be a net transfer of +z-momentum to the pore walls. In this instance the absolute value of the flux ratio would be less than the theoretical value of 1.25. Such a result was shown in Table IV. The converse of this behavior was observed when the axial pressure difference was negative, for which there would be a net transfer of -z-momentum to the pore walls.

Quantitatively, the problem of nonuniform pressure ordinary diffusion of gases in porous media had received little attention until the recent work of Evans, Watson, and Mason (64). These workers approached this problem in terms of the fundamental kinetic theory equations of diffusion for multicomponent gas mixtures (12, p. 517). Only the essential points of their treatment of this problem are presented here. A more comprehensive review of their theory is presented in Appendix IV.

The porous medium was visualized as a collection of "dust" particles which were uniformly distributed and fixed in space. In their treatment of the binary counterdiffusion problem, Evans, et al. considered the "dust" particles to be giant molecules. Thus, it was possible to apply the kinetic theory equations to a "ternary" mixture consisting of two Gases A and B and the dust "molecules" d.

In the case of uniform pressure ordinary diffusion, the only gradient would be the composition gradient and the above workers' treatment of this problem resulted in an equation equivalent to Equation (15). When pressure differences are present, both pressure diffusion and an external force must be considered. "The external force acts only on the dust particles, and is just sufficient to hold them stationary in space against the pressure gradient" (64). As pointed out in Appendix IV, the following equation was derived by Evans, et al. for the intermediate region of ordinary diffusion:

$$dy_A/dz + \left\{(1/n)\,(dn/dz) - J/\left[n\,(D_{AB})_e\right]\right\} y_A + J_A/\left[n\,(D_{NA})_e\right] = 0 \qquad (42),$$

where n is the total molecular concentration of real gas molecules, J is the total molecular flux based on the geometric cross-sectional area of the medium and referred to stationary co-ordinates, and J_A is a similar quantity for species A.

Integration of Equation (42) is no longer a straightforward problem since the pressure varies with z. This leads to the forced flow problem which Evans, et al. treated in terms of their dusty gas model and the kinetic theory diffusion equations. To compensate for the fact that the model provided for only a diffusion mechanism for flow, one parameter had to be made disposable. As outlined in Appendix IV, this treatment of the forced flow problem led to the following flow equation:

$$\beta J_A - J = (C_B/kTL)\,\Delta P \qquad (43),$$

where

$$\beta = 1 - (m_A/m_B)^{1/2} \qquad (44)$$

and

$$C_B = n\,(D_{Bd})_e/n_d \qquad (45).$$

In Equation (45), n_d is the concentration of dust "molecules," and $(D_{Bd})_e$ is the effective normal diffusion coefficient of Gas B with respect to the dust "molecules." Evans, et al. treated C_B as an empirical constant to be determined from flow experiments.

The term βJ_A in Equation (43) corresponded to a "slip" in the flow resulting from the simultaneous diffusion. As may be observed from this equation, there will be a net flux equal to βJ_A even when the pressure difference is zero. This is in agreement with previous theoretical and experimental results.

Equation (42) is a linear first-order differential equation for y_A and may be integrated from $z=0$ to $z=L$ after being combined with Equation (43). For normal diffusion and small pressure differences, the resulting equation may be written in the following form:

$$\exp^{*}\left\{-LJ/[n(D_{AB})_e]\right\}\ \left\{(1/\beta[J + (C_B/kTL)\,\Delta P] - Jy_{AL})\right\}$$

$$= \left\{1/\beta\ [J + (C_B/kTL)\,\Delta P] - Jy_{AO}\right\} \qquad (46).$$

where $\Delta P=0$, it may be readily shown that Equation (46) reduces to the integrated normal diffusion equation, Equation (10).

*exp denotes the power of e, the base of natural logarithms.

Evans, et al. (64) studied the normal counterdiffusion of helium and argon through a porous graphite in the presence of small axial pressure differences. Their experimental results agreed quite well with their predicted results. They found also that the empirical parameter C_B was independent of the pressure differences. As an additional test of their theoretical expressions, these workers determined the value of C_B from permeability measurements. This value agreed quite well with the values determined from their diffusion data.

The results of the nonuniform pressure study reported previously were used together with Equation (46) to test the applicability of the theory of Evans, et al. to the highly permeable fiber beds. Using the data obtained for Run No. 34, the parameter C_B was calculated from Equation (46). The value of this parameter was 3.0×10^3 sq. cm./sec. The data of Run No. 38 were used together with this value of C_B to calculate the pressure difference for this run. The calculated ΔP was -11×10^{-6} atm. and was in good agreement with the measured value of -10×10^{-6} atmosphere.

Although further experimentation would be needed to test rigorously the applicability of the theory of Evans, et al. to fiber beds, the above results indicated that this theory deserved further consideration. In view of the observed large effect of small axial pressure differences on normal diffusion, some such theory would undoubtedly be required to characterize quantitatively the transport of gases in most commercial problems concerned with diffusion through porous media, the drying of fiber beds included.

CONCLUSIONS

As a result of this study, the mechanisms and the resistance for the steady-state ordinary counterdiffusion of carbon dioxide and nitrogen through dry and partially saturated beds of 43-micron diameter nylon fibers under conditions of uniform pressure and temperature were characterized.

This diffusion process was accompanied by surface transport of carbon dioxide. Such transport was negligible below a pressure of about 0.5 atmosphere. From an analysis of the data obtained below this pressure, it was concluded that the bulk phase transport process was normal diffusion for both the dry and all of the partially saturated beds within the pressure range of 0.264 to 1.0 atmosphere. Therefore, the ordinary diffusion resistance of these beds was controlled by intermolecular collisions.

The normal diffusion process was analyzed primarily by means of the data obtained at a pressure of 0.264 atmosphere. As a result of these analyses, it was concluded that the diffusion process was not equimolal. In agreement with theory, the flux ratio was apparently governed by molecule-wall collisions and the related transport of axial momentum.

When the degree of saturation of the nylon fiber beds was less than about 0.5, the values of the ratio of the nitrogen to the carbon dioxide diffusion fluxes were approximately equal to the square root of the inverse ratio of the molecular weights of the gases, -1.25. These results and the results of analyses of the momentum transport taking place supported the conclusion that the net axial momentum transferred to the pore walls was zero when $\underline{s}$ was less than about 0.5.

When the degree of saturation was greater than 0.5, the value of the diffusion flux ratio was -1.34. This result was consistent with estimates of the momentum transport taking place in the system, which showed a marked decrease in molecule-wall collisions and a net transfer of -z-momentum to the pore walls as the degree of saturation increased above 0.5. These observations supported the theory that as the pore size increases, collisions of the molecules with the pore walls will decrease, and the flux ratio for normal counterdiffusion will approach a value equal to the inverse ratio of the molecular weights of the gases.

As the degree of saturation decreased, the effective normal diffusion coefficient increased. It was deduced that this behavior was associated with (1) an increase in the area available for transport of the gases, (2) a decrease in the resistance due to pore constrictions, (3) an increase in the branching and interconnecting of pores, and (4) an increase in the tortuosity factor.

Below a degree of saturation of 0.5, the relative effective normal diffusion coefficient was directly proportional to the nonwetting phase degree of saturation, $(1-\underline{s})$, raised to a power $\underline{n}$. For the beds studied, the value of this exponent was 1.084. In consideration of reported results of network model studies of porous media, the magnitude of this exponent was indicative of a highly branched pore structure.

Above a degree of saturation of 0.5, this proportionality no longer held. The observed diffusion resistance was much less than that expected from the results observed below a degree of saturation of 0.5. It was hypothesized that above $\underline{s}=0.5$ the pore structure was less highly branched and the pore tortuosity was smaller than below $\underline{s}=0.5$, and that the latter effect masked the former one.

Above a pressure of 0.5 atm., the diffusion process for the dry and the partially saturated nylon fiber beds appeared to deviate from normal diffusion.

In consideration of all of the experimental results, it was concluded that this behavior resulted from surface transport of carbon dioxide. At a pressure of 1.0 atm., surface transport accounted for 27% of the total observed transport of carbon dioxide for the bed partially saturated to a degree of 0.701, 3% when $\underline{s}$ equaled 0.108, and 15% for the dry bed.

The usual form of the normal diffusion equation was not applicable to normal diffusion accompanied by appreciable surface transport. When it was used the calculated values of the effective normal diffusion coefficient were lower than the actual values of the bulk phase transport coefficient. Likewise, the observed values of the flux ratio for normal diffusion in the presence of surface transport differed significantly from those pertaining to only normal diffusion, These observed effects of surface transport on the normal diffusion process were attributed to an exchange of momentum between the bulk phase gas molecules and the mobile adsorbate.

Besides surface transport, small axial pressure differences had a significant effect on the normal diffusion process. The observed transport rates for diffusion in the presence of axial pressure differences of about 0.01 mm. Hg were changed appreciably in comparison to "uniform" pressure diffusion rates. The effective normal diffusion coefficient was unaffected, however, by such pressure differences. These results were consistent with the experimental and theoretical results of Evans, Watson, and Mason (64) and with momentum transport considerations.

SUGGESTIONS FOR FUTURE WORK

In regard to the general problem of water vapor transport during the drying of fiber beds, additional studies under idealized conditions are needed before characterization of this process can be approached *in situ*. The results of the present study could be amplified by means of ordinary diffusion experiments made with partially saturated beds of nonporous fibers of various shapes and sizes. Nonadsorbing gases should be used to avoid the complications of surface transport. Of additional importance to the drying problem would be studies concerned with the effects of axial pressure differences and temperature differences on ordinary diffusion.

Intermediate diffusion may be of importance to gaseous diffusion in beds of wood pulp fibers, since *intra*fiber diffusion would probably be in the intermediate or even the Knudsen region of diffusion. The contribution to the overall diffusion resistance of wood pulp fiber beds made by intrafiber pores could be evaluated by varying the amount of *intra*fiber pore volume relative to *inter*fiber pore volume.

Surface transport of water vapor would undoubtedly be an important mode of mass transport during the drying of fiber beds. Besides studies concerned with normal diffusion accompanied by surface transport, studies of intermediate diffusion in the presence of surface transport would be of value. The surface transport process could best be characterized by making studies on a given test specimen with a nonadsorbing gas pair and then a gas pair for which one of the gases was highly adsorbable. Regarding the drying problem, the effects of temperature and pressure differences on the surface transport process would require study.

In reference to the general problem of diffusion in porous media, the dependence of the flux ratio on pore size deserves further consideration. Of course, characterization of the porous structure of porous materials would be helpful in defining the diffusion resistance of such materials. Visual studies might be instructive in this regard, as might analog simulation of these structures and electrical conduction studies.

NOMENCLATURE

A = cross-sectional area of test section of bed, sq. cm.

c_A = molar concentration of species A, moles/cc.

C_B = flow constant defined by Equation (48), sq. cm./sec.

D_{AB} = normal diffusion coefficient, sq. cm./sec.

D_{KA} = Knudsen diffusion coefficient, sq. cm./sec.

D_{NA} = intermediate diffusion coefficient, sq. cm./sec.

G_A = one-dimensional mass flux of species A with respect to stationary co-ordinates and based on total cross-sectional area, g./sec. sq. cm.

J_A = one-dimensional molecular flux of species A with respect to stationary co-ordinates and based on total cross-sectional area, molecules/sec. sq. cm.

$\vec{J}^*_A$ = molar flux of species A relative to the molar average velocity and based on total cross-sectional area, moles/sec. sq. cm.

k = Boltzmann's constant

L = geometric thickness of a test specimen, cm.

m_A = mass of a molecule of species A, g.

M_A = molecular weight of species A, g./mole

M_{AB} = axial momentum lost by species A per unit time per unit volume by collision with species B, dynes/cc.

M_{Aw} = axial momentum lost by species A per unit time by collisions with the wall per unit area, dynes/sq. cm.

n_A = molecular concentration of species A, molecules/cc.

$\vec{N}_A$ = molar flux of species A with respect to stationary co-ordinates and based on total cross-sectional area, moles/sec. sq. cm.

p_A = partial pressure of species A, atm.

P = total pressure, atm.

P_s = pore shape factor, dimensionless

r_{AB} = ratio of diffusion fluxes, N_B/N_A, dimensionless

R = universal gas constant

R_O = resistivity of a porous medium completely saturated with a wetting conducting solution, ohms/cm. cube

R_S = resistivity of a porous medium partially saturated with wetting conducting solution, ohms/cm. cube

R_T = radius of capillary tube, cm.

s = liquid wetting phase degree of saturation, liquid volume/total void volume, dimensionless

T = temperature, °K.

$\bar{u}_A$ = mean molecular speed of species A, cm./sec.

$\vec{v}_A$ = diffusion velocity of species A with respect to stationary co-ordinates, cm./sec.

$\vec{v}^*$ = molar average velocity, defined by Equation (4), cm./sec.

y_{AO} = mole fraction of species A at $z = 0$

y_{AL} = mole fraction of species A at $z = L$

z = z co-ordinate

$\alpha = 1 + N_B/N_A$

$\beta = 1 - (m_A/m_B)^{1/2}$

δ = diffusibility, ratio of effective diffusion coefficient to true diffusion coefficient, dimensionless

ϵ = porosity or fractional void volume of dry bed, dimensionless

θ = time, sec.

π = 3.1416.....

ρ_A = mass density of species A, g./cc.

τ = tortuosity factor, dimensionless

Subscripts:

A = gas species A

B = gas species B

C = carbon dioxide

e = effective, refers to property of porous medium

N = nitrogen

ACKNOWLEDGMENTS

To all of the people who contributed in various ways to the successful completion of this thesis, the author is sincerely grateful.

In particular, the guidance of the author's thesis advisory committee, the chairman, Mr. S. T. Han, and the members, Dr. J. A. Van den Akker, and the late Dr. G. R. Sears, contributed significantly to the completion of this study and is gratefully acknowledged.

The author is grateful also to Mr. H. W. Marx of the Machine Shop of The Institute of Paper Chemistry for constructing the diffusion chamber and contributing to its design.

A special note of gratitude is extended to my wife, Lorraine, for her continued patience and encouragement and for typing the original manuscript, and to Mark, Glenn, and Keith, my three sons, who provided additional incentive for completing this study.

LITERATURE CITED

1. Cowan, W. F. An investigation of the hot surface drying of glass fiber beds. Doctor's Dissertation. Appleton, Wis., The Institute of Paper Chemistry, 1961. 168 p.

2. Dreshfield, A. C. A study of transverse moisture distribution and movement during hot-surface drying of paper. Doctor's Dissertation. Appleton, Wis., The Institute of Paper Chemistry, 1956. 175 p.

3. Han, S. T., and Ulmanen, T., Tappi 41:185-9(1958).

4. McMaster, D. G. The thermal conductivity of dry and partially saturated fiber beds. Doctor's Dissertation. Appleton, Wis., The Institute of Paper Chemistry, 1963. 131 p.

5. Scott, D. S., and Dullien, F. A. L., A.I.Ch.E. Journal 8:113-17(1962).

6. Evans, R. B., III, Watson, G. M., and Mason, E. A., J. Chem. Phys. 35:2076-83(1961).

7. Dullien, F. A., and Scott, D. S., Chem. Eng. Sci. 17:771-5(1962).

8. Carman, P. C. Flow of gases through porous media. Chap. II. New York, Academic Press, 1956.

9. Present, R. D. Kinetic theory of gases. Chap. 4. New York, McGraw-Hill, 1958.

10. Rothfeld, L. B., A.I.Ch.E. Journal 9:19-24(1963).

11. Bird, R. B., Stewart, W. E., and Lightfoot, E. N. Transport phenomena. New York, John Wiley, 1960. 780 p.

12. Hirschfelder, J. O., Curtiss, C. F., and Bird, R. B. Molecular theory of gases and liquids. p. 539. New York, John Wiley, 1954.

13. Schaaf, S. A., Appl. Mech. Revs. 9:413-15(1956).

14. Pollard, W. G., and Present, R. D., Phys. Rev. 73:762-74(1948).

15. Rothfeld, L. B. Diffusion and flow of gases in porous catalysts. Doctor's Dissertation. Madison, Wis., University of Wisconsin, 1961. 373 p.

16. Present, R. D. Kinetic theory of gases. Chap. 8. New York, McGraw-Hill, 1958.

17. Wheeler, A. Advances in catalysis. Vol. 3, p. 249. New York, Academic Press, 1951.

18. Wicke, E., and Kallenbach, R., Kolloid Z. 97:135-51(1941); C.A. 37:8144(1943).

19. Hoogschagen, J., Ind. Eng. Chem. 47:907-13(1955).

20. Scott, D. S., and Cox, K. E., Can. J. Chem. Eng. 38:201-5(1960).

21. Evans, R. B., III, Watson, G. M., and Truitt, J., J. Chem. Eng. Data 6:522-5(1961).

22. Robertson, J. L., and Smith, J. M., A.I.Ch.E. Journal 9:342-7(1963).

23. McCarty, K. P., and Mason, E. A., Phys. Fluids 3:908-22(1960).

24. Fatt, I. The network model in the study of porous media. Doctor's Dissertation. Los Angeles, Cal., University of Southern California, 1955. 246 p.

25. Rose, W., Illinois State Geol. Survey Circ. 237, 1957. 31 p.

26. Hedley, W. H. Diffusion of gases through porous media. Doctor's Dissertation. St. Louis, Mo., Washington University, 1957. 145 p.

27. Kimura, M., Ueda, K., and Ofuka, T., A.I.Ch.E. Journal 5:267-8(1959).

28. Scheidegger, A. E. The physics of flow through porous media. Part IX. Canada, University of Toronto Press, 1959.

29. Penman, H. L., J. Agr. Sci. 30:437-62(1940).

30. Rust, R. H., Klute, A., and Gieseking, J. E., Soil Sci. 84:453-63(1957).

31. Dakshinamurti, C., Soil Sci. 88:209-12(1959).

32. Currie, J. A., Brit. J. Appl. Phys. 11:318-24(1960).

33. Archie, G. E. In Collins' Flow of fluids through porous materials. p. 38-9. New York, Reinhold, 1961.

34. Slawinski, A., J. chim. phys. 23:710-27(1926); C.A. 21:2590(1927).

35. Dye, R. F. A study of diffusion in porous media. Doctor's Dissertation. Atlanta, Ga., Georgia Institute of Technology, 1953. 83 p.

36. Wakao, N., and Smith, J. M., Chem. Eng. Sci. 17:825-34(1962).

37. Maxwell, J. C. Treatise on electricity and magnetism. p. 365. London, Oxford University Press, 1873; Fricke, H., and Morse, S., Phys. Rev. 25:361-7(1925).

38. Rayleigh, J. W., Phil. Mag. 34:481-502(1892).

39. Bruggeman, D. A. G., Ann. Physik 24:636(1935).

40. Millington, R. J., Science 130:100-2(1959).

41. Hashin, Z., and Shtrikman, S., J. Appl. Phys. 33:3125-31(1962).

42. Weissberg, H. L., J. Appl. Phys. 34:2636-9(1963).

43. Bliesner, W. C. A study of the porous structure of fibrous sheets using permeability techniques. Doctor's Dissertation. Appleton, Wis., The Institute of Paper Chemistry, 1963. 200 p.

44. Wyllie, M. R. J., and Gregory, A. R., Ind. Eng. Chem. 47:1379-88(1955).

45. Wang, Shu-Lung. The diffusion and flow of gases through porous media. Doctor's Dissertation. St. Louis, Mo., Washington University, 1953. 165 p.

46. Petersen, E. E., A.I.Ch.E. Journal 4:343-5(1958).

47. Michaels, A. E., A.I.Ch.E. Journal 5:270-1(1959).

48. Millington, R. J., and Quirk, J., Trans. Faraday Soc. 57:1200-7(1961).

49. Parker, J. D. An investigation of the permeability to water of partially saturated beds of glass fibers. Doctor's Dissertation. Appleton, Wis., The Institute of Paper Chemistry, 1958. 203 p.

50. Loschmidt, J., Wien Ber. 61:367(1870).

51. Stefan, A., Wien Ber. 68:385(1874).

52. Buckingham, E., U.S. Dept. Agr., Bur. Soils, Bull. No. 25, 1904.

53. International Critical Tables. Vol. I. p. 92. 1 e. New York, McGraw-Hill, 1926.

54. Myers, W. T., Jr. The rheology of synthetic fiber suspensions. Doctor's Dissertation. Appleton, Wis., The Institute of Paper Chemistry, 1962. 189 p.

55. du Pont de Nemours, E. I., and Company. Identification of fibers in textile materials. Bulletin X-156, Dec., 1961.

56. Jones, R. L. An investigation of the effect of fiber structural properties on the compression response of fibrous beds. Doctor's Dissertation. Appleton, Wis., The Institute of Paper Chemistry, 1962. 158 p.

57. Burnam, C. W. Personal communication, 1964.

58. Carson, F. T., J. Res. Natl. Bur. Stds. 12:567-85(1934).

59. Perry, J. H. Chemical engineers' handbook. p. 365-7. 3e. New York, McGraw-Hill, 1950.

60. Daynes, H. A. Gas analysis by measurement of thermal conductivity. Cambridge, England, Cambridge University Press, 1933.

61. Weitzel, D. H., and White, L. E., Rev. Sci. Instr. 26:290-2(1955).

62. Keulemans, A. I. M. Gas chromatography. Chap. 3. 2e. New York, Reinhold, 1960.

63. Schlichting, H. Boundary layer theory. 4th ed. p. 181-4, Chap. XXIII. New York, McGraw-Hill, 1960.

64. Evans, R. B., III, Watson, G. M., and Mason, E. A., J. Chem. Phys. 36:1894-1902(1962).

65. Hewitt, G. F., and Sharrat, E. W., Nature 198:952-7(1963).

66. Carman, P. C. Flow of gases through porous media. Chap. V. New York, Academic Press, Inc., 1956.

67. Adamson, A. W. Physical chemistry of surfaces. Chap. XI. New York, Interscience, 1960.

68. Crawford, V. A., and Tomkins, F. C., Trans. Faraday Soc. 46:504-14(1950).

69. Ray, G. C., and Box, E. O., Jr., Ind. Eng. Chem. 42:1315-18(1950).

70. Rutz, L. O., Graham, J. B., and Kammermeyer, K., J. Chem. Eng. Data 4:307-10(1959).

71. Salley, D. J., Textile Res. 5:493-508(1935).

72. Reyerson, L. H., and Peterson, L., J. Phys. Chem. 60:1172-6(1956).

73. Benson, S. W., and Seehof, J. M., J. Am. Chem. Soc. 75:3925-8(1953).

74. Noller, C. R. Textbook of organic chemistry. 2e. p. 31, 90. Phila., Pa., W. B. Saunders Company, 1958.

75. Tuul, J., J. Phys. Chem. 66:1736-7(1962).

76. Glasstone, S. Theoretical chemistry. Chap. IX. Princeton, New Jersey, D. Van Nostrand Company, Inc. 1961.

77. Haselton, W. R., Tappi 37:404-12(1954).

78. Henry, J. P., Chennakesvan, B., and Smith, J. M., A.I.Ch.E. Journal 7:10-12 (1961).

79. Damköhler, G. In Carman's Flow of gases through porous media. p. 105-6. New York, Academic Press, 1956.

80. Sears, G. W., J. Chem. Phys. 22:1252-3(1954).

81. Gilliland, E. R., Baddour, R. F., and Russell, J. L., A.I.Ch.E. Journal 4:90-6(1958).

82. Jeffries, R., J. Text. Inst. Trans. 51:T339-74(1960).

APPENDIX I

INTERMEDIATE DIFFUSION EQUATION

For the purpose of illustrating the momentum-transfer treatment of ordinary diffusion, a derivation of the intermediate diffusion equation using this method will be presented. This derivation is similar to that of Scott and Dullien (5) and is based on a circular capillary model. The one-dimensional steady counter-diffusion of Gases A and B through a circular capillary of radius R_T will be considered for conditions of uniform temperature and pressure and for an open system.

It can be assumed for this process that (1) shear stresses are negligible, (2) the gases behave ideally, (3) the concentrations and diffusion velocities are functions of the axial co-ordinate only, (4) transverse diffusion velocities are negligible, (5) $v_A \ll \bar{u}_A$, (6) the gas molecules are diffusely reflected after colliding with the tube wall, and (7) the expressions for the limiting values of M_{Aw} and M_{AB} are applicable to the intermediate region of diffusion.

The pressure drop for Gas A for this process is equal to the sum of the z-momentum transferred to the tube wall and that transferred to molecules of Gas B. A momentum balance over a length dz of the capillary may be written as

$$-dp_A/dz = [(2/R_T)\, M_{Aw}] + M_{AB} \qquad (14).$$

At the limit of Knudsen diffusion and under the assumption of negligible transverse diffusion velocities, Pollard and Present (14) derived an expression for M_{Aw}, Equation (19), based on a modified form of the Maxwell distribution law. For present purposes, it is appropriate to use a more precise expression for M_{Aw} developed by Smoluchowski (14), whose theory removed the assumption of negligible transverse velocity gradients. In the Smoluchowski theory, the flux at the tube

axis is $\pi/2$ times as great as that at the wall. According to this theory,

$$M_{Aw} = (n_A \bar{u}_A/4)\ (3\pi\ m_A v_A/8) \qquad (47).$$

It can be shown readily that, in the Knudsen region of diffusion, Equation (14) and Equation (47) can be combined to develop the Knudsen diffusion equation, Equation (13).

An expression for $\underline{M}_{\underline{A}\underline{B}}$ at the limit of normal diffusion may be derived from the Stefan-Maxwell equations (11, p. 570). This approach was used by Present (16), and a modified form of the expression resulting from his development, Equation (34), was presented previously. Expressed in terms of molecular quantities and for a capillary tube, Equation (34) would be

$$M_{AB} = kT\ n_A n_B (v_A - v_B)/(n\ D_{AB}) \qquad (48).$$

In the normal region of ordinary diffusion in a porous medium, Equation (48) can be combined with Equation (14) to develop the normal diffusion equation, Equation (10).

Assuming that Equations (47) and (48) are applicable to the intermediate region of ordinary diffusion, they can be combined with Equation (14) to give

$$-P\ dy_A/dz = 3\pi\ m_A \bar{u}_A J_A/(16\ R_T) + (kT/D_{AB})(y_B J_B - y_A J_B) \qquad (49),$$

since $\underline{J}_{\underline{A}} = \underline{n}_{\underline{A}}\underline{v}_{\underline{A}}$ and $\underline{n}_{\underline{A}}/\underline{n} = \underline{y}_{\underline{A}}$, etc. Application of the expression for the Knudsen diffusion coefficient, Equation (12), and the kinetic theory expression for $\bar{u}_A$ to Equation (49) results in the following expression:

$$-P\ dy_A/dz = kT\ J_A/D_{KA} + kT\ J_A(1 - \alpha y_A)/D_{AB} \qquad (50).$$

Rearrangement of Equation (50) into an integrable form, integration of this expression over the length L of the capillary, and modification of the resulting equation for application to a porous medium lead to the intermediate diffusion equation, Equation (15).

APPENDIX II

FLUX RATIO FOR NORMAL DIFFUSION

Consider the steady-state, normal counterdiffusion of two ideal gases at constant total pressure and constant temperature through a cylindrical capillary of radius R_T in an open system.

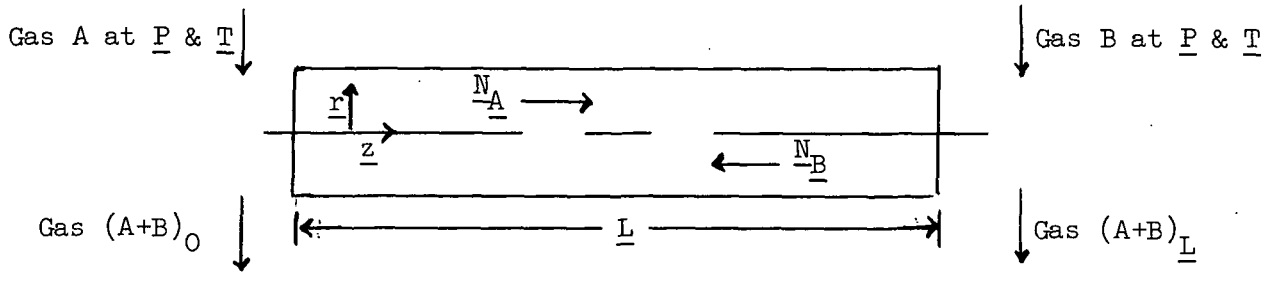

It usually has been taken for granted that the diffusion fluxes are independent of r. Dullien and Scott (7) have shown that this cannot be rigorously true.

The general form of the equation of motion is (11)

$$\rho D\vec{v}/D\theta = -\nabla P - [\nabla \cdot \vec{\tau}] + \rho\vec{g} \qquad (51),$$

where

$$D\vec{v}/D\theta = \partial\vec{v}/\partial\theta + v_x\,\partial\vec{v}/\partial_x + v_y\,\partial\vec{v}/\partial y + v_z\,\partial\vec{v}/\partial z \qquad (52).$$

For the above situation, neglecting end effects, Equation (51) reduces to

$$-(1/r)d(r\tau_{rz})/dr = \rho v_z dv_z/dz \qquad (53),$$

where τ_{rz} is the viscous flux of z-momentum in the radial direction, ρ is the over-all mass density, and v_z is the net transport velocity. Since

$$v_z = G/\rho \qquad (54),$$

where $\underline{G}$ is the net mass flux, Equation (53) becomes

$$d(r\tau_{rz})/dr = (rG^2/\rho^2)\, d\rho/dz \qquad (55).$$

Combining

$$\tau_{rz} = -\eta\, dv_z/dr \qquad (56),$$

where η is the viscosity coefficient, with Equations (54) and (55) gives

$$d[r(dG/dr)]/dr = -rG^2A' \qquad (57),$$

where

$$A' = (1/\rho\eta)d\rho/dz \qquad (58).$$

If $\underline{G}$ were independent of $\underline{r}$, the left member of Equation (57) would be zero; but the right member is zero generally only for $\underline{G}$=0. However, $\underline{G}$=0 is impossible as will be shown below.

For $\underline{G}$=0, it follows from Equation (55) that $\underline{r}\tau_{\underline{rz}}$ = constant, which can be true only if $\tau_{\underline{rz}} = 0$. From the kinetic theory of gases, the net shearing stress at the pore walls is

$$\tau_w = N_A M_A \frac{\bar{u}_A}{4} + N_B M_B \frac{\bar{u}_B}{4} \qquad (59).$$

Combining

$$\bar{u}_A/\bar{u}_B = (M_B/M_A)^{1/2} = \mu_{AB}^{1/2} \qquad (60)$$

with Equation (59) gives

$$\tau_w = (M_A\bar{u}_A N_A/4)(\mu_{AB}^{1/2}\, r_{AB} + 1) \qquad (61),$$

where

$$r_{AB} = N_B/N_A \qquad (62).$$

For $\tau_w=0$, $r_{AB}=-\mu_{AB}^{-0.5}$. However, by the definition of G,

$$G = N_A M_A + N_B M_B = M_A N_A(\mu_{AB} r_{AB} + 1) \quad (63),$$

$G=0$ implies that $r_{AB} = -\mu_{AB}^{-1}$. Therefore, the supposition that $G=0$ leads to contradiction. Therefore, G cannot be rigorously constant in a radial direction.

It will be shown, however, that the radial variation of G is negligibly small for small diameter capillaries. Carrying out the differentiation of Equation (57) gives

$$G'' + G'/r + A'G^2 = 0 \quad (64),$$

where G' and G'' are the first and second derivatives with respect to r, respectively. At the pore wall, Equation (64) becomes

$$-G_w'' - G_w'/R_T = A'G_w^2 < A'\bar{G}^2 \quad (65).$$

Since G_w'' will be negligibly small,

$$-G_w'/R_T < A'\bar{G}^2 \quad (66).$$

Therefore,

$$(G_0 - G_w)/\bar{G} < A'\bar{G} R_T^2 \quad (67),$$

where G_0 is the value of G at the center of the capillary.

The normal diffusion equation can be written in the following form

$$N_A = -[cD_{AB}/(y_B - y_A r_{AB})]\, dy_A/dz \quad (68),$$

where c is the molar density. Using Equation (68) as well as Equations (58) and (63), it can be shown that $A'\bar{G}$ will not exceed order one in c.g.s. units. Therefore, for $R_T \ll 1$ cm., the radial variation of G will be negligibly small.

A momentum balance on an incremental cylindrical shell for the process considered above gave

$$d(r\tau_{rz})/dr = (rG^2/\rho^2)d\rho/dz \qquad (55).$$

In view of the above results, Equation (55) can be integrated from $\underline{r}=0$ to $\underline{r}=\underline{R_T}$ to give

$$R_T \tau_w = (R^2/2)(G/\rho)^2 \, d\rho/dz \qquad (69),$$

where the average sign has been omitted over $\underline{G}$. Using Equation (63), Equation (69) can be written

$$\tau_w = [R_T N_A^2 M_A^2/(2\rho^2)](d\rho/dz)(\mu_{AB} r_{AB} + 1)^2 \qquad (70).$$

Combining Equation (70) with Equation (61) gives

$$(R_T N_A M_A/\rho^2)(d\rho/dz)(\mu_{AB} r_{AB} + 1)^2 = (\bar{u}_A/2)(\mu_{AB}^{1/2} r_{AB} + 1) \qquad (71).$$

For ideal gases

$$\rho = (PM_A/RT)(y_B \mu_{AB} + y_A) \qquad (72),$$

and

$$d\rho/dz = (PM_A/RT)(1 - \mu_{AB})(dy_A/dz) \qquad (73).$$

Combining Equations (68), (72), and (73) with Equation (71) gives

$$(dy_A/dz)^2 \, [1/(y_B - y_A r_{AB})(y_B \mu_{AB} + y_A)^2] = C_{AB} \qquad (74)$$

where

$$C_{AB} = [\bar{u}_A(\mu_{AB}^{1/2} \, r_{AB} + 1)]/[2D_{AB} R_T (\mu_{AB} r_{AB} + 1)^2 (\mu_{AB} - 1)] \qquad (75).$$

Taking square roots of both sides of Equation (74) and integrating gives

$$\int_{y_{AO}}^{y_{AL}} dy_A / \left\{[(1 - \mu_{AB})y_A + \mu_{AB}][-(1 + r_{AB})y_A + 1]^{1/2}\right\} = C_{AB}^{1/2} \int_0^L dz \qquad (76).$$

Integration of Equation (76) yields

$$\ell n(Y_{AL}/Y_{AO}) = E_{AB}\,[-(\mu_{AB}^{1/2} r_{AB} + 1)/(\mu_{AB} r_{AB} + 1)]^{1/2} \qquad (77),$$

where

$$Y_{AL} = [(1 - \alpha y_{AL})^{1/2} - B_{AB}]/[(1 - \alpha y_{AL})^{1/2} + B_{AB}] \qquad (78),$$

$$Y_{AO} = [(1 - \alpha y_{AO})^{1/2} - B_{AB}]/[(1 - \alpha y_{AO})^{1/2} + B_{AB}] \qquad (79),$$

$$E_{AB} = (\bar{u}_A^{1/2} L)/(2 D_{AB} R_T)^{1/2} \qquad (80),$$

and

$$B_{AB} = [(1 + \mu_{AB} r_{AB})/(1 - \mu_{AB})]^{1/2} \qquad (81).$$

Inspection of Equation (77) shows that for any physically meaningful values of $\underline{y}_{AL}$, $\underline{y}_{AO}$, and $\underline{R}_T$

$$\mu_{AB}^{-1} < r_{AB} < \mu_{AB}^{-1/2} \qquad (82),$$

where

$$\mu_{AB} > 1 \qquad (83).$$

The above treatment of the flux ratio for normal diffusion is essentially that of Dullien and Scott (7). This development was presented here because of its relevance to the present study and gaseous diffusion theory in general.

APPENDIX III

CALCULATION OF DIFFUSION COEFFICIENT

The equations used for calculating the diffusion fluxes, $\underline{N}_{\underline{N}}$ and $\underline{N}_{\underline{C}}$, will be developed, and the diffusion coefficient for Run No. 154 will be calculated.

Let $\underline{w}_{\underline{N1}}$ and $\underline{w}_{\underline{C1}}$ be the molar flow rates of nitrogen and carbon dioxide, respectively, entering the test cylinders, and $\underline{w}_{\underline{N2}}$ and $\underline{w}_{\underline{C2}}$ the molar flow rates leaving. Let $\underline{x}$ and $\underline{y}$ be the mole fractions of carbon dioxide in the effluent streams leaving the top and bottom test cylinders, respectively. Throughout this development ideal behavior of the gases is assumed. An over-all material balance on the test section of the fiber bed yields

$$w_{N1} + w_{C1} = w_{N2} + w_{C2} \tag{84}.$$

By means of an over-all carbon dioxide balance

$$w_{C1} = xw_{N2} + yw_{C2} \tag{85}.$$

Next, consider a carbon dioxide balance on the nitrogen or top side of the bed. No carbon dioxide enters in the pure nitrogen feed stream, but $\underline{N}_{\underline{C}}\underline{A}$ moles/sec. enter through the bed; $\underline{x}\underline{w}_{\underline{N2}}$ moles/sec. leave with the effluent stream from the top test cylinder. Therefore,

$$N_C A = xw_{N2} \tag{86},$$

where $\underline{A}$ is the area of the test section of the bed. By means of a nitrogen balance on the carbon dioxide or bottom side of the bed

$$N_N A = (1 - y)w_{C2} \tag{87}.$$

Equations (84) and (85) can be solved for $\underline{w}_{\underline{N2}}$ and $\underline{w}_{\underline{C2}}$. Combination of the resulting expression for $\underline{w}_{\underline{N2}}$ with Equation (86) and rearrangement yields

$$N_C A = x[y(w_{N1} + w_{C1}) - w_{C1}]/(y - x) \qquad (88).$$

Similarly, the expression for the nitrogen diffusion rate is

$$N_N A = (1 - y)[w_{C1} - x(w_{N1} + w_{C1})]/(y - x) \qquad (89).$$

Effective normal diffusion coefficients were calculated from Equation (10):

$$N_A = [(D_{AB})_e P/(\alpha RTL)]\ln[(1 - \alpha y_{AL})/(1 - \alpha y_{AO})] \qquad (10).$$

In terms of the present notation, $\underline{N_A} = \underline{N_C}$, $\underline{y_{AL}} = \underline{x}$, $\underline{y_{AO}} = \underline{y}$, and $\alpha = 1 + \underline{N_N}/\underline{N_C}$. From the data of Run No. 154,

$$33.4 \times 10^{-6} = (D_{AB})_e \frac{0.264}{(-0.26)(82.1)(313)(1.191)} \ln\left[\frac{1-(-0.26)(0.168)}{1-(-0.26)(0.805)}\right]$$

$$(D_{AB})_e = 0.1500 \text{ sq.cm./sec.}$$

APPENDIX IV

NONUNIFORM PRESSURE ORDINARY DIFFUSION

In the case of uniform pressure ordinary diffusion, the only gradients were the concentration gradients of the diffusing species. External forces in this situation are zero (6). When a pressure gradient exists, pressure diffusion and external forces appear (64). Evans, Watson, and Mason (64) treated this problem in terms of their "dusty gas" model of a porous medium, by which the medium is considered to be a collection of "dust" particles uniformly distributed and fixed in space. By considering the "dust" particles to be giant molecules, these workers treated the nonuniform pressure diffusion problem in terms of the kinetic theory diffusion equations for multicomponent gas mixtures (12, p. 517).

For a mixture of ν components and one-dimensional diffusion, the set of fundamental equations of diffusion was given as (64)

$$\sum_{i=1, i\neq j}^{\nu} (n_j J_i - n_i J_j)/[n'^2 (D'_{ij})_e] = d(n_j/n')/dz$$

$$+ (n_j/n' - n_j m_j/\rho')d \ln p'/dz$$

$$- [(n_j m_j)/(p'\rho')] \left[(\rho'/m_j)F_j - \sum_{k-1}^{\nu} n_k F_k\right] \qquad (90).$$

In this expression F_i is the external force acting on each molecule of species i, and n' is the total number of molecules per cc., including the particles of the porous medium. In this sense, p' is a fictitious pressure defined by $n'kT$. The unprimed quantities refer to only the real gas molecules. The first term on the right side of Equation (90) is the ordinary diffusion term, the second term is the pressure diffusion term, and the third term is the external force term.

Mason and his co-workers then proceeded to express the external force in terms of the gas pressure gradient. As stated before, the external force was

considered to act only on the dust particles and was just sufficient to keep them stationary against the pressure gradient. If F_d is the force on each particle of a thin slab of porous medium of cross-sectional area A, thickness dz, and composed of n_d dust particles per cc., then the total external force on the slab is $F_d (n_d A dz)$. If the gas has an excess pressure dP on one side of the slab, the force exerted by the gas on the slab would be $-AdP$. Therefore, it follows that

$$n_d F_d = dP/dz \qquad (91).$$

A "ternary" mixture of two gases, A and B, and the dust "molecules" d was then considered, and the set of equations of Equation (90) for $j=1$ were treated. Using Equation (91) along with the relations $P' = n'kT$ and $P = nkT$, the expression resulting from these operations was

$$(n_A J_B - n_B J_A)/[n'^2 (D'_{AB})_e] + (n_A J_d - n_d J_A)/[n'^2 (D'_{Ad})_e] = (1/n')dn_A/dz \qquad (92).$$

This expression was arrived at by Mason and his co-workers also from their dusty gas treatment of uniform pressure ordinary diffusion (6).

In their treatment of the uniform pressure case, these workers developed Equation (42), given previously in the text, from Equation (92). This was accomplished by including the properties pertaining to the dust "molecules" in the expressions for the effective normal and Knudsen diffusion coefficients. These expressions were in accord with the kinetic theory equations for these coefficients. For the intermediate region of ordinary diffusion, the above workers' treatment of the uniform pressure situation resulted in an expression which was equivalent to Equation (15), which had been developed by means of the momentum-transfer method of Maxwell and Stefan.

Mason and his co-workers then treated the forced flow problem by considering the set of equations given by Equation (90) corresponding to $j = d$. Using

Equation (91) and the relations $\underline{P} = \underline{n}\underline{k}\underline{T}$ and $\underline{n}'\underline{D}'_{\underline{i}\underline{j}} = \underline{n}\underline{D}_{\underline{i}\underline{j}}$ the following equation was obtained

$$\sum_{i=1, i\neq d}^{\upsilon} \left\{ n_d kT / [n(D_{id})_e] \right\} J_i = -dP/dz \qquad (93).$$

By specializing to a binary gas mixture and using the relations $\underline{J}_{\underline{B}} = \underline{J} - \underline{J}_{\underline{A}}$, $(\underline{D}_{\underline{B}\underline{d}}/\underline{D}_{\underline{A}\underline{d}}) = (\underline{m}_{\underline{A}}/\underline{m}_{\underline{B}})^{1/2}$ (6), and letting $\underline{C}_{\underline{B}} = \underline{n}\underline{D}_{\underline{B}\underline{d}}/\underline{n}_{\underline{d}}$, Equation (93) was resolved to the form

$$J - \beta J_A = -(C_B/kT)\,(dP/dz) \qquad (94).$$

From Equation (94), the flow equation given previously, Equation (43), was arrived at by treating $\underline{C}_{\underline{B}}$ as an empirical parameter to be determined from flow experiments.

The remainder of the treatment of nonuniform pressure ordinary diffusion by Mason and his co-workers was discussed previously as it applied to normal diffusion.